MORPHOLOGIC AND METABOLIC CHARACTERISTICS OF THE RHESUS VAGINA (*MACACA MULATTA*)

by

Daniel Morgan Ford

A THESIS
Presented to the Department of Anatomy
and the Graduate Division of the
University of Oregon Medical School
in partial fulfillment of
the requirements for the degree of
Doctor of Philosophy

June, 1971

AN ABSTRACT OF THE THESIS OF

Daniel Morgan Ford for the Doctor of Philosophy in Anatomy

Date of degree receipt:

Title: METABOLIC AND MORPHOLOGIC CHARACTERISTICS OF THE RHESUS VAGINA (*MACACA MULATTA*)

Approved: [redacted]

Despite the number of published investigations on the vagina of mammals, few studies have presented a morphologic characterization of the rhesus vagina and none has presented a consideration of glucose metabolism and the enzymes of glucose metabolism as put forth in this thesis. Morphologic studies of the rhesus vagina in the past were included in the consideration of the reproductive tract and were of necessity somewhat brief. The continued use of the rhesus monkey as a primate model for reproductive studies warranted this research. The morphologic and biochemical parameters were chosen to establish a base line against which investigations of a more experimental nature could be contrasted. There is a natural experimental aspect to normal function; that is, hormone levels vary with the course of the menstrual cycle.

In order to provide some insight into the relation of structure and function with the whole organ, observations were made at both the macro- and microscopic levels. Microchemical studies were not treated as isolated phenomena, but rather as subdivisions of the study of normal function in the rhesus vagina.

Both paraffin and fresh frozen techniques and stains for specific structural elements were used for morphologic study. Histochemical demonstration of enzyme

activity in frozen sections augmented both the morphologic and metabolic investigations. Microquantitative methods for metabolic measurement and enzyme assay, as modified by Adachi for skin and skin derivatives, facilitated the metabolic characterization of the vagina.

The epithelial lining of the rhesus vagina is quite different from that of woman, for it has developed exaggerations of the surface papillae, ridges, and rugae. The epithelial surface in the normal adult female is covered with keratinized teeth arranged in horizontally oriented combs which are in turn arranged as longitudinal columns. The teeth, which may be found in the upper two-thirds to three-fourths of the vaginal sheath, are sharp yet flexible.

Intricately well-developed subepithelial vascular and nervous plexi are supported in an organized but not particularly specialized connective tissue and muscle stroma. Stromal blood spaces in the walls of the vestibule and lower vagina attest the erectile nature of the region. Convolution of larger nerves in the vaginal wall may allow for stretching without damage to the nerve and provide a mechanism for stretch perception.

Cell shapes and dimensions varied with position in the epithelium and with time in the estrous cycle. Cells of the malpighian layers were frequently taller over the

peak of a stromal papilla. Corneal cells over the sides and apices of keratinized teeth were very compact. Cytologic phenomena correlated with increased thickness of the epithelium with the approach of ovulation and concomitant changes in metabolic state.

Specific yields from radioactive ^{14}C-glucose uptake were used to estimate (1) the contribution of the pentose-shunt to glucose metabolism, (2) carbon balance, (3) energy (ATP) balance, and (4) pyridine nucleotide balance. Based on ^{14}C-1- and ^{14}C-6-glucose metabolism, the pentose cycle accounted for 3,38% of overall glycolysis. The primary end product of glucose metabolism in rhesus vagina is lactic acid (95%). Carbon dioxide accounts for 4%.

For every 100 moles of glucose metabolized a net energy gain of 291 moles of ATP was generated. The net gain of reducing equivalents (NADH and NADPH) was 27 moles; NADH represented 92% of that. All pathways of glycolysis monitored here indicated a significant decrease in metabolism accompanying the ovulatory part of the cycle, usually followed by a luteal phase increase.

Histochemical studies demonstrated ovulatory phase decreases in the amount of glycogen in the stratum corneum, toluidine blue metachromasia in the stratum malpighi and stratum basale, and phosphorylase activity in the lower stratum malpighi and stratum basale.

Quantitative enzyme activity measurement revealed regional differences, suggesting that metabolic studies must be carefully controlled, so that samples will be taken from the same general region. Enzyme activities varied within the epithelium as well. Significant ovulatory decreases were demonstrated for glucose-6-phosphate dehydrogenase, pyruvate kinase, glyceraldehyde-3-phosphate dehydrogenase, and isocitrate dehydrogenase. The activity of malate dehydrogenase was significantly increased throughout the cycle (luteal higher than ovulatory higher than follicular).

The radiotracer data, considered with the changes in enzyme activities through the menstrual cycle support the following conclusions:

The vaginal epithelium of rhesus is not an inert tissue, but actively maintains itself with energy (ATP) secured for the most part by glycolysis via the Embden-Meyerhof pathway.

The basal and malpighian layers of the vaginal epithelium are the most metabolically active sites, while the stratum corneum is least active.

The pentose cycle is particularly active in the vaginal epithelium of the adult female rhesus with functioning hormonal systems.

Various of the changes in enzyme activities correlate with changes in overall metabolic activity, suggesting that the changes in enzyme activity may be an in vivo enzyme adaptation in the vagina.

APPROVED:

[redacted]

(Professor in Charge of Thesis)

[redacted]

(Chairman, Graduate Council

TABLE OF CONTENTS

LIST OF ILLUSTRATIONS

CHAPTER ONE. INTRODUCTION

I. The problem

This research was undertaken to characterize the vagina of the normal adult rhesus monkey (Macaca mulatta) vis à vis morphology and certain biochemical parameters in order to extablish a base line against which investigations of an experimental nature could be contrasted.

In order to provide some insight into the relation of structure and function with the whole organ, observations were made at both the macro- and microscopic levels. Microchemical studies were not treated as isolated phenomena, but as subdivisions of the study of normal function in the rhesus vagina. There is a natural experimental aspect to normal function; that is, variations relate to different hormonal levels in the course of the menstrual cycle.

Set forth in the ensuing chapters are studies of vaginal morphology at macro- and microscopic levels, vaginal metabolic interrelationships, and the enzymological ramifications of those metabolic factors, as explained by histochemical and microquantitative biochemical methods. The results are discussed in terms of the development and function of a normal rhesus female.

II. Development

The formation of a vagina in the urogenital system of

the fetal female represents the culmination of a dynamic interaction of mesodermal, ectodermal, and entodermal elements.

It is generally recognized that the upper four-fifths of the vagina derives from the fusion of the lower ends of the müllerian ducts (167). These paramesonephric structures form as grooves in the mesonephric ridges, which are taken into the ridges as ducts (8). Various observations indicate that the formation of the müllerian ducts is induced by the nearby wolffian (mesonephric) ducts: (1) experimental destruction of the wolffian duct is associated with the failure of the müllerian ducts to reach the cloaca; (2) the absence in man of müllerian ducts has been associated with a congenital lack of kidney which may result from retarded development of the ureter, embryonic agenesis of the ureter, or arrested development of the parent tissue (wolffian duct budding) of the ureter; (3) a basement membrane is initially lacking between the müllerian and wolffian ducts (167).

The urogenital sinus portion of the cloaca, which includes tissues of both entodermal and ectodermal origin, comprises the lower fifth of the vagina. The definitive epithelium of the vagina is thought to be derived from epithelial cells that migrated from the urogenital sinus under the lining of the upper four-fifths of the vagina

to excavate and replace that epithelium. No apparent line of histological demarcation separates the proliferative response of the vagina from that of the vestibule or, in certain species, from that of the skin beyond the vulva, the so-called sex skin (179). The evidence that the definitive vaginal epithelium in monkeys derives either entirely or for the most part from ectoderm of the cloacal membrane and/or proctodeum and that it reaches the vagina via the urogenital sinus is in line with the fact that the anal canal is lined with a squamous epithelium (178). Wells (167) suggested that the maternal hormones of pregnancy, rather than the fetal gonads, control the formation of the vagina, for the rapid decrease in maternal hormones after birth is followed by the regression of neonatal vaginal growth. Clark and Gorski (40) have found that the number of estrogen-binding sites in the cytoplasm of uterine cells reaches a maximum by day ten of neonatal life. After the peak is reached, the number of sites decreases and remains constant until days 22-23, indicating to Clark and Gorski that the ontogeny of the estrogen-binding protein is probably a property of the uterine cells and is not dependent on estrogen from the ovary. The same protein is present throughout postnatal development.

Whether a phenomenon of maternal hormone complement or an inherent feature of pudendal tissues, the proclivity

to femaleness is realized in the absence or inhibition of male hormone (including an excess of female hormone). In the case of exogenous estrogen in the fetal male, the timing of estrogen administration is an important aspect (176).

III. History of vaginal studies

A. Anatomy and endocrinology

Only a few studies of the rhesus reproductive tract have given much attention to the vagina. Only Allen (5) and Wislocki (171) provided thorough descriptions of rhesus vaginal morphology. Other studies that did include some general histological observations were those of Corner (44), Hartman (80), and Hisaw et al. (90).

The muco-columno-squamous interactions of the cervical epithelium have garnered a greater share of study than the vagina. Hormonal fluctuations influence the cervix in ways that can be observed both grossly and microscopically and more definitely than the vagina (41, 53, 75, 91, 92).

The need for the present study becomes apparent when one considers the references to the vagina of such primates as man, squirrel monkey, and macaque as being generally the same (24). Although the three are basically similar in their physiology, endocrinology, and basic structural organization, the studies of several investigators suggest

that the simplest macroscopic observations differentiate at a glance any one from the others (170, 172, 41, 25). Only Wislocki (170, 171) recorded that the longitudinal foldings of the vaginal wall were covered with a multitude of delicate transverse plicae (which, as we shall see in Chapter Three, represent only half the complexity of the mucosal morphology).

Most investigators have been interested in the vagina from an endocrinological point of view and chose a specific biochemical or morphologic criterion (e.g. the appearance of the smear) on which to base observations of experimental hormone efficacy. As a result the descriptions of the morphology of the normal adult rhesus vagina are inadequate.

The rhesus vagina lies in the base of the bowl created by the pelvic girdle and the perineal muscles. Its semicylindrical structure derives from the perineal muscles, those of the anal sphincter (70, 171), and the longitudinal and circular muscles of the vaginal wall. The vagina opens to the exterior by way of a vestibule and poorly differentiated labia minora between the specialized epidermal pads on the rump, the ischial callosities (137). The entire skin surface about the vaginal os, from the base of the tail to as far as the medial popliteal region exhibits a more or less permanent flush from the expanded

subepidermal blood vessels and spaces (171, 6, 42, 44, 80, 160).

The relatively smooth vestibule exhibits swellings which Wislocki (171) thought were analogous to the hymen. The epithelium of the vestibule is not much thicker than body surface skin, but becomes thicker closer to the inner two-thirds of the vagina where the surface of the wall proper is complexly elaborated into large and small folds and ridges (170, 171). The cervix extends into the vagina irregularly, so that the posterior lip is often larger than the anterior. Individual and age differences influence the conformation of the cervical surface and fornix.

The lining of both the vestibule and the vagina is similar to that in man in several respects, including a multilayered epithelium subject to variation according to ovarian activity (27, 70, 74, 127, 145, 158). As Wislocki (170, 171) has described the rhesus vagina, the topography of the vaginal lining is wholly dissimilar in the human and rhesus. The proliferation and differentiation of epithelial cells in the vagina of Homo and Macaca are very similar, although the rhesus may reach a stronger degree of keratinization.

The changing proportions of keratinized cells in the vaginal smear, first demonstrated in the rat by Long and Evans (119), have been correlated with those of other

animals including the rhesus monkey (5, 6, 45, 51, 130), the chimpanzee (57, 164), and the baboon (67, 81). Further studies, including the control of the hormonal complement by way of hormone administration to ovariectomized individuals, facilitated the correlation of vaginal epithelium smears with hormone action (21, 52, 142, 143, 144, 110, 166). Both estrogen and progesterone were shown to be necessary to induce the vaginal phenomena seen in the intact animal (39). Somewhat contrary to the recent work by Barker and Walker (13), wherein estrogen promoted keratinization and progesterone enhanced proliferation, Bullough (31) and Biggers and Claringbold (23) have found that estrogen stimulates cell division in mice.

After monitoring the appearance of cornified cells in the vaginal smear of rhesus, DeAllende et al. (51) found not one but two peaks of cornification: one about day 10-12 after menses and another 5-12 days later. Lamar et al. (112) noted a sudden liquefaction of the cervical mucus about day 10-12. An investigation by DeAllende of the state of the ovary at the time of the sudden changes in cornification of the vaginal cells and the liquefaction of cervical mucus revealed a preovulatory spurt of growth in the Graafian follicle that culminated in its dehiscence. Recent studies of the estrogen and progesterone levels in rhesus during the menstrual cycle correlate well with the

peaks of cornification found by DeAllende (94). That study confirms in rhesus the phenomena observed in man and other mammalian subjects (29, 128).

The cytological roles of estrogen and progesterone have been demonstrated to be the promotion of mitotic stimulation and surface cell heightening, respectively (31, 56). The synergistic action of the hormones in keratinization has been mentioned above. An antagonistic action has been described for progesterone, based on experimental manipulation (88, 90).

The usual time of ovulation in rhesus was well documented by the detailed records of Hartman (80) and Corner (45). Fortunately regularity is also usual, so the ovulatory times established by those authors can be used for calculations in other research.

B. Histochemistry

Histochemical investigations of the vaginal epithelium of primates have been few. Those on the vagina of rhesus are even fewer and deal only with the presence of glycogen in epithelial cells (165, 172). Studies on the histochemistry of the vagina of man, though not exhaustive, have included determinations of S-S and S-H groups, acid and alkaline phosphatase, ß-glucuronidase, succinic dehydrogenase, NAD diaphorase, α-naphthyl esterase, and

glycogen (16, 47, 59, 60). Additional esterases, phosphorylase, and branching enzyme have been added to the list of histochemical demonstrations in the vagina of rodents and other mammals (18, 20, 61, 63, 68, 78, 132, 154).

C. Carbohydrate metabolism

Studies of carbohydrate metabolism in the vagina of rhesus have been limited to demonstrations of glycogen and glycogenolytic enzymes. No more detailed investigations of carbohydrate metabolism have been made on the vaginal epithelium of any mammal, although many studies of carbohydrate metabolism have been done on the surface epithelium of skin.

IV. History of metabolic and microquantitative methods

The primary pathways of glucose metabolism have been clearly demonstrated in human and other mammalian skin and mucous membranes. Wohlgemuth (173) showed that human skin produces lactic acid from glucose in vitro. The integumental existence of the Embden-Meyerhof pathway was subsequently confirmed by numerous other works. Much of the qualitative demonstration of various glycolytic pathways was accomplished via histochemical methods especially those of the Krebs cycle and hexosemonophosphate shunt.

The localization and quantifaction of pepsin in the chief cells of the stomach (116, 117) initiated the general histochemical procedures. In those studies histological controls were used for comparison with the microchemical analyses. Greater accuracy and consistency derived from the further refinement of the quantitative histochemical methods (7, 125, 126), wherein freeze-dried sections were utilized instead of Linderstrøm-Lang's histological control. After applying Hoerr's (93) quick-freeze and drying method (dehydration at -30 to -40°C), Lowry dissected tissues of interest from the dried sections. To evaluate sample size, he determined protein content by the Folin phenol reaction and sample volume by multiplying the thickness of the section by its area, and measured dry weight with a quartz torsion balance or a quartz fiber "fish-pole" balance (120, 121, 122, 126). The greater convenience and reproducible 0.01 µg sensitivity of the quartz fiber balance make it the instrument of choice.

Because the Lowry group could not get more than a few micrograms of tissue from the dissections, they developed special methods for measuring very small quantities (e.g. 10^{-10} to 10^{-13} moles) of substances in tissues with as little as 10 µg wet weight. For greater sensitivity in microquantitative methods, Lowry et al. (126) refined their

fluorometric methods to measure adenosine triphosphatase, acid and alkaline phosphatases, cholinesterase, fumarase, and aldolase in 5-10 µg of brain tissue.

The Kaplan group (105) found that pyridine nucleotides (NAD^+ and $NADP^+$) could be made to fluoresce by heating them in strong alkali or a carbonyl compound. No treatment was necessary for measuring reduced pyridine nucleotides, for they have a natural fluorescence.

Fluorometry proved to be particularly good for the localization of enzymes, substrates, and coenzymes in tissue, because its sensitivity is about a thousand times finer than that of a spectrophotometric method. By stabilizing the fluorophor, Lowry et al. (124) modified the Kaplan procedure to measure still more enzymes, the first of which were lactic dehydrogenase, glucose-6-phosphate dehydrogenase, and 6-phosphogluconate dehydrogenase. Many other enzyme techniques have since been developed utilizing the principle of coupling--adding accessory enzymes--to assay almost any enzyme reaction fluorometrically, so long as the reaction can be linked to the oxidation of NADH or NADPH or to the reduction of NAD^+ or $NADP^+$ (123). With reference to the evolution of enzyme assay techniques, some enzymes do not yield easily to demonstration. In fact, phosphofructokinase is so delicate that the paper showing its purification was not

published until 1965 (118). It was 1968 before the enzyme was demonstrated in skin (4).

The microquantitative methods were quickly adapted by Hershey and Mendle (85) to the examination of human skin. That and subsequent studies by Hershey (82, 83, 84) suggested that the pentose shunt played an active role in glucose metabolism in skin. Although the demonstration of TCA cycle enzymes in skin (14, 46, 49, 72) and of hexosemonophosphate pathway enzymes (82, 84, 85) indicated their presence in skin, little information was proffered about the relationship of the pathways to each other or to the dynamics of carbohydrate metabolism as a whole.

The study by Berenblum et al. (17) demonstrating the high rate of aerobic glycolysis in skin (ca. 3 µg/mg/hr.) and that by Cruickshank and Trotter (48) indicating that oxygen tension influences the utilization of glucose for the production and oxidation of lactic acid were among the few studies contributing data on the dynamics of carbohydrate metabolism. Barron had suggested that the activity of the TCA cycle was limited in skin, opening the possibility that the glycolytic pathway plays a major role in ATP provision for biosynthesis.

The development of scintillation techniques for measuring carbon dioxide (140), lactate, lipid, and other

extractable fractions greatly facilitated the garnering of information concerning the various pathways of carbohydrate metabolism (64, 65). Micromodifications (2) and calculations utilizing pathway ratios for data interpretation (106, 151, 175) enabled the investigators of epithelial metabolism to fully characterize the metabolic patterns of a tissue, including carbon and energy balances.

Micromodifications of metabolic techniques and further development of microquantitative enzyme assays (based on the principle of coupling reactions to pyridine nucleotide systems, that is, the cycling method) have been continued (129, 141).

CHAPTER TWO. MATERIALS AND METHODS

I. Animals

Three adult rhesus females were maintained in separate cages in the intensive care room of the Oregon Regional Primate Research Center for the duration of this investigation. These three animals were the nucleus of the anatomical, histochemical, and microchemical studies of the rhesus vagina during the menstrual cycle. Twenty-three biopsy specimens were taken from the three animals during ten normal menstrual cycles. The cycle lengths averaged 27 days for animal 305-664, 26 days for animal 305-2074, and 28 days for animal 305-2259. No biopsy specimens were taken during summer months, even though only animal 2259 exhibited any irregular (longer) cycling during summer. Menstrual records for the three animals are included in appendix A. Preliminary studies were carried out on four additional animals; all seven females were healthy and menstruated regularly. None had undergone any major surgery.

Specimens were also procured from eight animals at the time of death. The condition of the animals at death is shown in Table I along with physical characteristics relevant to the studies. Dissection of the autopsy specimens constituted a major part of the macroscopic studies.

Gross observations of the vaginal lining of seven animals of various ages and states of ovarian function were also made (Table II, page 43) to further correlate the development of epithelial papillae with ovarian state.

II. Sampling

A. Biopsy

Vaginal specimens were removed under the supervision of the surgeon of the Oregon Regional Primate Research Center. Specimens from the four preliminary animals were taken with sterile scissors without anesthesia. The usual biopsy of the three test animals was made with a rongeur forceps* under general anesthesia by Surital in the dose range 6-15 mg/kilogram body weight as necessary for effect. The antiseptic powder, Neo-Predef, was sprayed liberally about the wound after the removal of the specimens. All biopsies were performed at 7:45 a.m. to allow adequate time for the glucose metabolism procedures.

For this investigation, the menstrual cycle was divided into three periods, approximating the follicular phase, the luteal phase, and the period of follicular-luteal interplay about ovulation. The peak hormonal

---

*Details of equipment and materials are listed in Appendix J along with the suppliers.

levels of the follicular phase are reached gradually and occur just before ovulation, which in rhesus monkeys is about days 10-15. Since it is difficult to pinpoint these peaks, biopsy periods were selected as postmenarchal* days 1-10, 10-15, and 15-25. Less ambiguity is associated with the third time period, since maximum progesterone concentration is reached quickly and maintained until shortly before the end of the cycle. Day 25 was selected as the cut-off date to ensure against missing the end of the cycle. Menarche cannot be predicted exactly, but rarely occurs before the 25th postmenarchal day.

Most biopsies were from the vaginal wall about midway along a line from the vaginal orifice to the fornix. The vagina was envisioned as having four walls, so that no wall would have more than one biopsy in any two-month span. The intent was to minimize the effects, if any, of wounding on phenomena already under the influence of fluctuating hormone levels.

B. Autopsy

Eight autopsy specimens were included in this research. Tissues were taken immediately after death and treated

---

*Menarche is used here in its literal meaning (the onset of menses) rather than in its common meaning as the first appearance of menstrual flow in the life of the individual.

according to the procedures planned for them, i.e., fixed in Hollande-Bouin solution for paraffin work, frozed for histochemistry, or dissected into 5 mg wet weight pieces for glucose metabolism studies. Observations of gross morphology were made at the time of autopsy. All available information on the surgical and menstrual histories and weight records for the year before sacrifice or biopsy were secured from the daily record files in the computer center of the Oregon Primate Center for all animals autopsied or biopsied, so that a reasonably accurate impression of the reproductive state of any given animal could be formulated.

Table I. Animals used in vaginal studies

ORPRC ID No.	Condition
Biopsies:	
305-2060	menstruating regularly; biopsy day 12
305-411	menstruating regularly; biopsy day 1-2
305-87	menstruating regularly; biopsy day 1-3
305-233	menstruating regularly; biopsy from vestibule day 13
305-2259	menstruating regularly; series of biopsies taken throughout menstrual cycle
305-2074	menstruating regularly; series of biopsies
305-664	menstruating regularly; series of biopsies
Autopsies:	
305-106	10 yrs. old; no regular menses for one year before sacrifice
305-254	age unknown; two weeks of menstrual discharge before sacrifice; animal appeared aged
305-98	at least 6 years old; hemioöphorectomized one week before sacrifice
315-3115	ovariectomized
305-3584	ovariectomized and adrenalectomized (steroid therapy)
305-4283	1 yr. old; high butter content milk diet
305-5034	80-day old infant
305-2089	apparently healthy female; day 7 of menstrual cycle
Observed only:	
305-216	ovariectomized
305-2300	hemioöphorectomized one week before sacrifice (observation time)
305-210	adult with ovaries; not cycling regularly age unknown
305-3585	adult with ovaries; age unknown
305-3598	adult with ovaries; age unknown
305-3587	adult with ovaries; age unknown
305-83	adult with ovaries; age unknown

III. Histological studies

A portion of each specimen was treated for paraffin embedding. Tissues were fixed four hours in Hollande's modification of Bouin's fixative* (96). Fixed tissues were placed directly in 70% ethyl alcohol for one hour, changed twice with 70% EtOH for one hour each, moved to 80% for one hour, and placed in 95% EtOH for 3 hours. The tissues were then placed in 100% EtOH for one hour, xylene for fifteen minutes, and "Paraplast" tissue embedding medium for four hours in a 57°C paraffin oven. Sections were cut from the paraffin embedded tissues at seven micra with a steel blade on a rotary microtome.** A water bath of 0.01% gelatin at 45°C was used for floating and spreading the sections before mounting on precleaned and prelabeled glass slides. The gelatin acted as an affixative when the slides were dried on a 45°C slide warmer for 4 hours or overnight. The slides were stored in microscope slide boxes until needed for staining.

In preparation for staining of the paraffin sections, the slides were deparaffinized in two changes of xylene (5 minutes each), placed in three changes of absolute alcohol (5 minutes each), and hydrated through 95%

---

*This and subsequent solutions and reagents are listed in Appendix B.

**Equipment and materials are listed with the model or catalog number and supplier in Appendix J.

alcohol to water. The following stains were used: Harris' hematoxylin and eosin (115); toluidine blue, buffered to pH 4.5 (134); periodic acid-Schiff reaction with control slides digested in 10% diastase in 0.02 M phosphate buffer, pH 6.0 (135); an unpublished modification of Roman's acid orcein-Verhoeff(153); and a ferric chloride demonstration of acid mucopolysaccharides (149).* After staining, the slides were dehydrated through alcohols, cleared in xylene, and coverslipped with "Permount" mounting medium.

To examine the undersculpturing of the vaginal epithelium and the intricacy of stromal papillary processes, a large piece of tissue including the vaginal wall, vestibule, and cervix from a reproductively patent female was incubated in 2N sodium bromide at 37° for four hours to split the epitheliostromal junction. The epithelium was then dissected from the stroma as a sheet, dehydrated through alcohols to xylene, allowed to dry, and mounted on a large glass slide for observation under a dissecting microscope.

IV. Histochemical studies

Immediately after biopsy or autopsy, a portion of

---

*The details of these histological procedures are given in Appendix C.

each tissue specimen was wrapped in aluminum foil, frozen on dry ice, and stored in liquid nitrogen at -96°C or in the freezer at -20°C. Later the tissues were mounted in ice and cut in various thicknesses (depending on the procedure to be done) with a steel blade in a cryostat at -20°C. Certain of the procedures required free-floating sections, so sections for those procedures were placed directly in screw-cap jars which had been equilibrated to -20°C within the cryostat. Cold fixatives for the procedures were added directly to the tissues in the jars, which were then placed in the refrigerator at 4°C for a prescribed time. The procedures were: the modified Bielschowsky silver impregnation technique for peripheral nerve endings (168, 169); the cholinesterase-silver technique for the demonstration of cutaneous nerves (152); and the DOPA (dihydroxyphenylalanine oxidase) reaction for cells with melanogenic potential (unpublished modification of Laidlaw and Blackberg [111] and Rappaport [148]).* Sections for the DOPA reaction were not fixed before incubation with the substrate.

Other histochemical procedures were carried out on sections affixed to slides. Such tissues were prepared by placing sections on "Tissue-Tac" coated, prelabeled

---

*The preceding and following histochemical procedures are presented in detail in Appendix D.

slides which had been allowed to equilibrate to -20°C in the cryostat. After the desired number of sections had been placed on a slide, the investigator affixed them to the slide by holding a finger to the glass below the sections, thereby melting them and allowing them to fuse with the dried affixative. The slides were then placed in small plastic slide boxes in the cryostat for storage until needed for staining. All slides so prepared were air dried for two hours just before staining. If the slides were not dried, the sections did not remain affixed to the slides during processing. Several different affixatives, various fixative solutions, and combinations of affixatives and fixatives were tried in attempts to eliminate the air-drying period, but none was successful.

After they had been dried, slides were either fixed in buffered 10% formalin or placed directly in the incubation medium without fixation. Slides were fixed for: alkaline phosphatase (69); acid phosphatase (12); acetyl- and butyrylcholinesterase (108, 136); the AOV stain for elastic fibers (153); a stain for acid mucopolysaccharides (149); and the PAS reaction with concomitant diastase control (135). The slides for PAS were fixed two hours in 100% ethyl alcohol. Acid phosphatase slides were fixed in 4.6% glutaraldehyde for two hours before incubation. Unfixed frozen sections were used to study phosphorylase

(157, 161); glucose-6-phosphate dehydrogenase (86); beta-glucuronidase (156); and aminopeptidase by the L-leucyl-β-naphthylamide method (138).

Reaction product depositions in the tissue sections were interpreted solely on the basis of localization and color intensity. The interpretations are necessarily oversimplified into the categories, absent (0), weak (1), moderate (2), and strong (3), which have been used in this and many other laboratories for several years. It should be noted that no greater accuracy accrues from using more classifications when observations are made on a continuum, as has been shown by Biggers and Claringbold (21) with discriminant analysis.

V. Microscopy and photomicrography

General observations and measurements were made with a Carl Zeiss GFL standard microscope equipped with 1, 2.5, 10, 40, and 100-power objectives, Kpl 8 x eyepieces, ocular micrometer, and a 50-60 Hertz 39-25-24 type transformer. The ocular micrometer was calibrated with a Carl Zeiss stage micrometer for each objective.

Photomicrographs were made with 4 x 5 inch Panatomic-X film in a Carl Zeiss Ultraphot II photomicroscope with a tungsten light source.

VI. Microchemical studies

A. Glucose metabolism

1. Procedure

a. Introduction

The metabolic studies were conducted on biopsy specimens from the three experimental animals. Immediately after biopsy, a specimen was placed on a watch glass on ice and dissected to provide samples of stroma-free epithelium weighing about 5 mg wet. To prevent the loss of tissue ability to metabolize glucose to CO_2, the tissue samples were held in buffered 100 mg% glucose solution (2). Within 15 to 25 minutes after biopsy, tissue samples were incubated in 100 microliters (2) of ^{14}C-glucose reaction mixture for one hour in the apparatus described in Appendix E. Blank tubes were run at the same time with the same radioactivity (.25 µc/tube) but without tissues. Specimens for blanks in post-incubation assays were held in buffered 100 mg% glucose solution at $4^{o}C$.

b. Carbon dioxide measurement

Carbon dioxide released from the incubating specimens was collected on hyamine hydroxide-saturated filter paper held above the specimens in a closed chamber, a technique that collects more than 95% of the CO_2 (2, 140). Details of the procedure are presented in Appendix E. After

Figure 1. Major pathways of glucose metabolism in skin and its derivatives

Hexosemonophate= Hexosemonophosphate

CO_2 is evolved from the TCA cycle

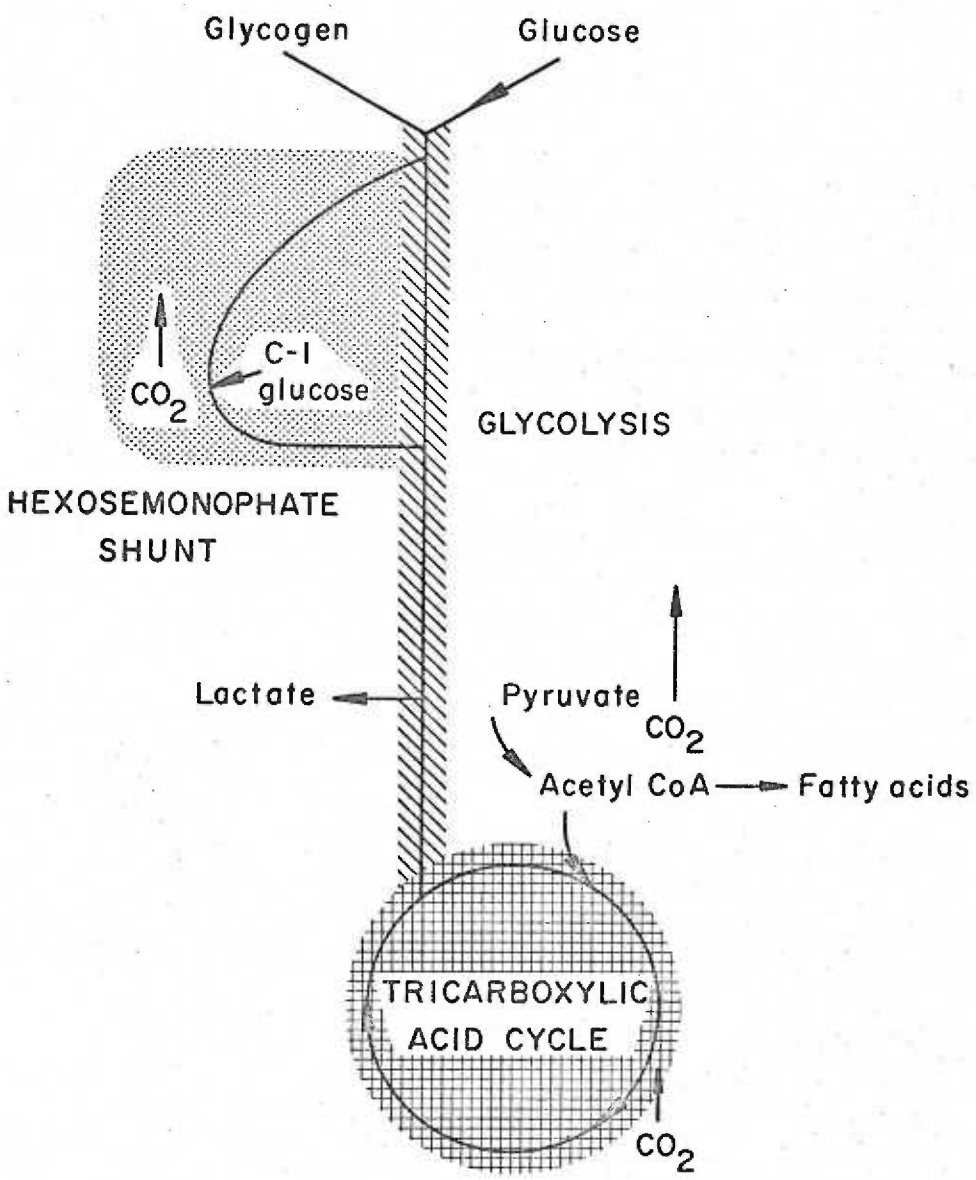
Glycogen
Glucose
CO_2
C-1
glucose
GLYCOLYSIS
HEXOSEMONOPHATE
SHUNT
Lactate
Pyruvate
CO_2
Acetyl CoA
Fatty acids
TRICARBOXYLIC
ACID CYCLE
CO_2

incubation, the filter paper was placed in a scintillation counting vial with 20 ml of scintillation medium.* The part of the apparatus with reagent mixture was held for further processing.

c. Lactate measurement

Tissue samples were added to "blank" reagent mixtures after incubation. Specimens and reagent mixtures were removed to tissue homogenization tubes and homogenized with 1 ml 3% TCA. Details of the entire lactate assay appear in Appendix E. Aliquots of 100λ were taken from each of the homogenates for the determination of lactate. The determination depends on cupric and calcium ion precipitation of glucose but not lactic acid from the homogenate solution. After centrifugation, a 100 λ aliquot of the remaining solution was applied to filter paper and air dried, and the paper was placed in a counting vial with 20 ml scintillation medium.

d. Glycogen determination

The homogenate remaining after the removal of an aliquot for lactate assay was centrifuged. One milliliter of

---

*5 g. of 2'-5'-diphenyloxazole (PPO) and 0.3 g. of p-bis-2' (5'-phenyloxazole) benzene (POPOP) per liter of toluene.

the supernatant was taken for glycogen determination, which is based on the alcoholic precipitation of glycogen from solution (159). After precipitation, the glycogen was dissolved in distilled water. An aliquot of the solution was applied to filter paper, air dried, and placed in a counting vial with 20 ml of scintillation fluid. Details of the procedure are given in Appendix E.

e. Lipid and protein-DNA measurements

Sediment remaining from the above centrifugation was washed three times with 500 λ of a 2:1 mixture of chloroform and methanol. The three washes from each tube were combined and evaporated under nitrogen until nearly dry. After the addition of 300 λ of heptane as a solvent to the small fraction of lipid extract, the solution was washed three times with double distilled water to remove water-soluble contaminants and water washings were discarded. The heptane-dissolved lipid was applied to filter paper, air dried, and placed in a counting vial with 20 ml of scintillation medium.

The lipid extracted sediment, suspended in a 250 λ distilled water, provided a 200 λ aliquot of protein and DNA residue which was applied to filter paper, air dried, and placed in a counting vial with 20 ml of scintillation fluid.

f. Counting

A Packard two-channel scintillation counter set for 900 volts counted all radioactive assay in these procedures. In all cases counts per minute were converted to disintegrations per minute, before further calculations.

2. Reagents

^{14}C-U-glucose (uniformly labeled glucose, specific activity 100 µc-3.8 mg)
^{14}C-1-glucose (glucose labeled in carbon-1-position, specific activity 50 µc/2.9 mg)
^{14}C-6-glucose (glucose labeled in carbon-6-position, specific activity 50 µc/3.0 mg
.54 M Krebs Ringer buffer
Hyamine hydroxide insodium hydroxide
10% Trichloracetic acid
3% Trichloracetic acid
Calcium hydroxide, powder
2N sodium chloride
10% glycogen solution
1% glucose solution
95% ethanol
Chloroform
Methanol
Heptane

3. Interpretation of metabolism data

The scintillation data from each fraction were converted to specific yields (percent of total counts). Estimation of the pentose cycle was calculated according to Katz et al. (106).

Method I.

$$\text{Pentose Cycle (PC)} = \frac{S}{3-2S}, \text{ where}$$

$$S = \frac{(G\text{-}1\text{-}CO_2) - (G\text{-}6\text{-}CO_2)}{1-(G\text{-}6\text{-}CO_2)} ,$$

and $G\text{-}1\text{-}CO_2$ and $G\text{-}6\text{-}CO_2$ represent the specific yields of carbon dioxide from glucose-1-^{14}C and glucose-6-^{14}C.

Method II.

$PC = \frac{1-\gamma}{1+2\gamma}$, where $\gamma = \frac{G1L}{G6L}$, and G1L and G6L represent the specific yields from lactic acid.

B. Quantitative enzyme assay

1. Procedural theory

So that the major steps and pathways of glucose metabolism in the rhesus vaginal epithelium could be more precisely quantified, seven selected enzymes, representing the major steps of predominant pathways determined in glucose metabolism studies, were assayed: glucose-6-phosphate dehydrogenase, phosphofructokinase, glyceraldehyde-3-phosphate dehydrogenase, pyruvate kinase, lactate dehydrogenase, isocitrate dehydrogenase, and malate dehydrogenase. Frozen sections (30 μ) of vaginal biopsy specimens were lyophilized. Dissections of the epithelium from the stroma were facilitated by the use of an angular piece of razor blade under a dissecting microscope. In parts of the study the epithelium was further dissected

into basal, malpighian, and corneal layers. Pieces of the epithelium weighing 1 μg ± 0.4 μg (determined with a "fishpole" quartz fiber balance) were used for the enzyme assay procedures.

Both epidermal homogenates and lyophilized sections of normal rhesus epidermis have been used in this laboratory to study the partial properties and characteristics of the seven enzymes assayed in this thesis. (3, 4, 98, 99, 100) Enzymes were assayed within the limits at which reaction rates were proportional to reaction time and enzyme amount. The optimal conditions determined in the previous studies for lyophilized tissues of rhesus epidermis were used in the enzyme assays of the rhesus vaginal epithelium. The assay conditions and constituents of the reaction mixtures for the seven enzymes appear with the detailed assay procedures in Appendix H.

a. The native fluorescence method for assay of NADH and NADPH

The assay for NADP-dependent enzymes depends on the stoichiometric reduction of $NADP^+$ to NADPH and the subsequent measurement of NADPH by virtue of its native fluorescence. In this thesis enzymes dependent on $NADP^+$ were G-6-PDH and ICDH. A similar mechanism is the basis of the assay for NAD^+-dependent G-3-PDH.

After an appropriate incubation period, the reaction

Figure 2. Enzymes measured in the major pathways of glucose metabolism.

1. glucose-6-phosphate dehydrogenase
2. phosphofructokinase
3. glyceraldehyde-3-phosphate dehydrogenase
4. pyruvate kinase
5. lactate dehydrogenase
6. isocitrate dehydrogenase
7. malate dehydrogenase

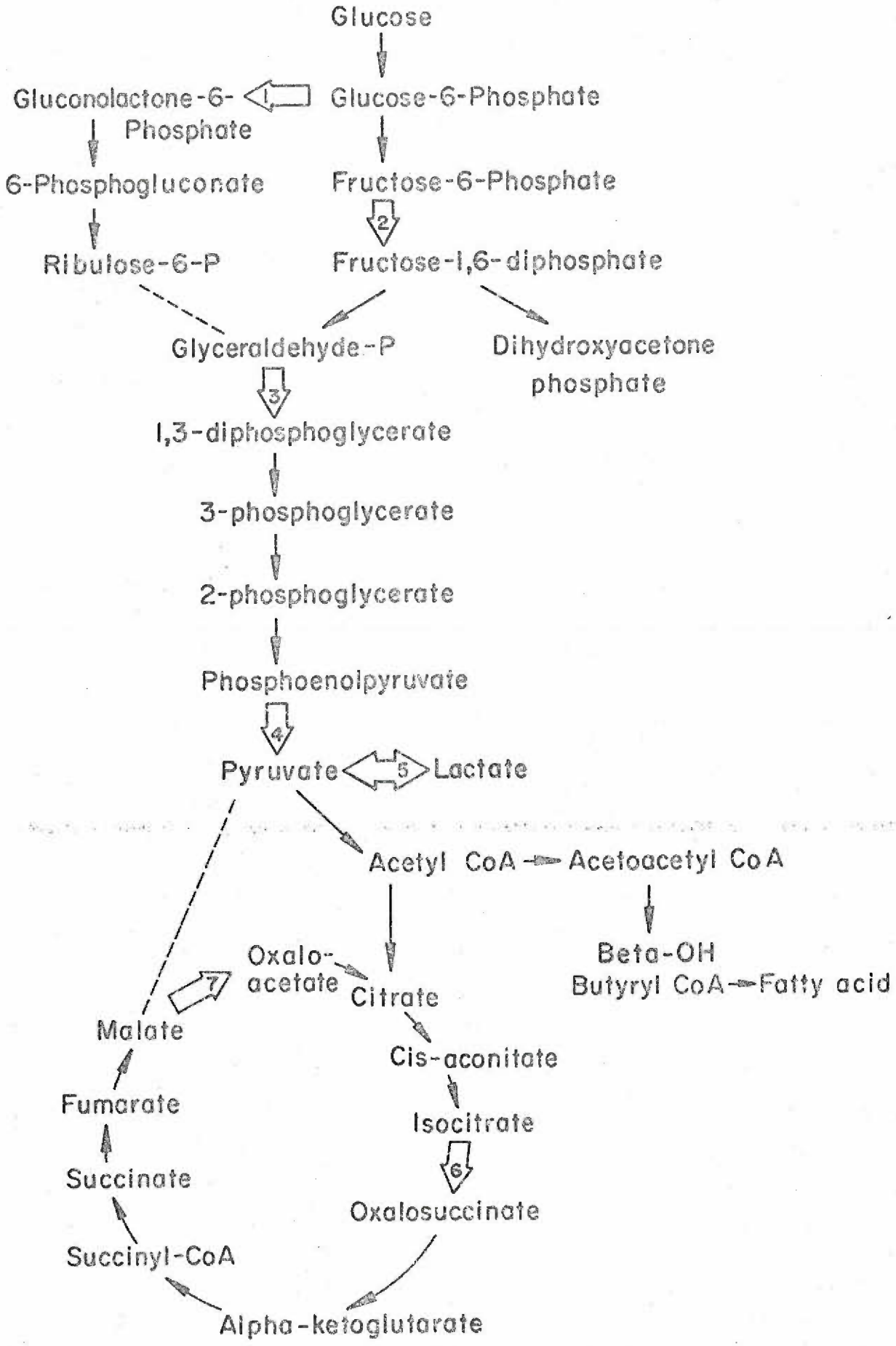
Glucose
Gluconolactone-6-Phosphate
1
Glucose-6-Phosphate
6-Phosphogluconate
Fructose-6-Phosphate
2
Ribulose-6-P
Fructose-1,6-diphosphate
Glyceraldehyde-P
Dihydroxyacetone phosphate
3
1,3-diphosphoglycerate
3-phosphoglycerate
2-phosphoglycerate
Phosphoenolpyruvate
4
Pyruvate
5
Lactate
Acetyl CoA
Acetoacetyl CoA
Beta-OH Butyryl CoA
Fatty acid
Oxalo-acetate
7
Citrate
Malate
Cis-aconitate
Fumarate
Isocitrate
Succinate
6
Oxalosuccinate
Succinyl-CoA
Alpha-ketoglutarate

was stopped by placing the tubes into water at 4°C. To maintain the natural fluorescence of the reduced pyridine nucleotide, the reaction mixture was diluted with 1 ml of 0.1 M carbonate buffer, pH 10.5.

In the Farrand fluorometer (Model A_2), the 365 mμ excitation wavelength was produced via the primary filter (Corning No. 5860). The emission wavelength was limited below 470 mμ by a secondary filtercomplex (Corning No.'s 4308, 5562, 3387). The excitation and emission maxima of reduced pyridine nucleotide are 360 mμ and 460 mμ, respectively.

The intensity of the fluorescence from reduced pyridine nucleotide is directly proportional to its concentration in solution. That intensity, as amplified in the fluorometer, was measured on a galvanometer.

b. The Strong alkali method for assay of NAD^+

Four of the seven enzymes studied required NADH as a cofactor. Those enzymes were PFK, pyruvate kinase, LDH, and MDH. The resultant NAD^+ had no native fluorescence but could be made fluorescent by the following treatment.

After incubation, the reaction was stopped by the addition of hydrochloric acid (to a final concentration of 0.2 - 0.5 N) which also destroyed unreacted NADH. Sodium

hydroxide (6.6 N, 100λ) was added to the acidified reaction mixture and incubated 15 minutes at 60°C (alternatives: 30 minutes at 37°C or one hour at room temperature). Such treatment produced a stable fluorescent agent, which after a five- to tenfold dilution with distilled water could be measured in the fluorometer as above.

Monthly standardization of nicotinamide adenine dinucleotide (NAD^+) and nicotinamide adenine dinucleotide phosphate ($NADP^+$) facilitated the monitoring of the stability of the reagents. The standardization procedure is given in Appendix E. The standardization depends on the reduction of NAD^+ or $NADP^+$ to NADH or NADPH. Freshly prepared 50 mM NADH was used as a spectrophotometric standard.

2. Reagents

a. Substrates

Glucose-6-phosphate (Sigma), disodium salt, 100 mM
Fructose-1,6-diphosphate (Calbiochem), 50 mM
Isocitrate (Sigma), trisodium salt, 100 mM
Pyruvate, (Sigma), trisodium salt, 100 mM
Oxaloacetic acid (Sigma), 100 mM

b. Auxiliary Enzymes

Aldolase (Sigma), 10 mg/ml
Trioseisomerase (Sigma), 10 mg/ml
Alpha glycerophosphate dehydrogenase (Sigma), 10 mg/ml
Lactate dehydrogenase (Sigma) 10 mg/ml
Alcohol dehydrogenase (Sigma), 5-6 mg/300 ml
Glucose-6-phosphate dehydrogenase

c. Buffers

Tris (hydroxymethyl) amino methane, 0.5 M, pH 7.5, 7.8-8.0, 7.8-8.2, 8.2-8.8
AMP_2 (2 amino-2-methyl-1,3-propanediol), 0.5 M, pH 8.6-8.8

d. Coenzymes and cofactors

NAD^+ (nicotinamide adenine dinucleotide) (Sigma), 100 mM
NADH (reduced nicotinamide adenine dinucleotide) (Sigma), 50 mM
$NADP^+$ (nicotinamide adenine dinucleotide phosphate) (Sigma), 10 mM
Albumin (5% bovine plasma)
Adenosine diphosphate, 50 mM
Adenosine triphosphate, 100 mM
Imidazole 0.2M, pH 7.0
Phosphoenolpyruvate, 100 mM
$MgCl_2$, 100 mM
$MnCl_2$, 1M
$MgSO_4$, 1M
KCL, 1M

e. Inhibitors

EDTA (ethylenediaminetetraacetic acid), 100 mM
Arsenate(sodium salt), 0.4 M
Mercaptoethanol, 1M

f. Fluorescence reagents

Carbonate buffer, 0.1M, pH 10.5
NaOH, 6.6N
HCL, 1N, 2N, 6N

VII. Statistical analyses

The raw data of the enzyme assay studies, corrected and converted to yield information in terms of moles/kg/hr, were subjected to analysis of variance considering population (i.e. the animal from which a biopsy specimen was

taken), time of menstrual cycle, and repetitions (i.e. determinations done under the same conditions). When significant differences were demonstrated, student's t-test was used to more exactly define the significance. The student's t-test was also used to determine the significance of differences within the glucose metabolism studies.

CHAPTER THREE. OBSERVATIONS AND RESULTS

I. Morphologic studies of the vagina

A. Epithelium

1. Gross morphology

a. Perineum and vulva

Macroscopic examinations of the rhesus vaginal tract provided the background against which the metabolic, histological, and quantitative biochemical studies could be contrasted.

The perineal skin of the adult female rhesus with normally functioning ovaries was always red; the intensity varied with age. The perineum of the younger adults grew progressively more flushed throughout the cycle and blanched periodically. I was not able to correlate blanching with impending menstruation as Corner suggested (44). The "sex skin" of the older adults remained a brilliant red throughout the cycle; the hue of the aged animals was dull when compared to that of the maximally flushed young. The color of the aged adult skin suggests that the vascular spaces lie deeper than those producing the more brilliant red; this point will be discussed in the section on microscopic anatomy.

The sex skin had a sparse but definite population of terminal (large) hairs and a larger number of short, fine vellus hairs.

There was no special structure at the vaginal orifice and no swelling to suggest the presence of a labium major; more importantly, the skin within 4 cm. of the orifice did not have the appearance of labia majora seen in other higher subhuman primates, e.g. the chimpanzee (62). The skin about the orifice was rather planar and made a sharp angle with the opening. The inner aspect of the vaginal orifice was glabrous, an observation borne out by later histological study. The hairs about the rima were all vellus(Fig. 3); the relationship between these hairs and the presence or absence of labia minora will be discussed in Chapter IV.

Figure 3. Split preparation to demonstrate vellus hairs at the edge of the vaginal orifice.

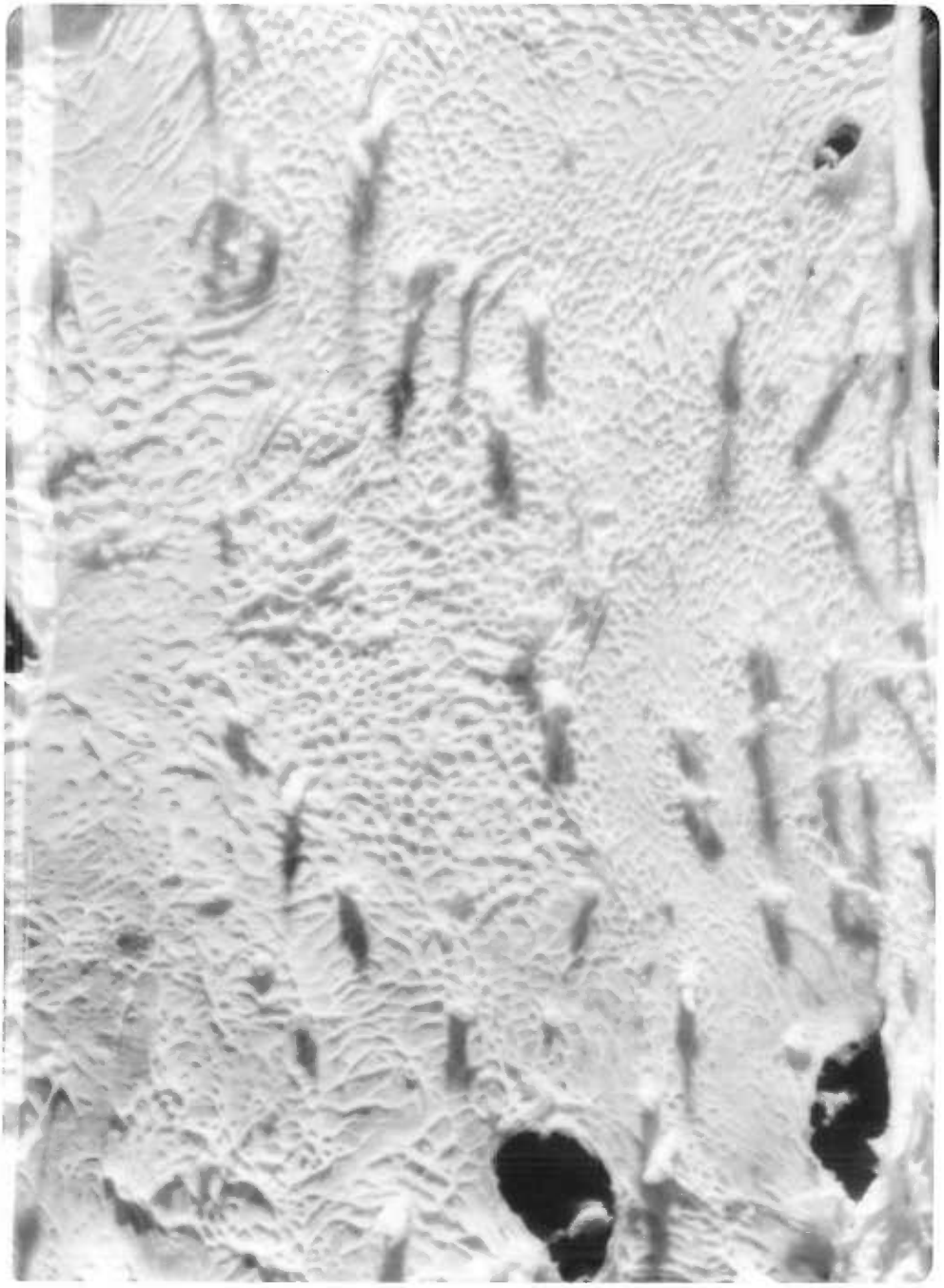

b. Vaginal wall

The smooth outer 1-2 cm. of the vaginal tract has been termed the vestibule, even though the average diameter is so narrow that the smooth epithelium is the only feature to distinguish the region from the vagina proper. The urethra opened into the anterior aspect of this portion of the tract.

The clitoris was prominent in the anteriormost part of the vestibule. The rhesus clitoris, like that of the chimpanzee, probably is not larger than that of women, but because of its reduced prepuce and frenula merely appears so.

A series of irregular longitudinal (parallel to the axis of the vagina) folds extending from the vestibule to the fornix appeared in greater or lesser numbers around the entire parietal circumference. The anterior and posterior rugae were always more definitely delineated; ridges of hillocks and rather deep valleys caused their irregularity. The surfaces of the hillocks were covered with, or thrown into, myriad acuminate processes projecting like teeth into the lumen and directed somewhat toward the cervical orifice. In the fornical half of the vagina, the folds spread until the valleys between were not well defined. Since the height of the combs of teeth was maintained in that region, the folds could not be said to have

flattened. The keratinized teeth are rather sharp to the touch, yet bend with pressure (Figs. 4 and 5).

Keratinized teeth lined the vaginal wall only in the female rhesus with functioning ovaries. Prepuberal, senile, and castrate animals had smooth vaginal epithelia from the vestibule to the cervix (Table II).

Figure 4. Surface view of keratinized teeth arranged in rows midway along length of vagina

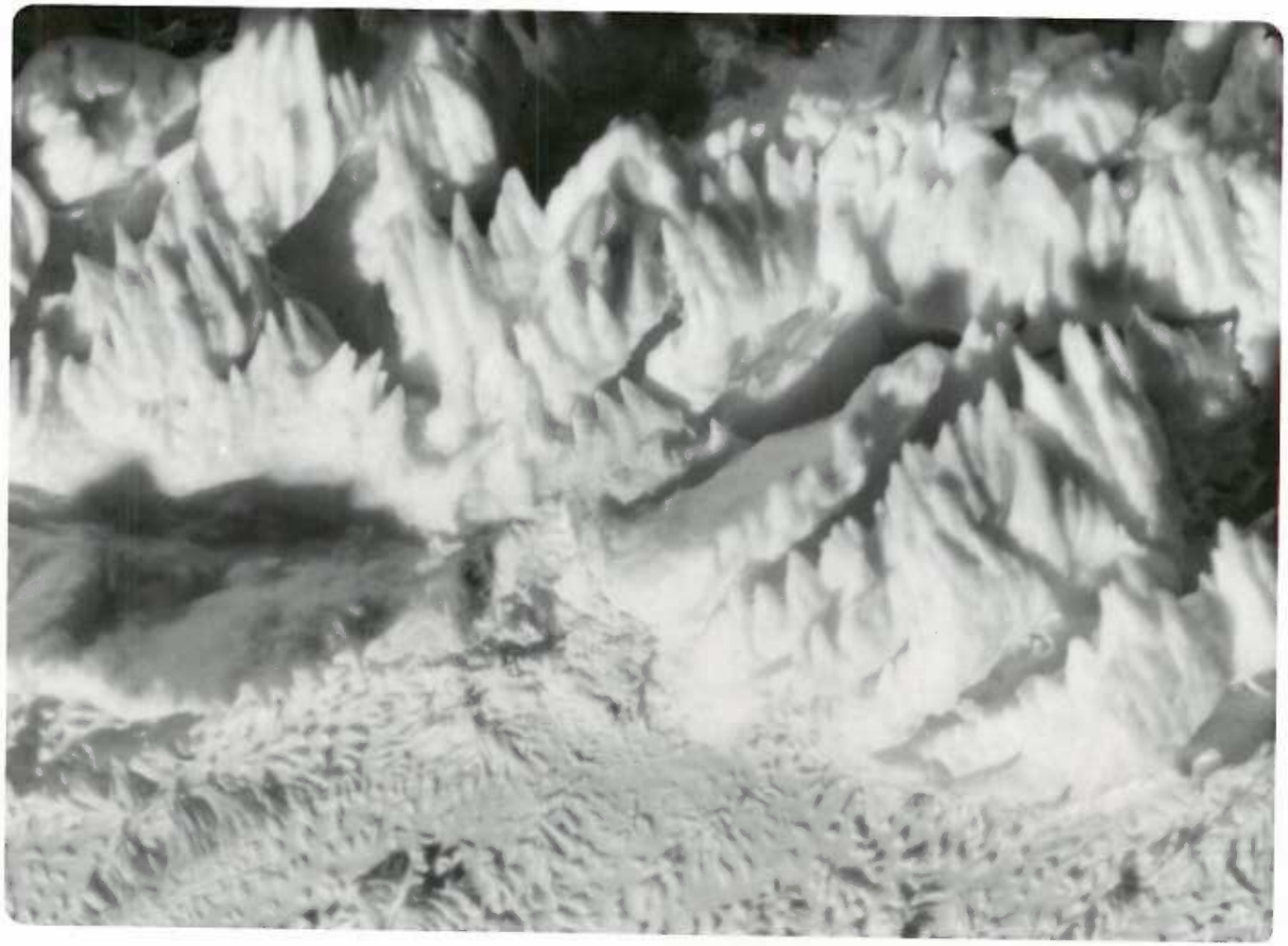

Figure 5. Cross-sectional view of keratinized teeth. Stained for elastic fibers with acid Orcein-Verhoeff. Initial magnification 44 x.

Table II. Topography of vaginal lining

ORPRC I.D. No.	Toothed	Smooth	Ovaries	Age
305-216	0	X	no	Adult
305-210	X	X	X	Adult
305-2300	X		X(one)	Adult
305-3585	X		X	Adult
305-3598	X		X	Adult
305-3587	X		X	Adult
305-0086	X		X	Adult
305-0664	X		X	Adult
305-2074	X		X	Adult
305-2259	X		X	Adult
305-0098	X		X(one)	Adult
305-4283	O		X	1 yr.
305-5034	O		X	80 day
305-2089	X		X	Adult
305-254	O		X	Senile?
305-3115	O	X	no	Adult
305-3584	O	X	no	Adult
305-411	X		X	Adult
305-87			X	Adult
305-233	O	X (vestibule)	X	Adult
305-106	O	X	X	Senile

c. Fornix and cervix

The usually smooth epithelium of the fornix was less smooth than that of the vestibule, for low folds frequently passed through it from the vaginal wall to and over the pars vaginalis of the cervix (Fig. 6). Sometimes the fornix looked like a fold circumscribing the cervix. Such a presentation may have been a reflection of parity.

The cervix protruded as much as a centimeter into the vaginal lumen at a very slight angle to the axis of the vagina. It appeared like a firm, even solid, button with pucker folds radiating from the center (the os cervix). The level of the os lay about even with the uppermost limit of the toothed portion of the vaginal wall. The fornical side of the cervix gave the impression of greater resilience than the inner aspect of the cervical canal. Cervical mucus filled the canal, exuded from the ox cervix, and was usually found over the surface of the vaginal wall. The average length of the vagina was 3.7 cm. to the os cervix and 4.5 cm. to the limit of the posterior fornix, which was usually 0.5 cm. deeper than the anterior.

2. Microscopic anatomy

a. Undersculpturing

In the female rhesus with adequately functional ovaries, the undersculpturing of the vaginal epithelium

(epithelio-stromal interdigitation) is very complex, consisting of major ridges encompassing many finer ridges to produce the cribriform (irregular honeycomb) appearance of the epithelial sheet and the rachitic profile of the cross section under the microscope. The undersculpturing of the epithelium of the vagina, cervix, vestibule, and fornix is so variably complex that the region of the tract can be identified from an inspection of the undersculpturing or its mirror image on the stromal side of the split epithelio-stromal junction (Figs. 7, 8, and 9).

The deep furrows in the surface of the vaginal wall between the major folds and plicae of keratinized teeth appeared on the undersurface of the epithelium as rather less sculptured ridges. Nevertheless, the ridges are undersculptured to a greater degree than that seen in any other area of complex dermoepidermal interaction. Between the ridges, myriad long, funnel-shaped infundibulae were arranged as a larger pocket (Figs. 10 and 11) so that the transverse section gave the appearance of a rachitic berry (Figs. 5, 12 and 13). The large pocket represented the undersurface of a keratinized tooth; smaller ridges delineated one keratinized tooth from another in the comb series. The epitheliostromal junction will be discussed further in the section on the lamina propria.

Figure 6. Split preparation of cervical epithelium (pars vaginalis). Folds are evident on the underside of the epithelium as well as on the surface where they appear as furrows.

Figure 7. Epithelial undersurface from parietal surface near vestibule

Figure 8. Split preparation of vaginal epithelium demonstrating undersurface

Figure 9. Stromal surface of split preparation. Many delicate papillae have coalesced in the dehydration and clearing process.

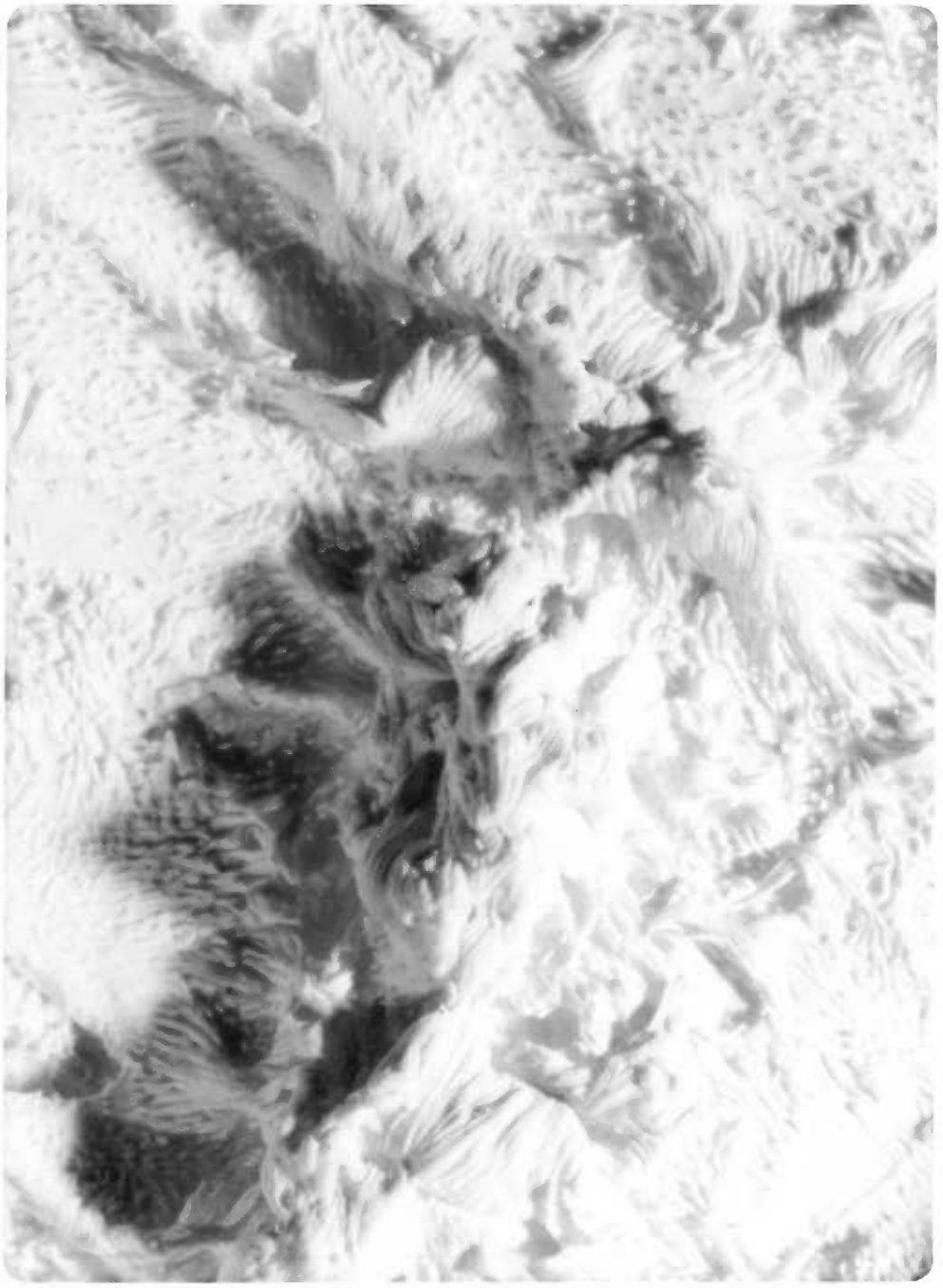

Figure 10. Closer view of underside of vaginal epithelium. High ridges represent deep furrows in surface. Minor ridges circumscribe long infundibula.

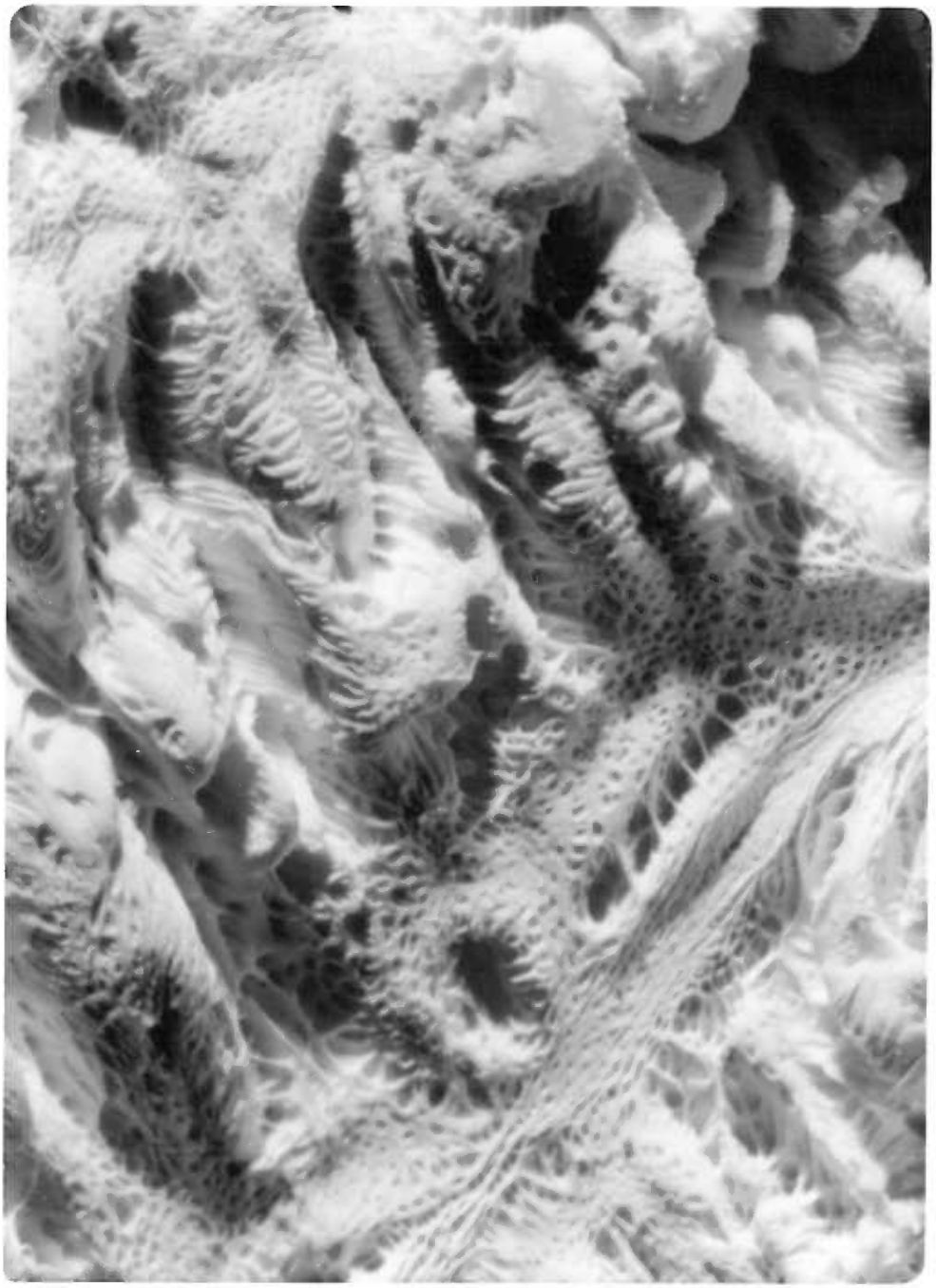

Figure 11. Pockets in the undersurface of the vaginal epithelium are composed of many infundibula.

Figure 12. Cross section of keratinized tooth demonstrating subdivisions of stromal papilla. Stained with toluidine blue. Initial magnification: 162.5 x.

b. General cellular morphology

Topographic variation in the vaginal wall was accompanied by some changes in the conformation of epithelial cells. Basal cells in regions of smooth epithelium (fornix, vestibule, and furrows of the vaginal wall) were generally cuboidal, 5 to 6 μ in diameter, arranged in a monolayer over the torose epitheliostromal interface. By contrast, the basal cells of the highly contorted epithelium of the vaginal wall ranged from cuboidal (6 to 13 μ diam.) to columnar (3 to 6 x 16 to 19 μ).

While the stroma was rather heavily infiltrated with leukocytes, the epithelium was generally free of them. An occasional neutrophil or eosinophil could be seen in the malpighian layers.

Spinous cells of the malpighian layers varied even more, from hexagonal cells of 10 to 20 μ diameter to horizontally oriented spindles of 10 x 20-30 μ . There were occasional areas of vertically oriented malpighian cells, but a horizontal mode was more usual. Large, distinct, basophilic nuclei were usual in the malpighian cells; so too were perinuclear clear spaces. Cells with apparently void cytoplasm and shrunken, heavily pyknotic nuclei occurred with varying frequency in the malpighian and corneal layers. Those cells resembled the "clear

cells" of epidermis over the general body surface (133), but occurred with greater frequency in the vaginal epithelium of the rhesus. Nonpyknotic nuclei (the majority) were found in the malpighian layers as far out as a level subjacent to the distinctly compact corneal layers, which would correspond to the granular layer of surface epidermis.

A PAS-positive material remained between the epithelial cells after diastase digestion, which was present in more and more intensely staining amounts from the basal layer to the corno-malpighian junction, where the heaviest concentration of PAS-positive-diastase-resistant granules, both intracellular and intercellular, occurred. Nearer the surface, the amount of PAS-positive material, though reduced , was greater than that before the junction and justifies the term"granular layer" or "stratum granulosum" to describe the zone of keratinization in the vaginal epithelium of the rhesus monkey.

The upper layers of the stratum malpighi exhibited some reduction of cell volume. Extreme compression in the lowest corneal layers usually made the junction between the strata malpighi and the corneum very distinct; no other epithelial cells were so compact. The juxtaposition of the upper malpighian and lower corneal layers constituted a transitional zone.

Once past the transitional zone, most of the nuclei lost the deep basophilia and shrank from an average diameter of 7 μ to one of 3 μ . The perinuclear clear space of the cells in the corneal layers, including those adjacent to the cornomalpighian junction, was normally much less obvious than that of the cells in the subjacent malpighian layers. The cells themselves had been "compressed" vertically so the vertical dimension was 1/3 to 1/2 that of the spinous cells adjacent to the junction. Although the compression would seem to have concentrated the cytoplasm of the keratinizing cells, in fact, they frequently appeared to have less cell substance than the neighboring spinous cells.

The process of vertical shrinking may have begun in the upper half of the stratum malpighi. The nuclear phenomena were such that corneal cells frequently appeared to have no nucleus. Beyond the granular layer the intracellular space increased, so that the vertical dimension changed from 1 to 3 μ in the stratum granulosum to 3 to 15 μ in the corneum. Not all the cells reenlarged; as many as 50 to 60% remained 1 to 2 μ at the widest vertical dimension. The unswollen cells apparently became the surface cells, for the surface was usually composed of two or three thin layers of compact cells. Presumably the swollen cells could not brook the surface tension of the dynamic epithelium, so were broken apart or quickly

sloughed from the surface. The valleys between the keratinized teeth were filled with just such sloughed keratinocytes during the middle of the menstrual cycle.

The number of pyknotic nuclei in the corneal layers, like that in the lowest malpighian layers, varied. Greater numbers of pyknotic nuclei appeared in the epithelium of specimens taken during menses; they were distributed more densely over the apex of a keratinized tooth, often forming a vertical band from the peak of the malpighian layer to the peak of the corneal layer.

c. Cyclic changes

1) Early (day 1 to 5)

Basal cells were relatively uniform in a monolayer. They were usually 5 μ in diameter (3 to 9 μ range), although by day 5 there were some columnar basal cells of 3 to 6 x 15 to 20 μ.

Cells of the malpighian layer were very distinct, their desmosomal connections being easily visible. Clear cells with pyknotic nuclei occurred in moderate to high numbers but were usually limited to the basal, lower third of the malpighian, and corneal layers. Spinous cells were usually 7.5 μ in diameter, but ranged in size from 7 x 16 to 10 x 22 μ.

The luminal surface of the stratum corneum is formed

of very loose nucleated squames. Some of the corneal cells were rather large (25 x 50 μ) but most were smaller. The stratum itself ranged in thickness from 30 μ to 90 μ. By day 5 some areas of the stratum corneum had reached 200 to 300 μ in thickness and some loculae between cells were 15 to 25 μ thick.

Most of the epithelial layers were highly compact. The thickness of the entire epithelium ranged from 25 to 50 cells and 100 to 500 μ. Greater thickness (400 to 600 μ) was attained by day 5.

2) Middle (day 7 to 15)

The conformation of basal cells was much less uniform than earlier, frequently appearing columnar and ranging from 10 μ in diameter to 5 to 6 x 10 to 16 μ. Cells were tallest over the peak of a dermal papilla.

Ten to 25% of the spinous cells had definite, large perinuclear clear spaces and were especially noticeable in the transitional zone where a "lacy" appearance was evidenced. The orientation of the malpighian cells was generally horizontal, but a vertical orientation was not rare. Cell dimensions were 6 to 12 μ x 25 to 35 μ.

Cells with pyknotic nuclei were limited to the outer corneum and the lower fourth of the malpighian layers. By comparison with the early period, they were rare.

During this part of the cycle, a few (but very few) neutrophils and eosinophils could be identified in the epithelium.

The stratum corneum during the ovulatory phases of the cycle was very thick (130 to 250 μ in some places; 12 to 18 μ in others). The layers were not very compact, yet the cells were flattened and attenuated; the outermost layer was obviously friable and splitting off. Large separations between cells and layers produced 20 to 50 μ spaces. A build-up of sloughed cells and cellular debris was found in the "valleys" between the very sharp peaks of keratinized teeth. The corneal layers over the sides and apex of such teeth were very compact.

The whole epithelium varied in thickness from 350 to 500 μ (25 to 50 cells) to 950 to 1450 μ (ca. 120 cells) in the most highly developed areas(toothed parts of the wall) to 150 to 250 μ (20 to 25 cells) and 550 to 900 μ (50 to 70 cells) in the less well-developed regions (the sulci between hillocks and folds). The rete ridges, spurs of epithelium extending into the stroma, did not vary in length (50 to 400 μ) with the menstrual cycle nor was there any variation in the numbers of ridges of any given length.

3) Late (days 17 to 25)

Basal cells were a relatively uniform cuboidal to columnar shape, 4 x 10 to 15 μ. More columnar cells appeared over the apex of a dermal papilla.

The stratum malpighi was much thinner in the luteal phase than in the early follicular phase of the cycle. Spinous cells were larger than basal cells, averaging 10 x 10 to 20 μ and becoming 3 x 25 μ higher up. Malpighian cells had a horizontal orientation at a lower level (closer to the basal layer) than those seen in specimens taken earlier in the cycle. Two or three hematocytes could be observed in a 2 cm. section of the wall.

Sloughing at the surface of the stratum corneum was more definite; the layers of the corneum were separated. Corneal thickness was relatively great, 250 to 330 μ in the valleys and about 350 μ at the peaks of keratinized teeth. There were many cells with pyknotic nuclei in the corneal layers but few in the lower malpighian strata.

The entire epithelium ranged from 550 to 650 μ (70 to 90 cells) in the thickest areas to 250 to 400 μ (45 to 80 cells).

B. Lamina propria

1. Microscopic anatomy

Judging from the paucity of bundles or cut ends, the adjacent subepithelial connective tissue was a relatively

homogeneous aggregation of short fibers, small vessels, and fine nerves. The upper layer of the stratum papillare of the stroma was three to six micra deep and free of cells; the basal lamina probably occupied much of that space. The stratum papillare is named for its relationship with the epithelium which seems to penetrate the stroma as many spurs (or rather, ridges, as has been shown by the split preparations), forming stromal papillae. Fine elastic fibers penetrated the basal lamina to end on the surfaces of basal cells (Figs. 13 and 14). These fibers splay from the ends of larger elastic bundles like the arms of a hydroid, their endings often giving the appearance of tiny bulbs.

Deeper stromal elements were much larger. Collagen bundles were well developed and compact, permeated occasionally by vessels, strands of muscle, and nerve trunks.

The lower stratum papillare and the remainder of the propria were well infiltrated by leukocytes. More dense accumulations of leukocytes and fibroblasts often appeared at the center of the base of a keratinized tooth. A well-developed plexus of large vessels in the stratum reticulare (Fig. 15) fed and received branches of the plexus of fine vessels subjacent to the epithelium. Many large arterial channels entered the midstromal plexus. The longitudinal and circumvesting coats of smooth muscle were not so

Figure 13. Fine elastic fibers in a small stromal papilla. Acid Orcein-Verhoeff stain. Initial magnification: 375 x

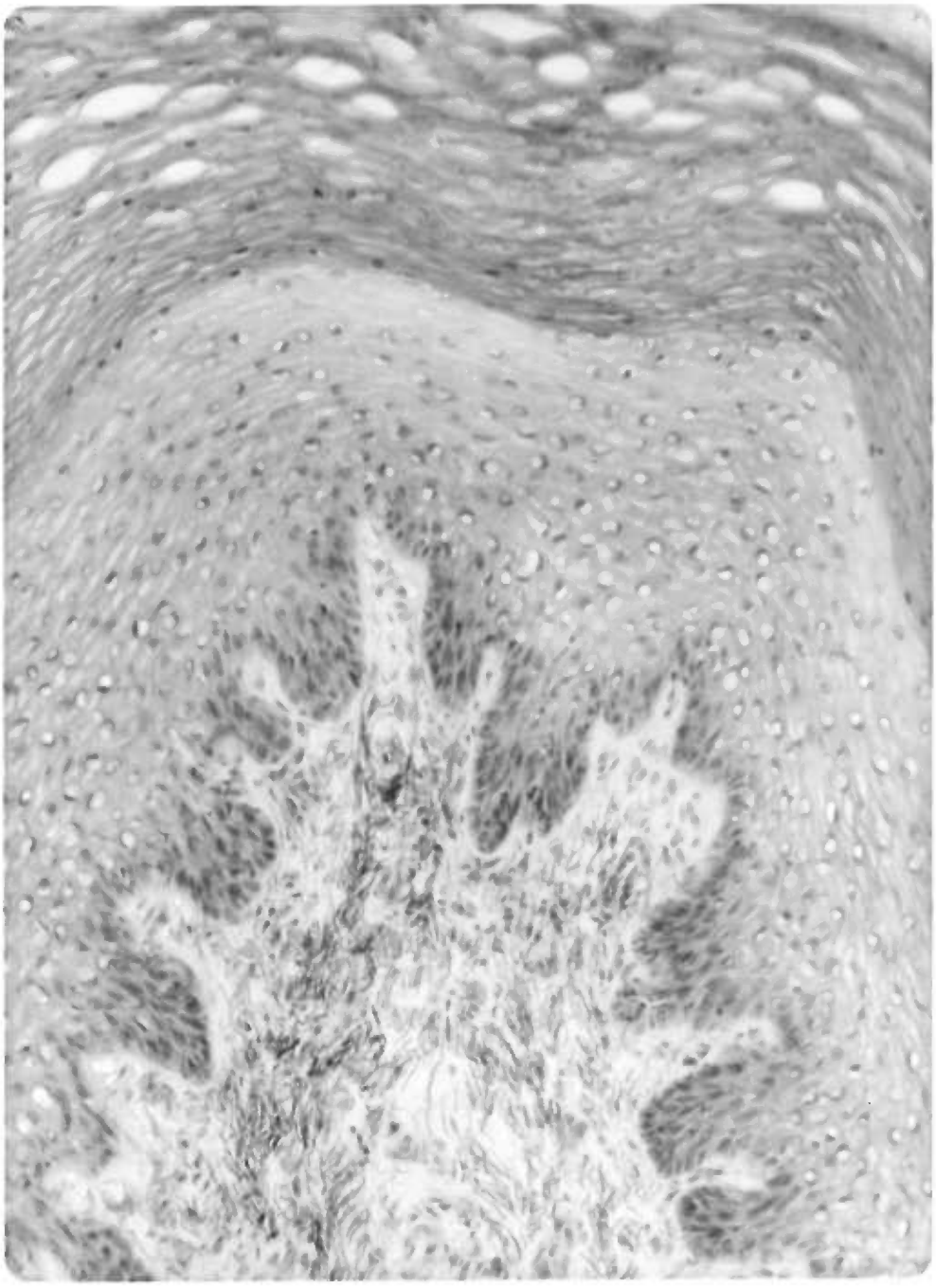

Figure 14. Fine elastic fiber attachments to basal epithelial cells. Acid Orcein-Verhoeff stain. Initial magnification: 375 x

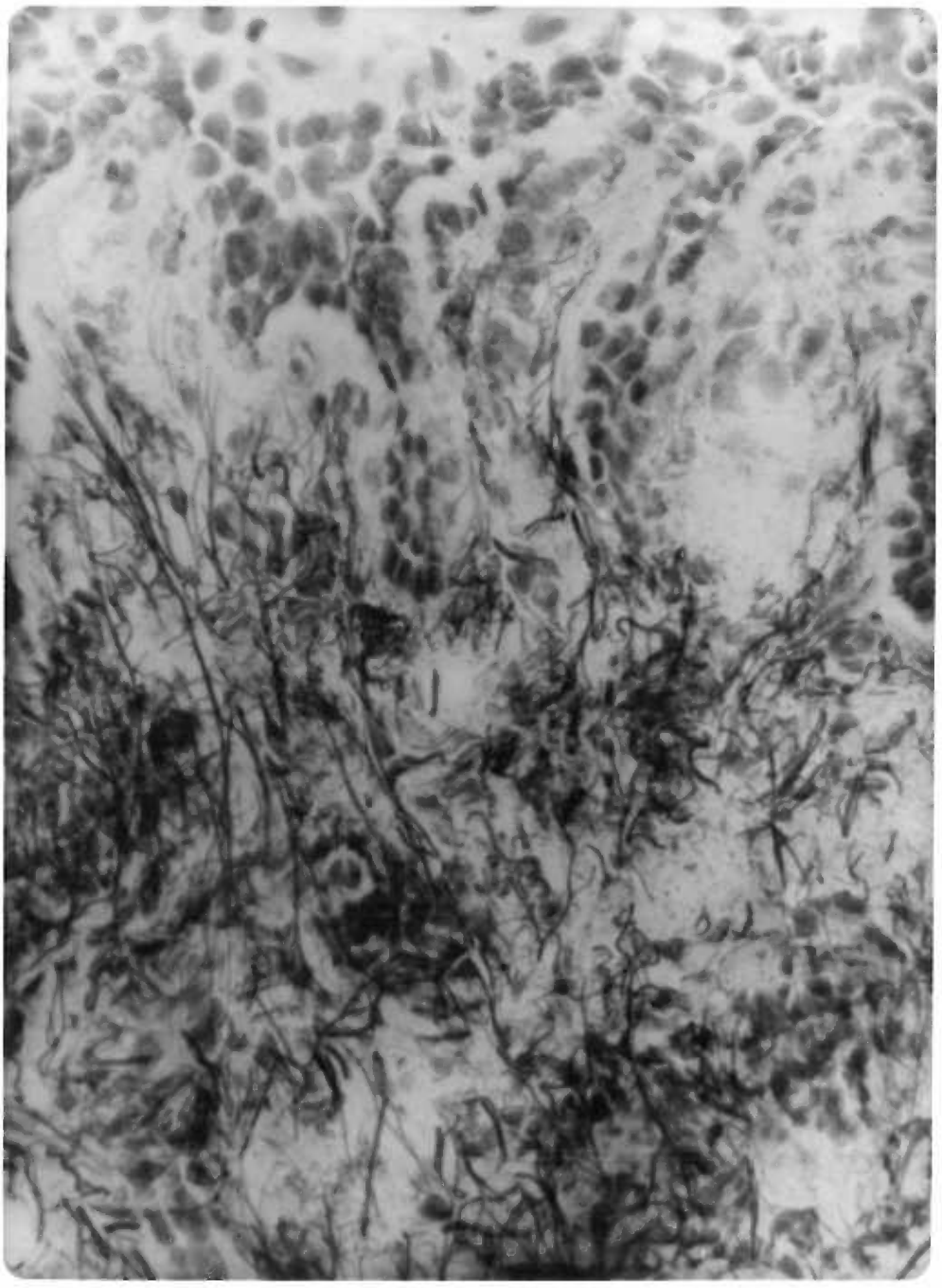

Figure 15. Vascular complement of vaginal wall. Alkaline phosphatase preparation. Initial magnification: 40 x

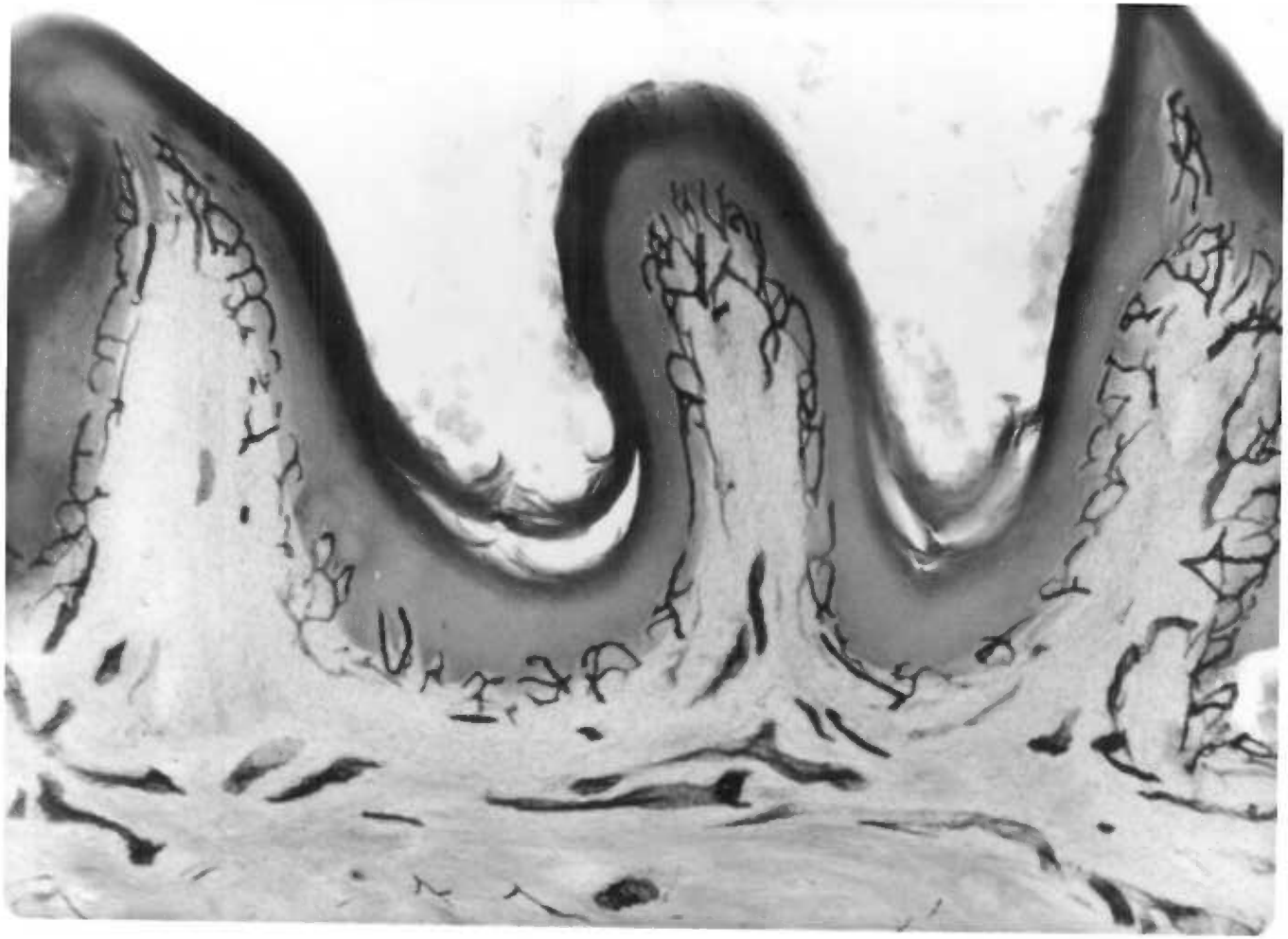

Figure 16. Subepithelial capillary plexus within an infundibulum of a keratinized tooth. Alkaline phosphatase preparation. Initial magnification: 157.25 x

extensive as those of the uterus or rectum, but they did invest most of the vaginal wall. Coursing through the deep proprial substance of the vulva were large elements of striated bulbocavernosus muscle. In the same region, slightly above the striated muscle, was a large, multilobed sebaceous gland emptying via a well-developed sinoid duct into the vestibule. Two layers of cuboidal cells constituted the walls of the duct, which opened onto the surface of the vestibule through a funnel-shaped infundibulum. The sebaceous complex at this level corresponds to the glands of Bartholin. Fatty spaces of the spongiosa between the muscle and the sebaceous glands extended only a short way up into the stroma along the vaginal wall from the vulva and vestibule, so that there was no spongiosa around most of the vagina. Connective tissue in the wall was found among and beyond the smooth muscles to complete the parietal capsule.

The vascular complement of the vaginal wall, like that of skin, was best developed in the stroma around various structures and in the upper stroma just below the basal layer of epithelium. The elaborate subepithelial plexus resembled the subepidermal plexuses of such specialized areas as the glabrous lip, the palm, or the sole. The elaboration of vessels was most complex in those regions of the wall that have complex epithelial formations.

As can be seen in Figure 16, the capillary plexuses proliferated into all the infundibula of the keratinized teeth.

Fine nerves and nerve endings also formed a plexus in the stroma directly below the epithelium (Figs. 17 and 18). The plexus was fed by nerves from large trunks deeper in the stroma. The muscles of the vaginal stroma were heavily invested with both fine and large nerves. Blood vessels and vascular spaces, especially those in the vulva and lower vestibule, were also replete with nerves around their capsules and thus provided evidence for the erectile nature of these tissues. Subepithelial nerve endings in the vagina were interesting for their regional variation as well as for their structure.

Observation of the finest nerves was facilitated by the superimposition of silver granules on the sulfide crystals of the cholinesterase reaction (152). Much of the nervous complement of the vaginal wall could not be visualized with the silver technique alone. The nonspecific (butyryl) cholinesterase reactivity of the parietal nerves was consistently better than that of acetylcholinesterase. Subepithelial nerve endings in the wall were best developed in the regions of greatest epithelial elaboration; indeed, the endings within a keratinized tooth were more complex than most others (Figs. 19 and 20).

The nerve endings of the sulci and furrows between the combs of teeth and folds were greatly reduced compared with those of the keratinized teeth. The glomar conformation of the fine endings was also found in the clitoris. The exact conformation of the endings is highly variable, but those of the clitoris were often larger and even more complex. The stroma of the clitoris and adjacent tissues was literally filled with nerves, forming a mesh in those erectile tissues. Those nerves and the nerves of the parietal stroma had a rather wavy appearance like that of collagen bundles.

Small, dendritic, argyrophilic cells appeared in the basal epithelial and subepithelial layers of the vaginal wall and vestibule close to the fine nerves.

Observable particularly in the immature rhesus were vater-pacini pressure receptors in the adventitial connections ventral to the clitoris, between that structure and supporting structures and between the clitoris and the vagina. Sebaceous follicles in adjacent vulvar regions displayed obvious hair follicle end organs. Subepithelial endings in the fornix were sparse and not at all complex. Much of the vaginal nerve supply came via the perineal branch of the pudendal nerve; other sources were the hypogastric and uterine nerves. There were no serosae about the vagina, except where the rectovaginal pouch came close to the posterior fornix.

Figure 17. Fine nerves and nerve endings beneath the epithelium of the vaginal wall. Silver-enhanced butyrylcholinesterase preparation. Initial magnification: 125 x

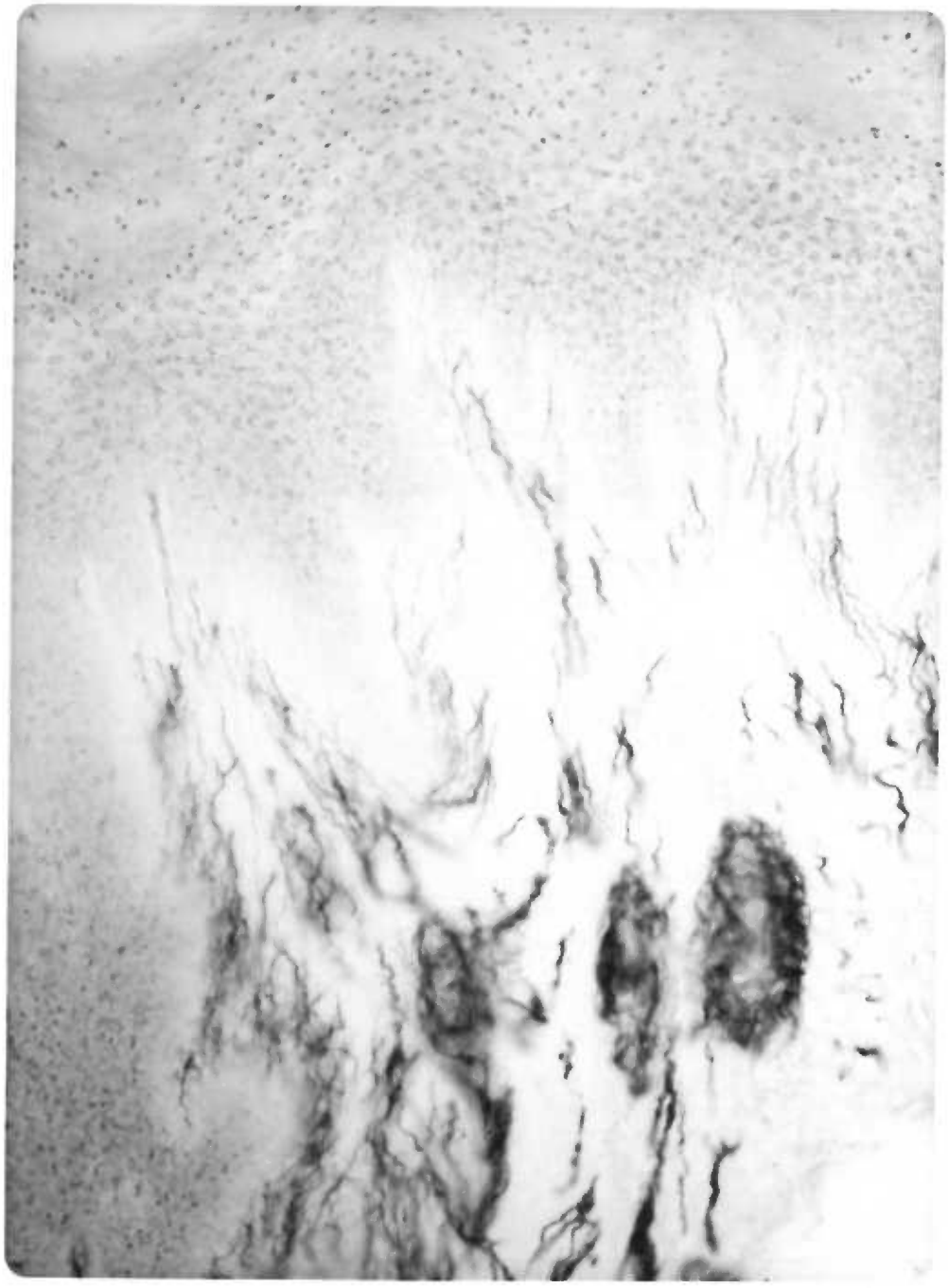

Figure 18. Fine nerves and nerve endings subjacent to the epithelium of a furrow in the wall. Silver-enhanced butyrylcholinesterase preparation. Initial magnification: 187.5 x

Figure 19. Fine nerve endings in a cross section of the wall. Silver-enhanced butyryl-cholinesterase preparation. Initial magnification: 240 x

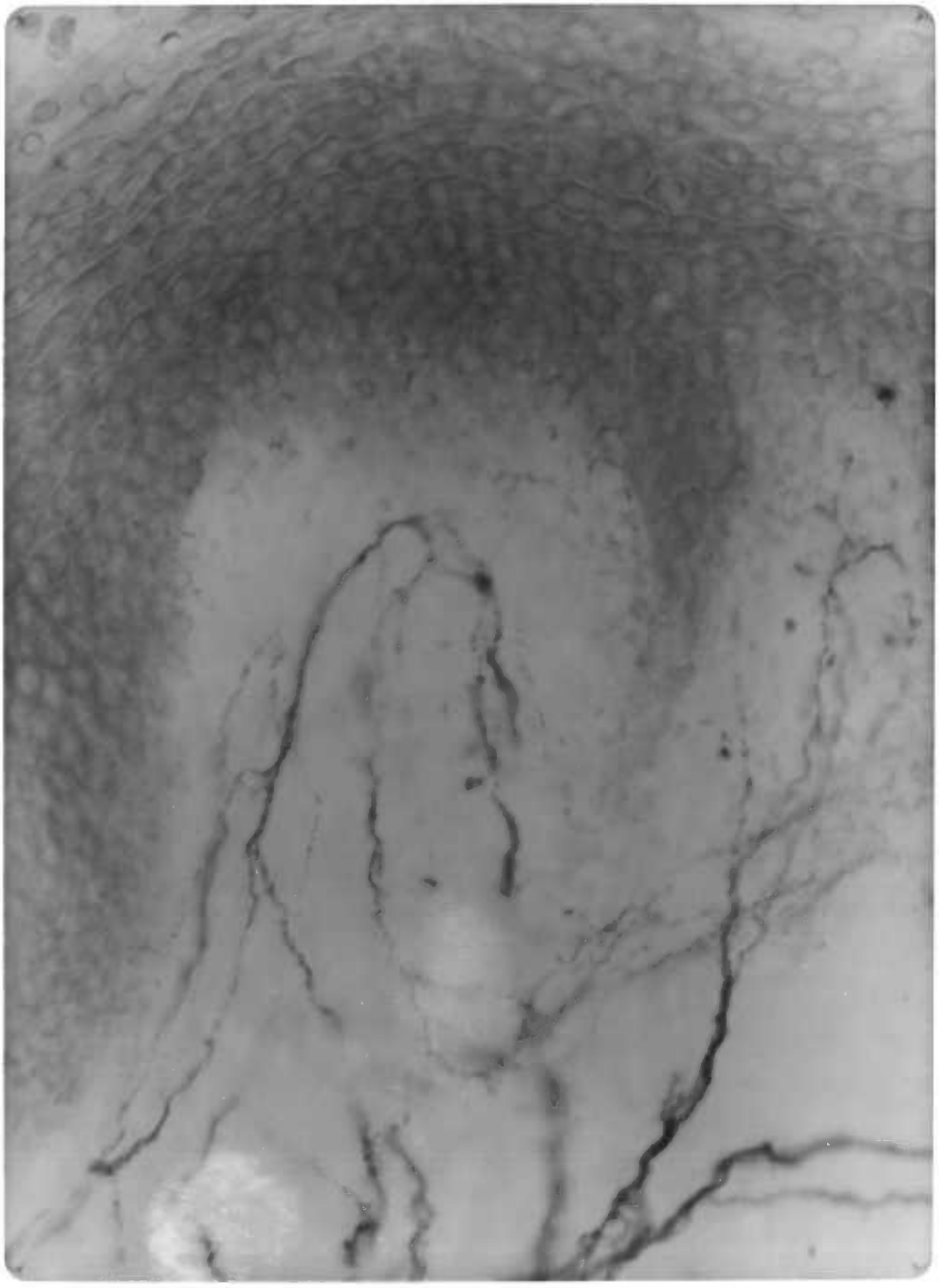

Figure 20. Nerve ending within a keratinized tooth. Silver-enhanced butyryl-cholinesterase preparation. Initial magnification: 600 x

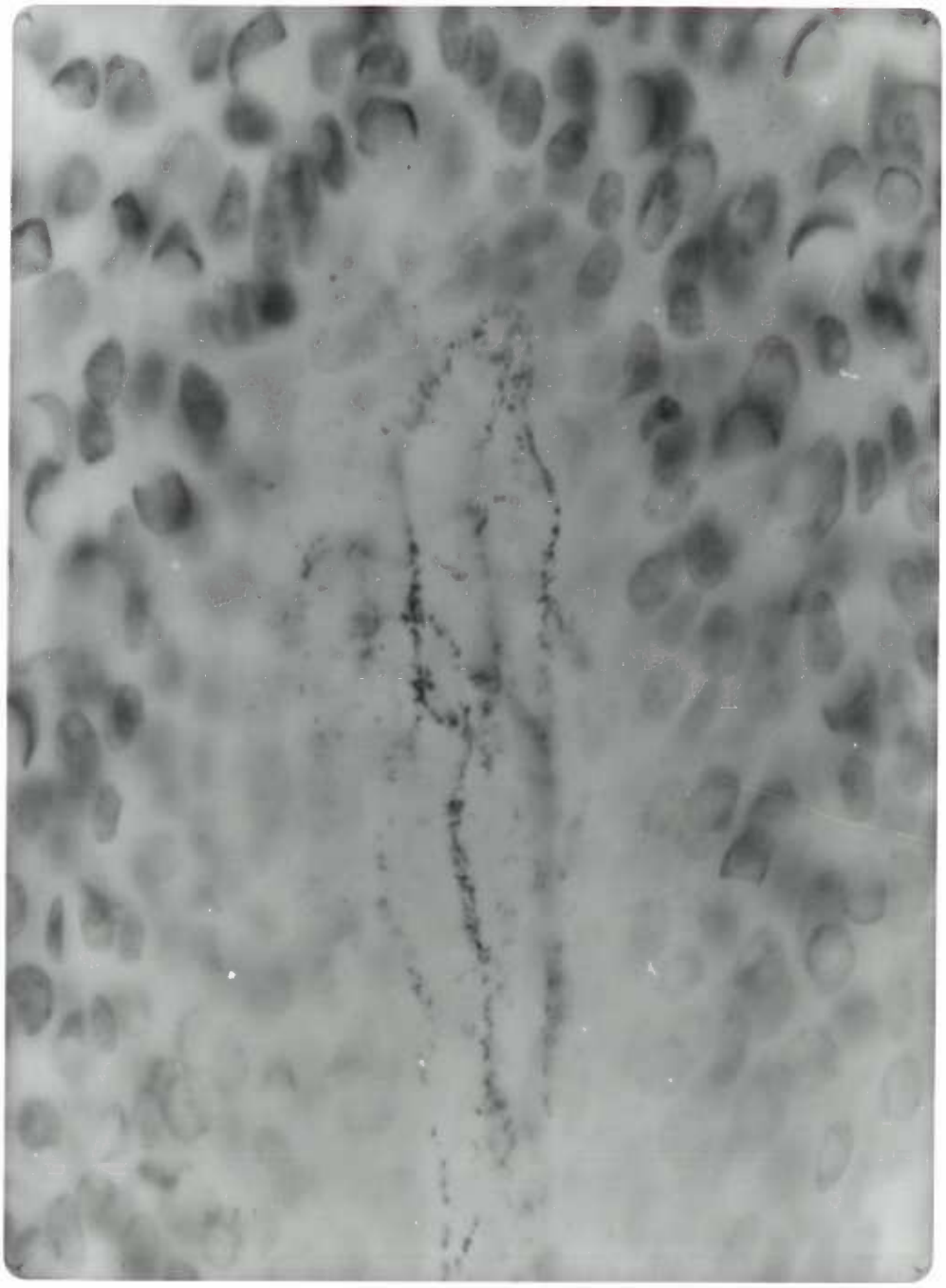

II. Metabolic studies of the vagina

A. Glucose metabolism

Preliminary studies of glucose metabolism were performed with radioactive glucose labeled in three different ways: uniformly labeled; labeled in the 1-position; and labeled in the 6-position. The results of these studies provided information about the predominant pathways of metabolism and the general pattern of energy exchange. The conclusions, based on the metabolic studies, led to histochemical and quantitative microchemical analysis of some key enzymes of those more prominent pathways. The information derived from studies with ^{14}C-1 and -6-glucose was used to assess the contribution of the hexose-monophosphate shunt to the utilization of glucose in the vagina.

The mean specific yields from ^{14}C-glucose in the normal rhesus vagina are given in Table III. The absolute yields in Tables VII and VIII will be discussed after examination of the specific yields as they relate to (1) pentose shunt contributions, (2) carbon balance, (3) energy balance, and (4) pyridine nucleotide balance. The ^{14}C-1- and ^{14}C-6-glucose results are useful in estimating the portion of exogenous glucose that is diverted to the pentose shunt. (The methods of estimation have been presented in the chapter on materials and methods.) Sample

calculations can be found in Appendix F. Based on ^{14}C-1- and ^{14}C-6-glucose metabolism, the pentose cycle accounted for 3.38% $\pm$ .291^{SE} of overall glycolysis. As can be seen in Table III, by far the greatest product of glucose metabolism in rhesus vaginal epithelium was lactic acid. This is also apparent in the consideration of carbon balance, (Table IV) based on the complete metabolism of 100 moles of glucose, where 568 of 600 available moles of carbon appear in lactic acid.

The primary reactions responsible for ATP production are those involving glyceraldehyde-3-phosphate dehydrogenase and pyruvate kinase, which together account for about 81%. The TCA cycle contribution is 15%, a relatively minor contribution, yet greater than that found in normal skin (97). The major ATP usage in carbohydrate metabolism occurs early in the Embden-Meyerhof pathway with the reactions of hexokinase and phosphofructokinase. The net energy gain is 291 moles of ATP $\pm$ 3.7^{SE} generated from 100 moles of glucose (Table IV).

The basic reducing agents for many metabolic reactions, including several along the glycolytic pathway, are NADH and NADPH, which are generated at the reaction of glyceraldehyde-3-phosphate dehydrogenase and the pentose shunt, respectively. Reduced nicotinamide adenine dinucleotide production (92%) far surpassed that of NADPH

(8%). The primary utilization of reduced pyridine nucleotides occurred with the formation of lactate, the primary reaction product of glycolysis in the rhesus vagina. The net formation of reducing equivalents was 27 moles of NADH and NADPH (Table VI).

The portion of exogenous radioactive glucose metabolized to lipid, glycogen, protein, and DNA accounted for less than 1% of the total radioactivity recovered. Nevertheless, these essentially preliminary metabolic studies indicate that there is a significant drop in the ^{14}C incorporation into lipid from the follicular phase (.5%) to the ovulatory phase (.1%).

The amount of carbon dioxide produced from uniformly labeled glucose (Table VII, Fig. 21) decreased from 17.72 x 10^4 μmole/kg/hr in the early part of the cycle (d 1 to 5) to 13.32 x 10^4 μmole/kg/hr in the middle of the cycle (d 1 to 15). The difference is significant at $p = .05$. A subsequent increase in the glucose to CO_2 rate from the middle to 18.212 x 10^4 μmole/kg/hr in the late part of the cycle is significant only near the $p = 0.1$ level. There is no significant difference between the mean rates of CO_2 production in the early and late periods.

A drop in the amount ^{14}C-U-glucose metabolized to lactate (Table VII, Fig 22) in the early cycle (15.47 x 10^5 μmole lactate/kg/hr) is even more highly significant ($p = .02$) than the decrease in the CO_2 study. The

increase in lactate production from the middle (10.3 x 10^5 µmole/kg/hr) to the late part of the cycle (15.313 x 10^5 µmole/kg/hr) is significant only at p = 0.1, but the t-value does approach that of the p = .05 level. The rates of lactate production in the early and late periods do not differ significantly.

Since the molecular weight of glycogen cannot be accurately determined, the rate of glycogen synthesis from glucose is usually expressed as the per cent incorporation based on the radioactive glucose recovered in the glycogen fraction. Alternatively glycogen is expressed as a per cent of CO_2 or lactate (Appendix F).

The increased rate of labeled glycogen production (Table VII, Fig. 23) from .133% in the middle to .22% in the late part of the cycle is significant at the p = 0.1 level. The early cycle PI of .18 is not significantly different from either the middle or the late cycle values.

Table III. Specific yield of products from labelled glucose

Label position	U		1		6	
		SE*		SE		SE
CO_2	4.8 %	± .2	9.9%	± .7	1.3%	± .16
Lactate	94.6%	± .2	89.5%	± .7	97.8%	± .4
Lipid	0.3%	± .05	.5% (Follicular) .1% (Ovulatory)		0.3%	± .04
Glycogen	0.2%	± .01	0.2%	± .03	0.4%	± .08
Protein/ DNA	0.3%	± .03	0.1%	± .01	0.5%	± .2

Values given as means of five determinations

*Standard error of the mean

Table IV. Carbon Balance

(Theoretical calculation based on 100 moles of glucose)

Moles of carbon incorporated from pool of 600

CO_2..... 28.6

Lactate... 567.5

Lipid..... 1.6

Glycogen.... 1.05

Protein/DNA. 1.55

N= 5

TableV. Balance of Energy Transformations

(Theoretical calculation based on 100 moles of glucose)

N = 5

	ATP formation from reaction of:	
Cytoplasmic	G-3-PDH.....	197
	Pyruvate kinase.....	197
Mitochondrial	TCA cycle.....	73.6
	Pyruvate decarboxylase	20.8
	Net ATP formation	488
	ATP utilization by reaction of:	
	Hexokinase.....	100
	Phosphofructokinase..	97
	Acetyl CoA carboxylase, etcetera.....	negligible
	Net ATP utilization	197
	Net energy gain	291

Table VI. Pyridine nucleotide balance (Theoretical calculation based on glycolysis of 100 moles of glucose; N = 5)

NADPH formation from:	
Pentose cycle.....	18.6
NADH from:	
G-3-PDH.....197	
Total reduced pyridine nucleotide.....	215.6
NADH, NADPH utilization in formation of:	
Fatty acid.....	negligible
Glycerol (from G3P)..	negligible
Lactate.....	189
Total utilization....	189
Net reducing equivalent formation.....	26.6

Table VII. ^{14}C-U-Glucose metabolism in menstrual cycle

(Time vs. rate of incorporation)

Cycle time	µmole x 10^4 CO_2/Kg/hr	µmole x 10^5 Lact./Kg/hr	Percent incorporation into Glycogen
	SE*	SE	SE
Early (d 1-5) N =15	17.72 ± 1.2	15.466 ± 1.4	0.18±0.03
Middle (d 7-15) N =35	13.32 ± 1.41	10.298 ± 1.56	0.133±0.025
Late (d 17-25) N = 30	18.212 ± 2.456	15.313 ± 2.52	0.218±0.05

SIGNIFICANCE:

	Early vs. Middle	Middle vs. Late
CO_2	p = .05	p = .1
Lactate	p = .02	p = .1
Glycogen	p > .1	p = .1

* Standard error of the mean

Table VIII. Metabolism of ^{14}C-U-, ^{14}C-1-, and ^{14}C-6-Glucose

(Label position vs. rate of incorporation)

	μmole x 10^4 CO_2/Kg/hr		μmole x 10^5 Lact./Kg/hr		Percent incorporation into Glycogen	
		SE*		SE		SE
^{14}C-U-Glucose N=75	13.32	±1.19	10.3	±1.38	0.13	±.03
^{14}C- 1-Glucose N=25	20.99	±6.8	12.81	±7.11	0.05	±.01
^{14}C-6-Glucose N=25	1.36	±.05	7.26	±2.64	0.08	±.03

*Standard error of the mean

All biopsies from mid-cycle

Figure 21. Mean values of ^{14}C-carbon dioxide determined from ^{14}C-glucose metabolism
N = 23

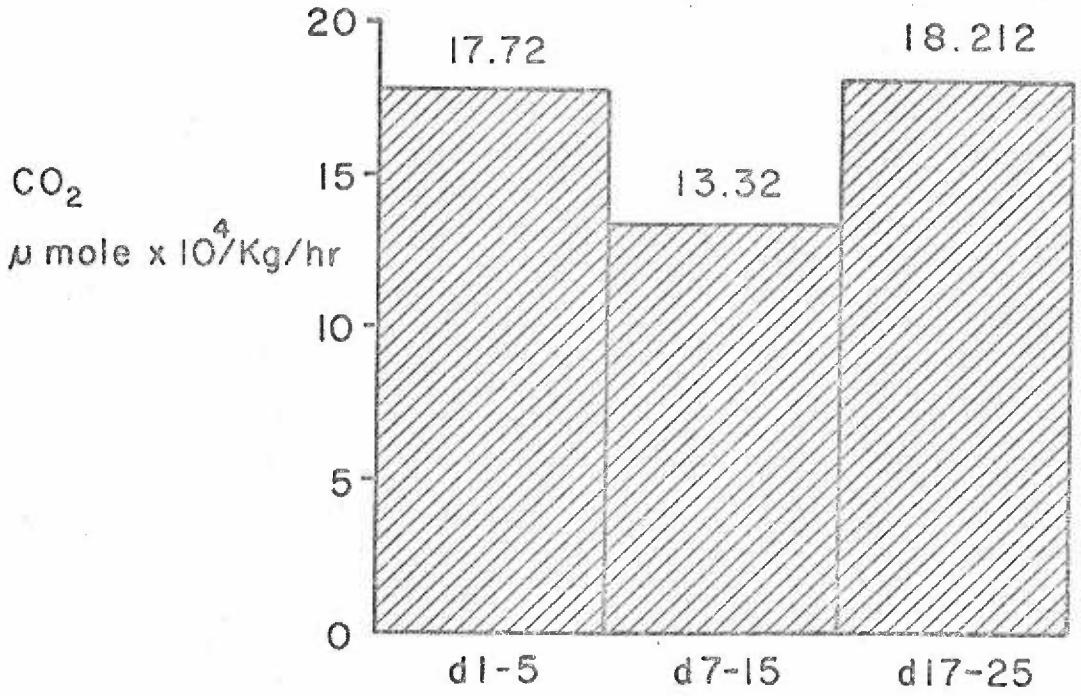

Fig 21 ^{14}Carbon Dioxide Recovered in Course of Cycle

Figure 22. Mean values of ^{14}C-lactate produced from ^{14}C-glucose metabolism

N = 23

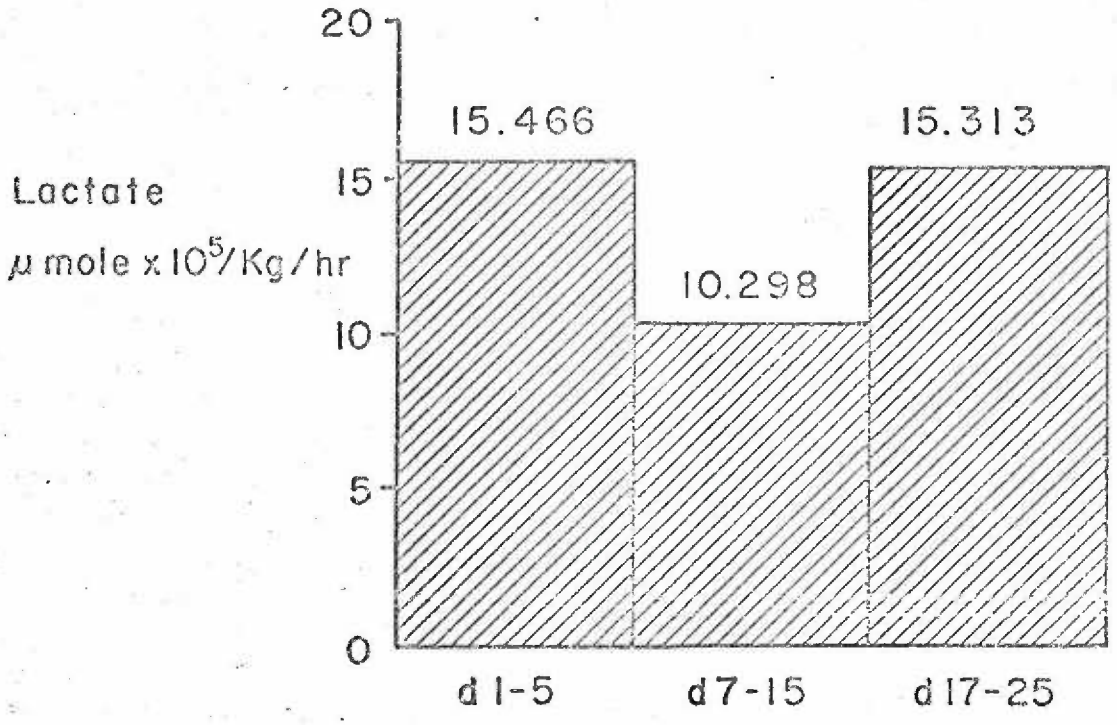

Fig 22 ^{14}C-Lactate Recovered in Course of Cycle

Figure 23. Mean values of ^{14}C-glycogen produced from ^{14}C-glucose metabolism

N = 23

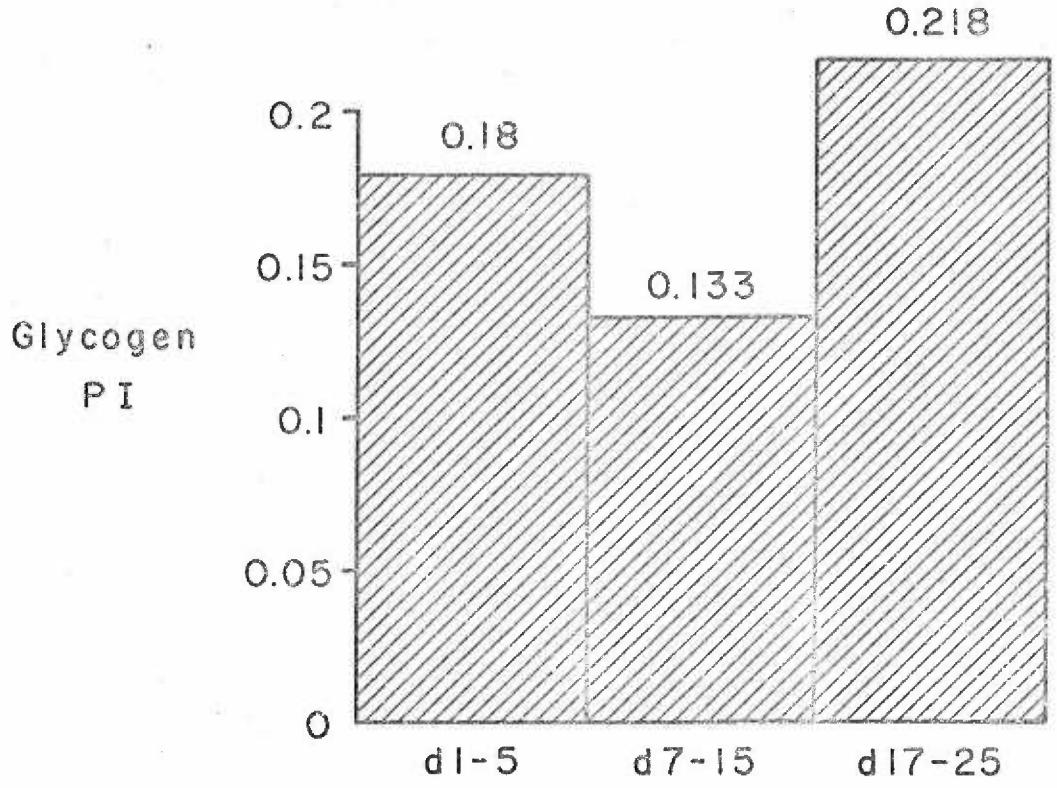

Fig 23 ^{14}C-Glycogen Recovered in Course of Cycle
PI = percent incorporation of available radioactive glucose

B. Histochemistry

To determine the location of enzymatic (and other histochemically demonstrable) changes within the vagina, sections of quick-frozen tissues were incubated with appropriate substrates and indicators for glycogen, metachromasia, phosphorylase, glucose-6-phosphate dehydrogenase, β-glucuronidase, leucine aminopeptidase, alkaline and acid phosphatase, acetyl- and butyrylcholinesterase.

Glycogen deposits, measured by the PAS reaction and diastase digestion in the vaginal epithelium and directly subjacent stroma, were maintained at relatively constant levels except in the stratum corneum. Early in the cycle (d 1 to 7), the corneum exhibited a heavy concentration of glycogen, which was decreased to a weak level through the middle of the cycle (d 11 to 17) and returned to a moderate-strong deposition by day 23. The intercellular spaces of the stratum corneum remained rather strongly PAS-positive after diastase digestion, whereas those of the malpighian layers were only weakly positive. Though the PAS-positive reaction between malpighian cells became more intense the closer the cells were to the stratum granulosum, the junction was immediately apparent by the extraordinary increase in staining reaction and cellular compression in the strata granulosum and corneum.

Metachromasia, associated with regularly polymeric

molecules in the vaginal lining stained with toluidine blue, underwent some characteristic changes in the course of the cycle. While metachromasia in the lamina propria maintained a relatively constant weak intensity, in the basal and malpighian layers it dropped from moderate or strong in the early follicular phase of the cycle (d 1 to 7) to weak through the middle of the cycle (d 10 to 20). Near the end of the cycle (d 25), metachromatic staining often increased slightly in the basal and malpighian layers. With rare exceptions, there was no metachromasia in the corneal layers, and even when there was, the metachromatic elements were rare.

The level of phosphorylase activity in the vaginal wall ranged from weak to very strong. The stroma was generally not reactive through most of the cycle; however, there was weak activity about mid-cycle (d 13 to 17) and weak to moderate activity in stromal fibroblasts throughout the cycle. In the basal and lower malpighian cells, the pattern of change in phosphorylase reaction product was the same, although the levels of intensity were different: a gradual decline from the first day of menstruation to day 11, after which the level was constant until the end of the cycle. In the basal layer, the decrease was from moderate to zero, that of the lower malpighian cells from strong and moderate to weak. The upper

malpighian cells exhibited a constant reaction intensity range of moderate to strong. Phosphorylase activity in the corneal layers was low (very weak) at the beginning and end of the cycle, but was relatively constant through the remainder of the cycle (d 3 to 23) at a weak to moderate intensity.

Generally no glucose-6-phosphate dehydrogenase activity could be demonstrated in the general stroma or stratum corneum. Stromal blood vessels and fibroblasts displayed a moderate to strong reaction product deposition for this enzyme, one of the gateways of the pentose shunt. Reactivity was relatively constant through the cycle for the epithelial layers, although there were indications of a drop in activity about day 15 to 20. The intensity of staining was different from one cell layer to the next. Within basal cells there was strong reaction next to the dermo-epidermal junction, especially in the vault over a dermal papilla; the rest was only weakly reactive. As the cell passed into the lower malpighian layer, the staining intensity increased to moderate. Still higher in the malpighian layers, G-6-PDH activity was strong. The most intense stain was deposited in the cells of the upper malpighian layers at the cornomalpighian junction, especially in the apex of a keratinized tooth.

The distributional intensity gradient of

β-glucuronidase was reversed from that of G-6-PDH, i.e. the strongest reaction occurred in the basal layer and decreased as the cells moved toward the surface. The upper malpighian and corneal layers exhibited weak or only trace reactivity. In the general stroma, there was no β-glucuronidase reaction product. Blood vessels and fibroblast cell surfaces displayed moderate to strong reactivity; stronger closer to the dermoepidermal junction. In all epithelial layers, enzyme activity increased through the middle of the cycle and decreased through menstruation.

Leucine aminopeptidase had a distribution of reaction product similar to that of β-glucuronidase. The stroma directly subjacent to the epithelium exhibited a general low level of activity. Blood vessels and fibroblasts in that region also had weak to moderate activity. Basal cells displayed moderate to strong LAP reactivity, but the reaction level gradually subsided in the malpighian layers until the corneal layers, where no reaction product could be found. No significant changes were observed through the menstrual cycle.

The greatest alkaline phosphatase activity was observed in the stromal blood vessels, especially the subepithelial capillaries. Little or no reaction was seen in the stroma, although several connective tissue elements

did exhibit a low-level surface reactivity. The intensity of vascular reaction product ranged from moderate to very strong and varied with the time course of the menstrual cycle; the variation occurred on the lower end of the range. That is to say, there were always very reactive vessels, but more of the previously moderately reactive larger vessels displayed strong reactions in the ovulatory stages of the cycle. Cyclic changes were not found in other structures. Weak alkaline phosphatase activity was observed irregularly throughout the basal and malpighian layers. A moderate level of reaction product was deposited rather uniformly in the stratum corneum at the cornomalpighian junction, decreasing in intensity toward the surface.

Except for some weak-to-moderate acid phosphatase activity in the lower malpighian cells, the subcorneal tissues had no acid phosphatase product deposition. The moderate and strong reactivity displayed by the stratum corneum at the cornomalpighian junction decreased in the direction of the vaginal lumen; reaction intensity was frequently greater in the "valleys" between keratinized teeth. Reaction levels were relatively constant throughout the menstrual cycle.

For the most part, cholinesterase activity was limited to subepithelial nerves. Some very weak activity was noted,

however, for both the acetyl- and butyrylcholinesterase reactions in the corneal layer at the cornomalpighian junction. Stromal nerves more immediately subjacent to the epithelium had more intense reaction product deposition than more proximal nerve fibers or trunks. The strong level of reactivity of butyrylcholinesterase-positive nerves was more consistent than the moderate-to-strong reactivity of acetylcholinesterase. The levels of activity were relatively constant throughout the menstrual cycle. As mentioned in the chapter on morphology, visualization of the nerves was greatly facilitated by the superimposition of silver grains on the sulfide crystals of the cholinesterase reaction. In those silver preparations, some dendritic argyrophilic cells were observed in the lower vagina and vulva.

Dopa oxidase activity was limited to a few parabasal dendritic cells near the vulva.

Table IX. Histochemical changes in vaginal wall

	Glycogen	Toluidine Blue Metachromasia	Phosphorylase	Glucose-6-phosphate dehydrogenase	β-glucuronidase
Stratum Corneum	F:3-4 O:0-1 L:1-2	0	1-2	0	0-1
Upper Stratum Malpighi	2-4	F:2-3 O:0-1 L:1-2	2-3	3	0-1
Lower Stratum Malpighi	1-3	F:2 O:1 L:1-2	F:2-3 O:1 L:1	1-2	1-2
Stratum Basale	0	F:2 O:0-1 L:1	F:2 O:0 L:0	1-3	3
Stroma	1	0-1 BV's:2-3 BL:2-3	F:0 O:0-1 L:0	0 BV's:1-3	0 BV's:2-3

Reaction Product Intensities:
4- very strong
3- strong
2-moderate
1- weak
0- negative

BV- blood vessel
BL- basal lamina
NN- nerves

Changes through the cycle are indicated by the inclusion of values for follicular F, ovulatory O,and luteal L phases.

Table IX. Continued

	Leucine-amino-peptidase	Alkaline Phos-phatase	Acid Phos-phatase	Acetyl-Cholin-esterase	Butyryl-Cholin-esterase
Stratum Corneum	0	2-3	2-3	0-1	0-1
Upper Stratum Malpighi	0-1	0-2	0-1	0	0
Lower Stratum Malpighi	1-2	0-2	0-2	0	0
Stratum Basale	1-3	0-1	0-1	0	0
Stroma	0-3 BV's:1	0-1 BV's:2-4	0	0 NN:1-3	0 NN:2-3

C. Quantitative enzyme assay

1. Enzymes and interaction

After the histochemical studies, a survey of seven enzymes was carried out on each biopsy and several of the autopsy specimens. Glucose-6-phosphate dehydrogenase was used to corroborate the observations made from histochemical preparations. The assay in conjunction with the histochemical demonstration of G-6-PDH provided a finer insight into the tissue localization of the enzyme and its cyclic changes.

2. Intravaginal regional variation

Student's t-test corroborated my earlier hypothesis that for certain enzymes, enzyme activity varies according to the region--whether fornix, wall, or vestibule--and that therefore all biopsies should be taken from the same general region along the length of the vagina. For example, glucose-6-phosphate dehydrogenase activity in the fornix at 13 moles/kg/hr was significantly higher ($p = .01$) than the 5 moles/kg/hr seen in the vaginal wall in the same time period. The levels of lactate dehydrogenase and pyruvate kinase activity in the fornix were significantly lower (again at $p = .01$) than those of the wall. However, LDH activity in the fornix was not significantly different from that of the

biopsy of the wall taken from the same animal on the same day. The activity of that biopsy represents the lower limit of the range of activity for that time period and is itself significantly different from the representative sample. Fornical glyceraldehyde-3-phosphate dehydrogenase activity was lower than that measured in the wall but was significantly different only at the 90% level ($p = 0.1$). There was no significant difference between fornical isocitrate dehydrogenase or malate dehydrogenase activity and the activity of those enzymes in the wall.

Enzymatic activity in vestibular epithelium was uniformly higher than that of wall epithelium, except for LDH and ICDH, which, though higher, were within the range of the wall activity.

Table X. Regional variation in enzyme activity (in moles/Kg/ hr)

	Fornix (d 23)	Wall (d 23)	Significance (p =)
G6PDH	13.304	5.942	0.01
LDH	2.556	6.848	0.01
P Kinase	1.274	2.985	0.01
G3PDH	0.135	0.237	0.1
ICDH	0.113	0.138	NS
MDH	7.14	5.628	NS

N = 5 in each case

Table XI. Regional variation in enzyme activity (in moles/Kg/hr)

	Vestibule (d 13; N=5)	Wall (mean d 11-15) (N=20)	Significance (p=)
G6PDH	10.09	2.21	0.01
LDH	5.29	3.35	NS
P Kinase	3.96	1.11	0.01
PFK	0.12	0.07	0.05
G3PDH	1.099	0.212	0.01
ICDH	0.201	0.05	NS
MDH	10.321	4.27	0.01

3. Intraepithelial location

Histochemical preparations indicate that glucose-6-phosphate dehydrogenase activity is strong in the basalmost epithelial cells but not in spinous layers until the uppermost malpighian cells at the corno-malpighian junction where the level of reaction product deposition is again strong. Indeed, the reaction looks strongest in the granular layer, so one would expect a quantitative assay of G6PDH to reveal a relationship like: stratum corneum < stratum granulosum $\geq$ strata malpighi and basale. The second relation would be expected, because the strong activity of the basal cells might be diluted (in activity per microgram dry weight) by the mediocre level of activity in the malpighian layers with which they were dissected.

The variation between animals vis à vis enzyme assay activity was not a significant factor. Nevertheless, what differences did exist were accentuated by dissecting the epithelium into three parts according to stage of differentiation: 1) stratum corneum; (2) lowermost stratum corneum and uppermost stratum malpighi, constituting the stratum granulosum; (3) the remainder of the stratum malpighi and basal layer. Repetition of the dissection and assay minimized the confusing individual variation.

Glucose-6-phosphate dehydrogenase was lowest in the stratum corneum, as can be seen in Table XII. The increase in G6PDH activity from the corneal to granular layers is significant at the 98% level ($p = .02$). The basal layer exhibited a still higher level of activity that is different from that of the granular and corneal layers by increments that are significant at the $p = .05$ and $p = .01$ levels, respectively. The distinction between basal layer activity and that of the granular and corneal layers was equally clear for the lactate dehydrogenase assay. Here, however, the basal cells had a much lower activity than the granulosum and corneum ($p = .02$ and $p = .01$), which were, in turn, not significantly different from each other. The three layers exhibited pyruvate kinase activity at nearly equal rates of activity; the differences were not statistically significant. The same equipotency was observed with the phosphofructokinase assay, although there are indications that the cornomalpighian junction had higher activity than either of the other zones (in one case the differences were significant at $p = .05$ with respect to the corneum and at $p = .01$ with respect to the basalis). There has not been a significant difference between the basal and corneal layers with respect to PFK. The gradient of enzyme activity for glyceraldehyde-3-phosphate dehydrogenase was opposite from

that of G6PDH and was more subtle. There was no significant difference between the stratum corneum and the stratum granulosum, nor was there any significance in the difference between the stratum granulosum and stratum basale, yet the difference between the stratum corneum and stratum basale was significant at the 95% level ($p = .05$).

Table XII. Intraepithelial location of enzyme activity

	Stratum Corneum		Stratum Granulosum		Stratum Basale	
	moles/ kg/hr	Significance S.C. vs S.G.	moles/ kg/hr	Significance S.C. vs S.B.	moles/ kg/hr	Significance S.C. vs S.B.
G6PDH	0.624	p = .02	2.21	p = .05	3.984	p = .01
LDH	7.255	NS	11.378	p = .02	3.436	p = .01
P Kinase	1.44	NS	1.58	NS	1.78	NS
PFK	0.053	NS	0.069	NS	0.05	NS
G3PDH	0.438	NS	0.279	NS	0.198	p = .05

N=25 in each case

4. Individual difference (between test animals)

To determine the validity of considering all the assay data for a particular enzyme as a homogeneous population, a three-factor analysis of variance was performed on each of the seven enzymes studied for three populations (animals) and three time periods of the menstrual cycle, each with five reptitions. The results of the analysis are summarized in Table XIII according to the significance level of the factors.

Significant differences ($p = .05$) due to population variance were exhibited by glucose-6-phosphate dehydrogenase. All other enzymes showed no significant variation between biopsy courses. The significant differences shown by G6PDH should be interpreted with caution, however, for the analysis of interaction of population and time indicates that the time factor was responsible for much of the variation attributed to population. The lack of significant differences within the other six enzyme studies for the same populations also casts suspicion on the differences for G-6-PDH.

Table XIII. Summary of analysis of variance

Enzyme	Population	Time	Population x Time
G6PDH	*	**	**
P kinase	NS	**	**
G3PDH	NS	*	*
ICDH	NS	*	NS
MDH	NS	*	NS
PFK	NS	NS	NS
LDH	NS	NS	NS

** 99% level (p = .01)

* 95% level (p = .05)

NS Not significant

5. Time and enzyme activity

The three-factor analysis of variance gave some insight into the effect of biopsy time and level of enzyme activity. As can be seen in the summary of ANOV, G-6-PDH and P-kinase showed highly significant differences for the Time factor and for the Population x Time interaction. G-3-PDH, ICDH, and MDH had significant differences between time periods of the cycle. G-3-PDH showed a significant Population x Time interaction. None of the factors or interactions was significant for PFK or LDH.

A review of the analyses suggests that time is the single most important factor. With exception of G-6-PDH, the effect of differences between animals was not significant, although its interaction with time was significant for nearly half of the enzymes. The third factor, repetition of individual observations at each time period and population, was not significant in any study, and thus indicated that there was no significant systematic error in data collection.

Table XIV. Mean enzyme activity in course of cycle (in moles/Kg/hr)

Enzyme	Time Period in Cycle				
	Early (d 1-5)	p=	Middle (d 7-15)	p=	Late (d 17-25)
G6PDH	6.98	0.01	2.21	0.01	4.75
P Kinase	1.77	0.05	1.11	0.01	2.28
G3PDH	0.325	0.05	0.212	0.05	0.345
ICDH	0.153	0.05	0.05	0.05	0.113
MDH	4.09	NS	4.27	0.05	5.55
PFK	0.054	NS	0.07	NS	0.05
LDH	4.7	NS	3.35	NS	5.39

N=75 in each case

The mean values for enzyme activities in each of three time periods are presented in Table XIV. The time periods were selected to approximate the times of prime follicular phase(estrogen) activity and luteal phase (progesterone) activity as well as the estrogen-progesterone interaction associated with ovulation, which occurs between days 10 and 15 in the rhesus monkey. The observations on day 7 were included in the middle time period to decrease the chance of including any changes associated with the drop in estrogen titer just before ovulation. As it happened, inclusion of those observations with either the early or middle group did very little to change the mean values of those time periods. It is true, however, that using mean values reduced some of the changes, so that some apparently similar changes, as noted from mean values, were not equally significant. The statistical determination of significance considers the number of observations and the similarity of those observations to each other.

Figure 24. Mean enzyme activity determinations of glucose-6-phosphate dehydrogenase and pyruvate kinase
N = 23

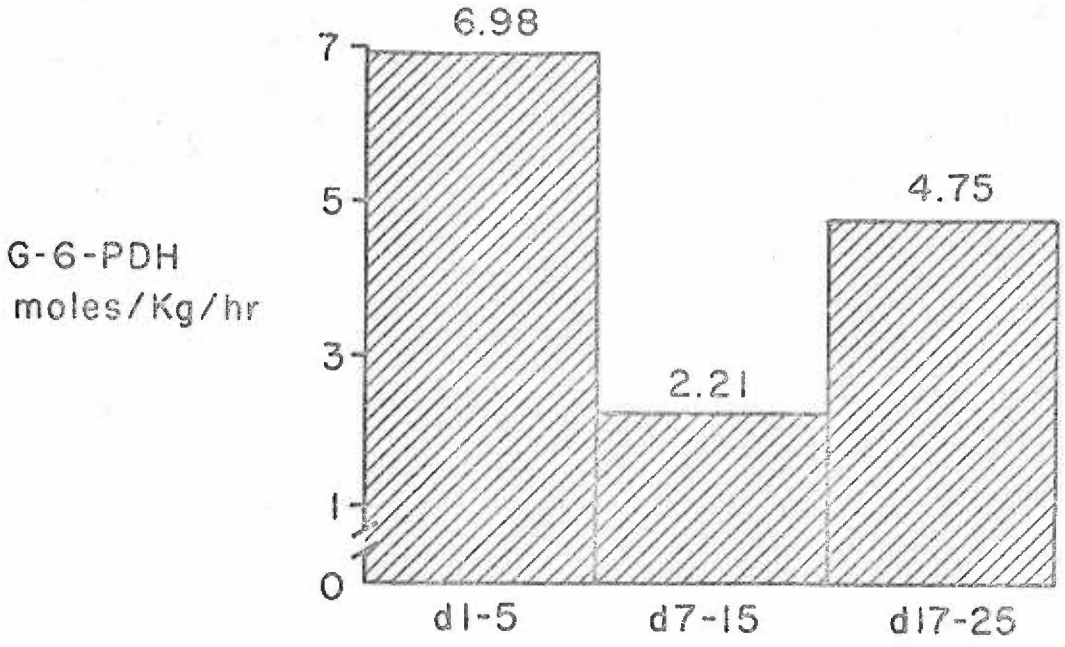

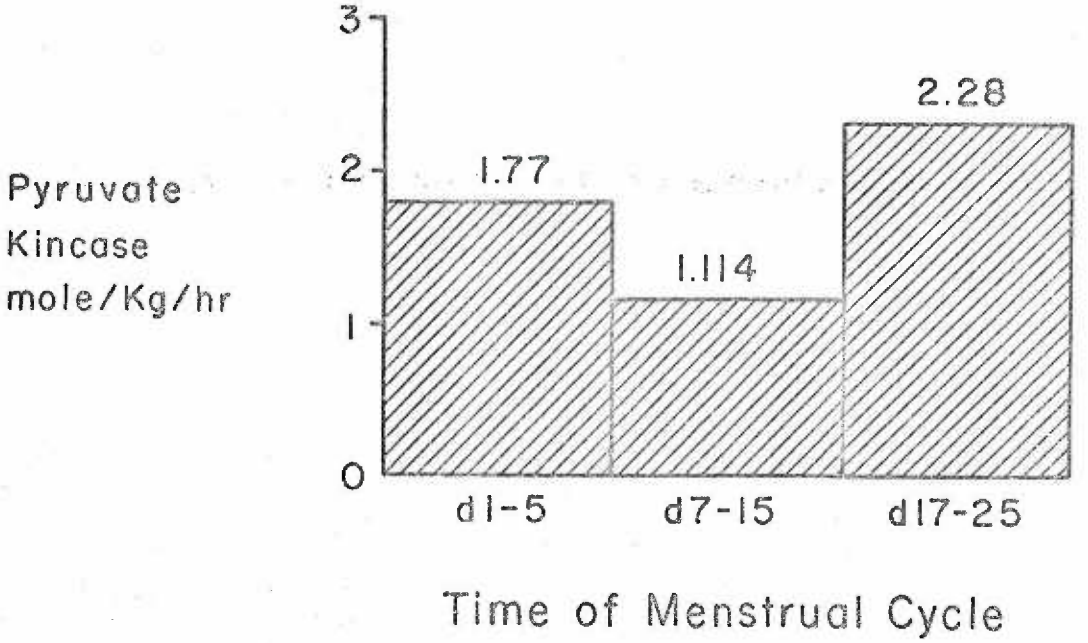

Fig 24 Mean Enzyme Activity in Course of Cycle

Figure 25. Mean enzyme activity determinations of phosphofructokinase and lactic dehydrogenase
N = 23

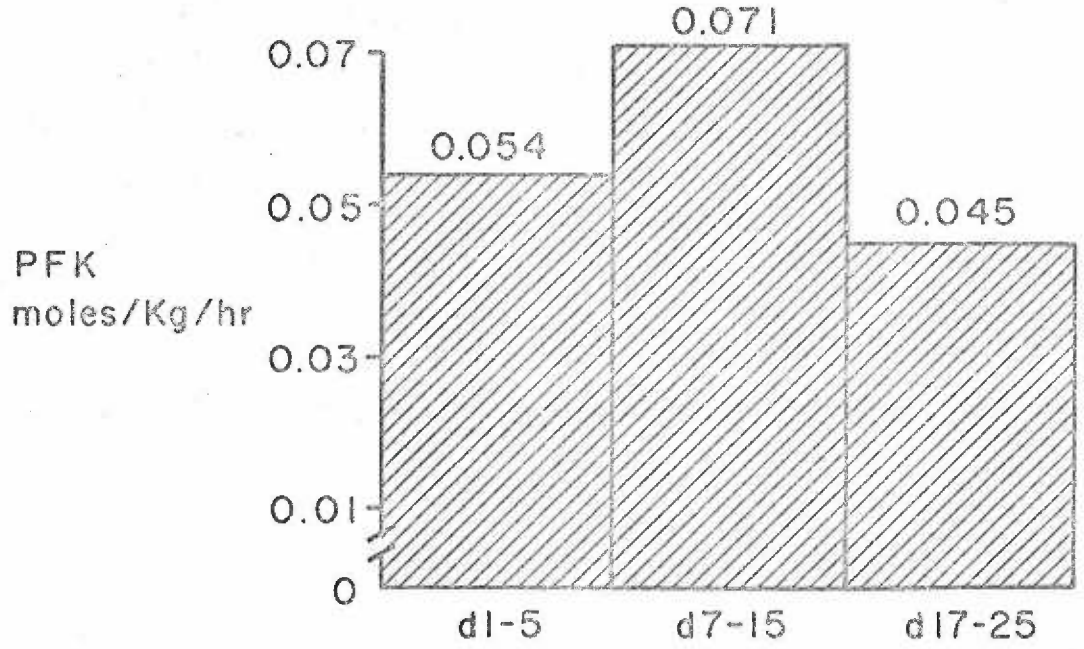

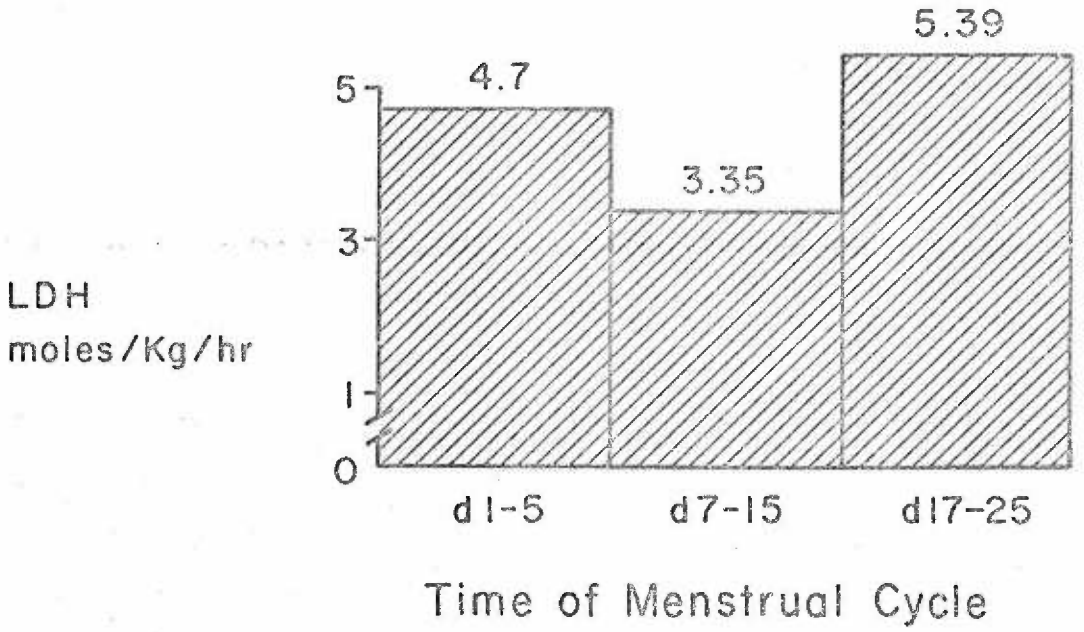

Fig 25 Mean Enzyme Activity in Course of Cycle

Figure 26. Mean enzyme activity determinations of glyceraldehyde-3-phosphate dehydrogenase, isocitric dehydrogenase, and malic dehydrogenase
N = 23

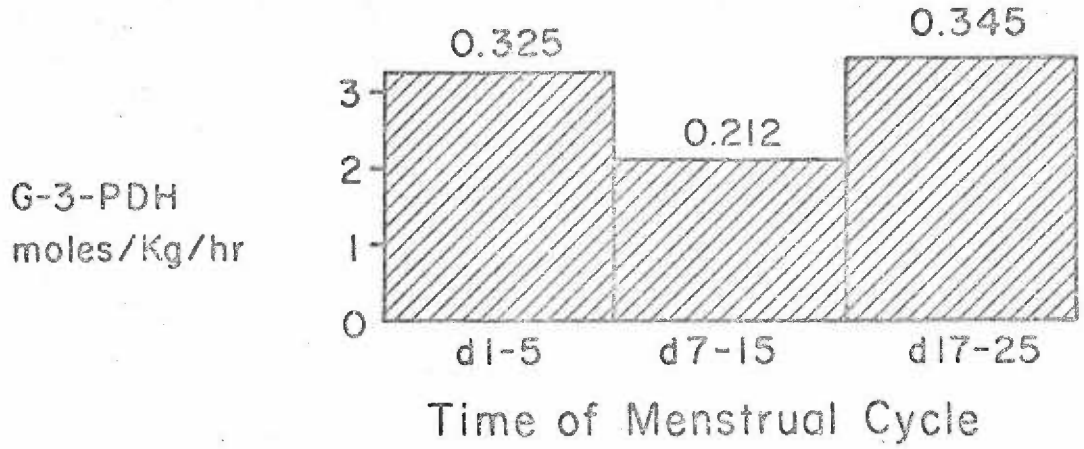

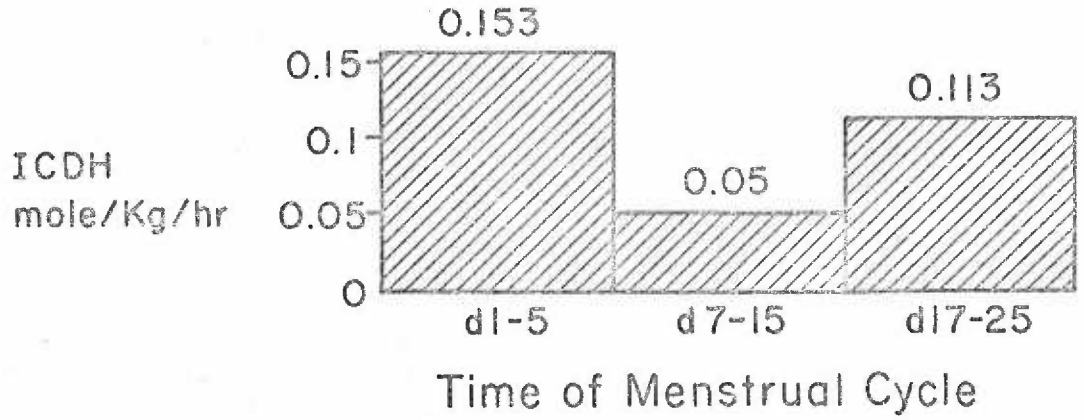

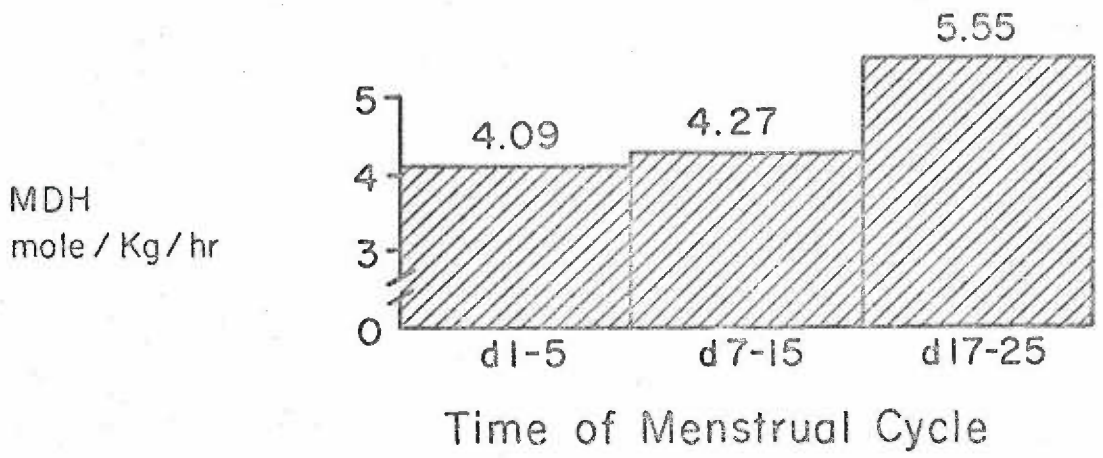

Fig 26 Mean Enzyme Activity in Course of Cycle

A significant drop in the activity of glucose-6-phosphate dehydrogenase through the middle of the cycle was followed by an increase in the late cycle to a level near that of the early part of the cycle. Similar significant decreases through the middle of the cycle occurred for pyruvate kinase, glyceraldehyde-3-phosphate dehydrogenase, and isocitrate dehydrogenase. The activities during the late stage of the cycle for each of the four enzymes were similar to those of the early period. Malate dehydrogenase in the vaginal epithelium exhibited relatively constant activity throughout most of the cycle, but showed increasing activity during the 12th to 25th postmenarchal days. The changes observed in the table for phosphofructokinase and lactic dehydrogenase do not brook statistical analysis. The mean assay values for each enzyme, biopsy time, and animal will be found in Appendix I. It now becomes apparent that the significance of enzymatic change in the vaginal epithelium depands on the particular enzyme tested and is different from one enzyme to another.

CHAPTER FOUR. DISCUSSION

The discussion of the observations presented will concentrate on two aspects of the study: (1) the morphology of the vulva and vagina and (2) metabolism. The histochemical findings will not be discussed separately. In this work, glucose metabolism was studied by investigating both the total reaction and certain intermediate reactions (by measuring the activity of the enzymes catalyzing those key reactions). All enzymes studied were assayed under optimal conditions, so assay values represent metabolic potential, not necessarily physiological activity. The primary worth of the individual values can be found in comparative studies. The role of hormones in morphology and metabolism will be considered in each section.

I. Morphology

The distribution and color intensity of the sex skin, though individually variable, is influenced in all cases by hormonal fluctuations, both natural and experimental (10, 87, 90, 113, 146). The influence of estrogens and progesterones on sex skin has also been demonstrated in other primates and mammals (39, 57, 66, 67, 76, 81, 155, 177). The production of red color in the sex skin has

not always been ascribed to vascular phenomena. Corner (44) was convinced that an epidermal pigment was the chromogenic agent.

The development of labia minora, a striking feature of the genitalia in woman, contrasts with the rima pudendi of rhesus, which is not particularly specialized. The distribution of vellus hair follicles and nerves suggests that the edges of the rhesus vaginal orifice are analogous to the labia minora. Rhesus exhibits well-developed ischial callosities; Wislocki (170) correlated the presence of ischial callosities with the reduction of external genitalia.

The rhesus clitoris, like that of the chimpanzee (62), does not have a well-developed hood or frenula. As in woman, the urethra opens into the vestibule, which is proportionately more narrow in rhesus. The suggestion of tissue folds in some other macaques and baboons probably corresponds to the hymen of woman, but the thin folds of sensitive skin about the human vestibule have no counterpart in rhesus. Wislocki (170) suggested that there is some tissue swelling at the junction of the vestibule and vagina in all "Simiae"; however, he could not exclude the possibility that the bulbus cavernosus muscle produces that swelling.

The terms "functionalis" and "basalis" commonly

applied by reproductive physiologists to uterine epithelium have been extended to the vaginal epithelium. Such an extrapolation is valid with reference to the extensive desquamation of surface layers from the vaginal epithelium of rodents, but the desquamation is much more subtle in primates. Changes in the upper layers of the vaginal epithelium might be more suitably compared with those occurring in the hair follicle or the skin epidermis. Just as the cycle of proliferation, regression, and quiescence in the follicle indicates the dynamic character of this ectodermal derivative, so in the vaginal epithelium functionality is not a property of any specific layer. All cells in all layers are in a state of metabolic and functional flux subject to modification by exogenous factors. Over the general body surface, the epidermis itself undergoes cyclic changes in proliferation and desquamation (30, 32, 35).

Mucous crypts or glands do not develop in the vaginal lining of rhesus as they do in some other mammals, so the moist epithelium of rhesus vagina is not a true mucous membrane. The "mucous" surfaces are in fact keratinizing themselves into oblivion as far as cellular activity is concerned. They are, indeed, metabolically relatively inactive as shown in Chapter Three.

In estrogen-stimulated immature mice, vaginal

keratinization was found to proceed by degrees, rather than continuously, as it does in surface epidermis (43). The layered appearance of pyknotic nuclei in the vaginal epithelium of rhesus in Chapter Three of this work also suggested stepwise differentiation. Such graded keratinization has not been recorded in the ultrastructural studies of the vagina of man (11, 77).

The keratinizing nature of mucous membranes has been supported by work on rodents and other mammals in vivo and in vitro (9, 18, 19, 102, 103, 104, 114). Research on the nature of keratinization in the oral mucosae (131, 150) indicates that the process is the same as that seen in such definitely keratinizing structures as hair and claws, but differs in the amount of fibrous material built up intracellularly. The mucosae do not form the stratum corneum seen in body surface epidermis but rather a surface from which the cells tend to slough individually (107). A true horny layer can be induced in the vagina of the mouse by estrogen treatment (162).

Observations of the vaginal epithelium split from the underlying stroma facilitated an appreciation of the complex epitheliostromal interaction. In conjunction with the microscopic and microchemical studies, those gross observations helped provide a better reference for the vagina as an organ--a whole, the parts of which were under

scrutiny, and to which the observations of the parts could be related. The various studies supported each other in the characterization of the vagina as a dynamic structure, functioning under the influence of external factors. The peculiarity of the surface of the vaginal lining is striking. That the underside of the epithelium should be even more complex was expected, yet the degree of complexity was surprising. Although the topographic character had been suggested by Wislocki (170, 171), no one since has noted the interaction between epithelium and stroma. The delicate intricacy of the epitheliostromal junction could not have been envisioned with histological sections. Just as the true nature of the dermoepidermal junction was thought to be epidermal pegs until Montagna (133) showed that it was composed of ridges, so that of the epitheliostromal junction could never be adequately interpreted from histological sections.

The vaginal wall of woman is grooved by transverse rugae which are themselves divided by furrows of variable depth, giving the general impression of papillae. Except that the papillae are more numerous near the orifice of the vagina (70), the analogy between the papillae of woman and the keratinized teeth of rhesus would be strong.

The development of specialized surface topography in the vagina of rhesus is probably dependent on a

critical minimal level of ovarian hormone, which brings about the formation of keratinized denticulate papillae in the vaginal lining of the menarchal to the premenopausal female. Thus, cyclic variations are affected by fluctuating sex hormones. Obviously, the formation of keratinized teeth in the epithelium is directly related to ovarian function; however, whether estrogen is the primary factor responsible for the presence or absence of those denticles awaits further study. The primary topographic development in rhesus is analogous to a chemical buffer, in that hormonal changes beyond that initial threshold must be abnormally large to produce any further macroscopic change. With sufficient exogenous estradiol, Bachman et al. (10) induced anomalous edema and folding in the areas of the perineum and face of rhesus that normally become flushed under the influence of the hormones of the menstrual cycle.

Wislocki (171) claimed that the keratinized teeth were obliterated in parous individuals. The observations presented in Chapter Three suggest that natural obliteration occurs only in the senile rhesus.

In the adult rhesus with functioning ovaries, the epithelium of the vagina varies in thickness from about 500 μ through menstruation to 1000 to 1500 μ near ovulation and to 500 to 800 μ again in the later half of the

cycle. The epithelium is especially thick compared with the surface epidermal thickness (137). The vaginal epithelia of juvenile, senile, and castrate rhesus are only a few cells deep and vary from 10 to 40 micra in thickness. In those specimens, the layers of epithelial cell differentiation seen in the normal adult vagina cannot be so easily identified. The extraordinary vertical compression of cells in the granular and corneal layers is particularly noticeable in the vaginal epithelium of the normal adult.

The granular layer of vaginal epithelium was a constant feature in rhesus, even in sections from the wall during the late menstrual period when maximal desquamation should already have taken place. Such a zone of keratinization was not present in the epithelia of immature of castrate rhesus females. That observation concurs with the conclusion reached by Dierks (55): the "Verhornungszone" is present only with sufficient hormonal stimulation. Dierks also claimed (54) that during menses in woman the granular layer is sloughed with the higher layers of the epithelium. Loss of the granular layer was not observed in rhesus.

The degree to which cells of the stratum corneum slough from the vaginal surface when a smear is taken does change during the cycle. Hartman (80) has indicated that

the desquamation of cells from the vaginal surface is a better indicator of ovulatory state than the count of leukocytes, sex skin reddening, or bleeding. Support for that statement recently came from Mauro et al. (130), who established an index of maturation for rhesus vaginal smears based on the number of parabasal cells, intermediate cells, and superficial cells per hundred epithelial cells counted.

The presence or absence of leukocytes in vaginal smears has been claimed as the critical principle on which to classify smears (22); the appearance of those blood cells was supposed to result from the infiltration of and passage through the epithelial layers of the vaginal mucosa. However, light microscopy shows that the numbers of leukocytes in the vaginal epithelium of rhesus are nowhere near large enough to explain the appearance of neutrophils and eosinophils in the vaginal smear (5, Chapter Three, this work). Using electron microscopic techniques, Eddy and Walker (56) observed increased numbers of leukocytes in the vaginal epithelium after progesterone treatment of ovariectomized mice. Although the ultrastructural characteristics of leukocytes are unique, the necessarily miniscule size of a sample for electron microscopy may bias any observation of significant increase. Blood cells in a smear cannot be accounted for

by migration through the vaginal epithelium, for too few can be seen in the epithelium itself. An endometrial source for leukocytes in vaginal smears seems more probable.

The complex topography of the vaginal lining of rhesus derives from an epitheliostromal interaction under the influence of functioning ovaries. The intricate and deep undersculpturing of the vaginal epithelium is consistent with the hypothesis of increased epitheliostromal interdigitation in regions subject to friction and abrasion. The denticulate lining of rhesus vagina does increase the surface area, whether or not it was an adaptation for that purpose. The cellular detritus which accumulates between the keratinized teeth, in conjunction with the complex topography, provides an excellent harbor for microorganisms. The semirigid keratinized teeth must act as stimulators of the intromitted penis. The surface adaptation may have come about primarily to insure ejaculation.

Nerve endings of the stromal stratum papillare within keratinized teeth are more complex than those seen elsewhere in the vaginal wall. Those endings suggest that the denticles contribute to the female's sex behavior as well as to the male's. By comparison with the vulva and vestibule, the population of fine subepithelial nerve endings

in the wall of the vagina was reduced. The undulations of the many nerve trunks deeper in the stroma would allow stretching of the vaginal wall without injury to the nerves (109). As well as being the source of the sub-epithelial nerve plexus, the wavy nerves must also be the receptor mechanism for stretching and deep pressure. Especially in the lower vagina and vestibule, deep pressure is also sensed by pacinian corpuscles in the outer capsule and attachments.

The difference in staining intensity of acetyl-cholinesterase and butyrylcholinesterase in the nerves of the vagina was similar to that of body surface skin as noted by Montagna et al. (137). Why BChe is stronger than AChe in rhesus is beyond speculation at this time.

The effects of the experimental manipulation of hormone levels on vaginal phenomena have been studied by several investigators in various mammals. Clark and Birch (39) and Biggers and Claringbold (22) have determined that both estrogen and progesterone are needed for the full effect. The influence of hormones on mitosis in the vaginal epithelium has been charted by Biggers and Claringbold (23); the influence on mitosis in the epidermis of surface skin was studied by Bullough (31), who found that estrogens definitely stimulate cell division.

The cytological roles of estrogen and progesterone

have been examined electronmicroscopically by Eddy and Walker (56) in the castrate female mouse. The administration of estrogen led to faster keratinization of epithelial cells, whereas progesterone produced increased proliferation in terms of epithelial thickness. Progesterone treatment was followed by the heightening and mucification of surface cells and the invasion of leukocytes into the epithelium, without mucification or keratinization of other cells. The apparent decrease in the thickness of the vaginal epithelium in late cycle does not support the role for progesterone. The vaginal epithelium of rhesus does, however, continue to increase in thickness after ovulation; this is partially consistent with the theory of Eddy and Walker.

The primary source of energy for mitosis, according to Bullough and Johnson (33), is glucose. That the great stores of glycogen in the epithelium of the vagina represent an energy depot accords with the theory that energy storage is proportional to the distance from a vascular supply of nutrients. The basal layer of the vaginal epithelium, where the greatest mitotic activity is found, is void of glycogen. That void echoes the finding of Bradfield (26) that glycogen is not deposited in the germinal layers of the epidermis. The glycogen in the malpighian layers of the epithelium, where one would expect cellular

activity requiring energy, is not static, as evidenced by the levels of phosphorylase demonstrated in the malpighian cells.

Gregoire (71) has claimed that during the cycle there is no change in the amount of glycogen in the vaginal epithelium of normally cycling rhesus. The dissection techniques and radioactive method used in the present study indicate that the increase in the amount of epithelial glycogen is significant at least ninety per cent of the time. The preliminary observations of glycogen in immature and castrate animals agree with the observation that glycogen is deposited in the vaginal epithelium only with sufficient stimulation by ovarian hormones (71).

II. Metabolism

To my knowledge, there has been no published description of the precise pathway of glucose metabolism in the rhesus vagina. One of the difficulties of such a study lies in the inherent problem of obtaining large samples of epithelium uncontaminated by other tissue from the vaginal wall. Previous biochemical investigations have studied only whole tissue specimens. Knowledge of the energy metabolism of epithelium alone has been lacking. Attempts to split the epithelium from the stroma by enzymatic digestion were not satisfactory for metabolic

studies, as indicated by comparison of the study of Brooks et al. (28) and the data of Bullough and Laurence (34). The elimination of the need for large amounts of tissue has made Adachi's micromodifications of glucose metabolism assay ideal for such a situation. Supported by microquantitative enzyme assay studies, those glucose pathway studies gave a very good initial characterization of the metabolic patterns in the vaginal epithelium of rhesus.

Glucose, the major exogenous nutrient energy source of the vaginal epithelium, is metabolized primarily through the Embden-Meyerhof pathway and pentose cycle. As in normal surface skin (1), the TCA cycle is much less utilized in vaginal epithelium than in muscle or liver. On the other hand, the involvement of the pentose cycle is much greater in vaginal epithelium than in muscle. Tables III and IV indicate that the main end-product of glucose metabolism in the vaginal epithelium is lactate, as it is in normal skin (1, 65). Whereas the specific yield of lactate in muscle is about 50% (15) and that in adipose tissue about 30% (106), lactate accounts for 95% of the end product of glucose metabolism in the vaginal epithelium. Such a high specific yield was also found in another highly active tissue, human hair follicles (2). Because there is no circulatory mechanism in the

epithelium to remove it, lactic acid builds up in those tissues beyond the level that would normally result from anaerobic glycolysis.

As mentioned, the TCA cycle is not one of the major sites of glucose metabolism in the rhesus vagina. Only 15% of the ATP produced from glycolysis derives from the TCA cycle; another 81% is produced from the reactions involving glyceraldehyde-3-phosphate dehydrogenase and pyruvate kinase. The potential energy of ATP is utilized for the most part in the reactions of hexokinase and phosphofructokinase. The net energy gain via glycolysis, starting with the theoretical 100 moles of glucose, was 27 moles. The balance of cytoplasmic-reduced pyridine nucleotides indicates that there are sufficient reducing equivalents for synthetic processes.

Glucose metabolism via the pentose cycle results in the production of ribose for nucleic acid metabolism and the reduction of nicotinamide adenine dinucleotide phosphate (NADPH) necessary for fatty acid synthesis. One would like to know, therefore, to what degree the pentose cycle contributes to the total glucose metabolism of vaginal epithelium. A general idea of the involvement was gained by comparing the fates of the carbon molecules from the C-1 and C-6 positions of the glucose molecule as it is metabolized to CO_2. Carbon from the C-1 position

appears in the CO_2 produced from the pentose cycle and the Embden-Meyerhof pathway, whereas that from the C-6 position is in the CO_2 from the E-M pathway and the TCA cycle. The ratio of CO_2 from the C-1 position to that from the C-6 position will be greater than unity when the pentose cycle plays an active role in the glucose metabolism of rhesus vagina. Following the calculations of Katz et al. (106), the pentose cycle accounts for about 3.5% of glycolysis. Though that may be a low percentage, consider that less than 1% of the radioactive glucose was metabolized to lipid, glycogen, protein, and nucleic acid. There is as yet no accurate way to measure the amount of recycling that takes place in the pentose cycle. Because the Katz methods take into consideration the fact that a carbon atom in the glucose molecule has more than one chance to become CO_2 in the pentose cycle, they are far superior to the old method of C-1 to C-6 comparison.

Although less than 1% of the ^{14}C-glucose is metabolized to lipid, the decrease in radioactive lipid found in the ovulatory phase is statistically significant. Together with the decreases in CO_2 and lactate, the lipid drop suggests a general metabolic deceleration at the time of ovulation. It is unlikely that the decrease in lipid synthesis from ^{14}C-glucose has any physiological

significance.

Preliminary studies in which the entire carbon, pyridine nucleotide, and adenosine triphosphate balances were calculated indicated that no significant changes in those balances accompanied the hormonal changes of the normal menstrual cycle of rhesus. In view of the statistically significant decreases revealed by the enzyme assay and uniformly labeled ^{14}C-glucose studies, metabolic investigations in greater depth may well support the subtle changes in those parameters that parallel the metabolic decreases at ovulation.

The three major products of glucose metabolism in the vagina of rhesus--lactate (95%), CO_2 (<5%), and glycogen (<1%)-- exhibit decreased incorporation of labeled glucose in the ovulatory stage of the menstrual cycle. The suggestion of a low turnover of the large deposit of glycogen is clear. The level of phosphorylase activity, however, indicates that a fast turnover of a small portion of the glycogen pool is more likely and is reminiscent of the situation in epidermis (1). The PAS demonstration of epithelial glycogen in the vagina suggested that only the stratum corneum exhibits cyclic fluctuations in the glycogen complement.

The histochemical demonstration and microquantitative assay for glucose-6-phosphate dehydrogenase are of

practical use in predicting metabolic changes via the pentose cycle, an increase in which would be indicative of nuclear activity. One would also expect elevated pentose cycle activity to result in increased NADPH production for lipogenesis. Decreases in G-6-PDH activity suggested by histochemical and quantitative microassays indicate that the increased thickness of the vaginal epithelium beyond the time of ovulation probably results more from cellular enlargement than from continued mitosis. Microdissection of epithelial strata for subsequent enzyme assay corroborated the gradient of G-6-PDH activity demonstrated by histochemical method in which the greatest activity was localized in the basal layer and the least activity in the stratum corneum. The advantage of the two techniques used in conjunction was also demonstrated, for the highly variable amount of stratum corneum in adjacent millimeter pieces of tissue could obviously yield abnormally low activities.

The level of beta-glucuronidase activity in the vaginal epithelium increases through the ovulatory period and decreases through the menses. That fluctuation corresponds to the changes in plasma estrogen titer and supports the role of beta-glucuronidase in estrogen metabolism (12). Beta-glucuronidases are found in almost all tissues and may soon be indicated in the mechanisms of action of

many substances (e.g. hormones like estrogen, progesterone, prolactin, or growth hormone), since activity levels are seen to fluctuate with or inversely to those substances. These enzymes hydrolyze a variety of conjugated glucuronides, the aglucuron radical of which is responsible for substrate specificity (58, 163). The physiological role is not clear.

The histochemical demonstration of several enzymes gave the impression of greater activity in the axes of keratinized teeth than in adjacent epithelial areas. The concentration of glycogen in the axis of a tooth was increased, as was the number of pyknotic nuclei. Acid phosphatase was the exception, for its activity was greater in the valleys between the keratinized teeth. The most logical explanation for increased enzyme activity, glycogen, and pyknotic nuclear concentrations in the axes of denticles would be the increased number of cells in those areas. If such is the case, the increase is subtle; an increase in cell number paralleling that of the activities was not observed. The high acid phosphatase activity is probably the result of the normal lysosomal activity of epithelial exfoliation in an area where the superficial cells do not easily slough but are trapped between the denticles.

The results and observations presented in this thesis have indicated some trends in morphological and

biochemical phenomena accompanying the menstrual cycle of rhesus. The exact time of ovulation was not determined in any of the cycles. As can be noted from Appendix A, however, the menstrual cycles were regular so that extrapolation from the detailed chronicles of Hartman (80), Corner (44), Allen (5), and Davis and Hartman (50) suggested that ovulation was occurring in the time period 10 to 15 days after the onset of menses.

Since the middle time period of the cycle frequently exhibits a depressed level of metabolic and specific enzyme activities, perhaps the gap between the peak estrogen concentration in the system and that of progesterone is wider in rhesus than was previously believed. A more likely explanation becomes apparent from the results of Hopper and Tullner (94) and Johansson et al. (101), who show that the estrogen level drops lower and the progesterone level rises faster than was suggested by earlier workers.

The changes seen in the vagina of rhesus and man warrant the conclusion reached by Huffman (95): the vagina is a more sensitive target organ for ovarian function than others, e.g. breast development, pubic hair, pudendal flush. Much earlier than do the other target organs, the vagina changes in surface conformation, initiation of cornification, change in size of the vaginal

orifice, lengthening of the vaginal canal, and alteration of the size and shape of the cervix.

The radiotracer data, considered with the changes in enzyme activities in the vagina through the menstrual cycle, support the following conclusions:

The vaginal epithelium of rhesus is not an inert tissue, but actively maintains itself with energy (ATP) secured for the most part by glycolysis via the Embden-Meyerhof pathway (ca. 80%) and partially by pathways within mitochondria (ca. 15%).

The basal and malpighian layers of the vaginal epithelium are the most metabolically active sites, and the stratum corneum is least active--a conclusion expected on the basis of metabolic patterns in surface skin.

The vaginal epithelium of adult rhesus with functioning hormonal systems actively utilized glucose via the Embden-Meyerhof pathway and tricarboxylic acid cycle. The pentose cycle is particularly active, supplying NADPH and ribose for lipid and nucleic acid syntheses.

Various changes in enzyme activities correlate with changes in total metabolic activity and thus suggest that the changes in enzyme activity may be an in vivo enzyme adaptation in

the vagina.

The present study has recorded only the initial steps toward a fuller understanding of the hormonal interrelationship with energy metabolism in the vagina of rhesus. I have attempted to add an enzymatic facet to the general metabolic explanation of hormone effects, but only further study can prove the relationships unequivocally. There is still much to be learned about the mechanisms and regulating factors that govern glucose metabolism at different stages of the menstrual cycle.

An aspect of the vagina not examined by this study relates to the absorption of substances by moist epithelia and the nature of the difference between fully keratinizing and partially keratinizing surfaces. That an epithelium as thick as that of the vagina should permit or even facilitate rapid absorption of materials is a phenomenon of great theoretical interest, which, if adequately explained, would have many practical applications in medicine. How are the absorptive properties of skin changed when the surface is hydrated, as by occlusion? Are the cytological characteristics of the corneal cells changed to resemble those of oral or vaginal epithelia? Do microvilli develop on surface cells? If the apparently void intracellular spaces of the outer corneal layers of the vagina of rhesus result from tissue processing,

the soluble substances filling those spaces could facilitate the transmission of substances from the surface to the inner epithelial layers and stromal vessels.

To date, the epithelium of the rhesus vagina has not undergone a thorough ultrastructural examination. That investigation should be made to elucidate the unique topography of the vaginal lining. Most of the vaginal fine structure studies have been directed to rodents (37, 43, 56, 147). There has been some correlation of ultrastructural features and physiologic and histochemical observations of estrus in rodents (36, 37). Two further morphological relationships in rhesus vagina need to be examined by ultramicrotechniques: (1) the tiny bulbous endings of the fine elastic fibers that appear fuzzy by electron microscopy; (2) the free nerve endings in the lower vagina and vulva that are abundant in and about the clitoris.

Other work remains for the morphologist. Mitotic indices and cell turnover times should be plotted for each stage of the menstrual cycle. Again changes in the fibrous elements of the stroma, in blood vessels, and in epithelial cells should be studied in neonate, adolescent, and senile animals. Electron histochemistry is badly needed to correlate structure and hormone action and to elucidate the site of action.

Although the lipid component of glucose metabolism was small, the significant changes exhibited suggest that ^{14}C-acetate incorporation investigations should be made in the course of the menstrual cycle. Metabolic studies should be carried out on castrate individuals under the influence of exogenous hormone. Microquantitative enzyme assay of key regulatory enzymes (hexokinase and phosphofructokinase) should be carried out in greater depth.

Now that some changes have been charted, the information should have diagnostic value, if it is supported by further study to pinpoint to the day the changes in cytologic, metabolic, and enzyme activity. Full correlation of ovarian function with those activities will require determination of estrogen and progesterone titers in the system and "bimanual palpation" (44, 80).

This investigation of normal anatomy and biochemistry may facilitate successful study of disease states. The knowledge of how similar to and how different rhesus vagina is from that of woman will make the use of rhesus a better model for studies of man.

REFERENCES

1. Adachi, K. Metabolism of glycogen in the skin and the effect of X-rays. J. Invest. Derm., 1961. 37, 381-395.

2. Adachi, K. & Uno, H. Glucose metabolism of growing and resting human hair follicles. Am. J. Physiol., 1968. 215(5), 1234-1239.

3. Adachi, K. & Yamasawa, S. Quantitative histochemistry of the primate skin VII. pyruvate kinase. J. Invest. Derm., 1966. 47, 289-292.

4. Adachi, K. & Yamasawa, S. Quantitative histochemistry of the primate skin X. phosphoglucoisomerase, phosphofructokinase, and trisephosphate isomerase. J. Invest. Derm., 1968. 50, 180-185.

5. Allen, Edgar. The menstrual cycle of the monkey, Macacus rhesus: observations on normal animals, the effects of removal of the ovaries and the effects of injections of ovaries and placental extracts into spayed animals. Carnegie Inst. Wash. Contr. to Embry., 1927, No. 98. 19, 1-44.

6. Allen, Edgar. Sex characteristics in monkeys. Proc. Soc. Exp. Biol. & Medic., 1928. 25, 325-327.

7. Anfinsen, C. B., Lowry, O., & Hastings, A. The application of the freezing-drying technique to retinal histochemistry. J. Cell. Comp. Physiol., 1942. 20, 231-237.

8. Arey, L. B. Developmental Anatomy, seventh ed. Philadelphia: Saunders, 1965.

9. Asscher, A. W. & Turner, C. J. Vaginal sulphhydryl and disulfide groups during the estrous cycle of the mouse. Nature (London), 1955. 175, 900-901.

10. Bachman, C., Collip, J., & Selye, H. The effects of prolonged oestriol administration upon the sex skin of Macaca mulatta. Proc. Roy. Soc., B., 1935. 117, 16-21.

11. Bahr, G., & Moberger, G. Beitrag zur Kenntnis der Feinstruktur des Vaginal-epithels des Menschen. Z. Geburtsch. Gynäkol., 1956. 146, 33-42.

12. Barka, Tibor & Anderson, Paul J. Histochemistry: theory, practice, and bibliography. New York: Harper and Row, 1963.

13. Barker, T. E. & Walker, B. E. Initiation of irreversible differentiation in vaginal epithelium. Anat. Rec., 1966. 154, 149-159.

14. Barron, G., Mayer, J., & Miller, Z. The metabolism of skin. Effects of vesicant agents. J. Invest. Derm., 1948. 11, 97.

15. Beatty, C., Peterson, R. Basinger, G., & Bocek, R. M. Major metabolic pathways for carbohydrate metabolism of voluntary skeletal muscle. Am. J. Physiol., 1966. 210, 404-410.

16. Bejdl, W. Die saure Phosphatase in Haut und Vagina des Menschen und ihre Bedeutung für die Verhornung. Z. Zellforsch. Mikroskop. Anat., 1954. 40, 389-400.

17. Berenblum, I., Chain, E., & Heatley, N. The metabolism of normal and neoplastic skin epithelium. Am. J. Cancer, 1940. 38, 367-371.

18. Bern, H., Alfert, M. & Blair, J. Cytochemical studies of keratin formation and of epithelial metaplasia in the rodent vagina and prostate. J. Histochem., 1957. 5, 105-119.

19. Bern, H., & Lawrence, D. Influence of vitamin A on keratinization. In E. Butcher & R. Signnaes (Eds.) Fundamentals of keratinization. Washington, D.C.: AAAS, 1962.

20. Biggers, J. D. The carbohydrate components of the vagina of the normal and ovariectomized mouse during oestrogenic stimulation. J. Anat. (London), 1953. 87, 327-336.

21. Biggers, J. D. & Claringbold, P. J. Criteria of the vaginal response to estrogens. J. Endocrin., 1954. 11, 277-284.

22. Biggers, J. & Claringbold, P. Optimum conditions for the local (intravaginal) action of estrogens. Australial J. Biol., 1954. 7, 118-139.

23. Biggers, J. & Claringbold, P. Mitotic activity in the vaginal epithelium of the mouse following local estrogenic stimulation. J. Anat., 1955. 89, 124-131.

24. Bo, W. J. The effect of progesterone and progesterone-estrogen on the glycogen deposition in the vagina of the squirrel monkey. Am. J. Obstet. Gynec., 1970. 107, 524-530.

25. Bolk, L. Beitrage zur Affen-anatomie VI: Zür Entwicklung und vergleichende Anatomie des Tractus Urethro-vaginalis der Primaten. Zeitschr. f. Morph. u. Anthro., 1907. 10, 25.

26. Bradfield, J. R. G. Glycogen of vertebrate epidermis. Nature (London), 1951. 167, 40.

27. Braus, Hermann. Anatomie des Menschen v. II. Munchen: Springer Verlag, 1956. pp. 502-509.

28. Brooks, S. C., Godefroi, V. C. & Simpson, W. L. Metabolic studies on skin. I. Isolation of various mouse skin components; their oxygen consumption and utilization of 1-^{16}C-acetate. J. Invest. Derm., 1963. 40, 305-315.

29. Brown, J. B. Estrogen excretion in normal and abnormal menstrual cycles. In C. W. Lloyd (Ed.) Recent progress in the endocrinology of reproduction. New York: Academic Press, 1959.

30. Bullough, W. S. Mitotic activity in the adult male mouse, Mus musculus L. The diurnal cycles and their relation to waking and sleeping. Proc. Roy Soc. (London), 1948. 135, 212-33.

31. Bullough, W. S. Oestrogens, carbohydrate metabolism, and mitosis. In Ciba Fdn. Colloquia on Endocrinology, 1953. 6, 278-294.

32. Bullough, W. S. The control of mitotic activity in adult mammalian tissues. Biol. Rev., 1962. 37, 307-342.

33. Bullough, W. S. & Johnson, M. The energy relations of mitotic activity in adult mouse epidermis. Proc. Roy. Soc. Ser. B., 1951. 138, 562-575.

34. Bullough, W. S. & Laurence, E. G. The mitotic activity of the follicle. In W. Montagna & R. E. Wllis (Eds.) The biology of hair growth. New York: Acad. Press, 1958.

35. Bullough, W. S. & Laurence, E. B. Stress and adrenaline in relation to the dirunal cycle of epidermal mitotic activity in adult male mice. Proc. Roy. Soc. (London) Ser. B., 1961. 154, 540-556.

36. Burgos, M. H. & Wislocki, G. B. The cyclical changes in the guinea pig's uterus, cervix, vagina and sexual skin, investigated by histological and histochemical means. Endocrinology, 1956. 59, 93-118.

37. Burgos, M. & Wislocki, G. The cyclical changes in the mucosa of the guinea pig's uterus, cervix and vagina, and in the sexual skin, investigated by the electron microscope. Endocrinology, 1958. 63, 106-121.

38. Burton, J. Histochemical demonstration of acid phosphatase by an improved azo-dye method. J. Histochem. Cytochem., 1954. 2, 88, 94.

39. Clark, G. & Birch, H. G. Observations of the sex skin and the sex cycle in the chimpanzee. Endocrin., 1948. 43, 218-231.

40. Clark, J. & Gorski, J. Ontogeny of the estrogen receptor during early uterine development. Science, 1970. 169, 76-78.

41. Clark, O. H. & Corner, G. W. The cervix uteri of the rhesus monkey. Anat. Rec., 1935. 63, 247-252.

42. Collings, M. R. A study of the cutaneous reddening and swelling about the genitalia of the monkey, Macaca rhesus. Anat. Rec., 1926. 33, 271-286.

43. Cooper, R. A., Cardiff, R. D., & Wellings, S. R. Ultrastructure of vaginal keratinization in estrogen treated immature BALB/c CRGL mice. Z. Zellforsch., 1967. 77, 377-403.

44. Corner, G. W. Ovulation and menstruation in Macacus rhesus. Carnegie Inst. Wash. Contr. to Embryology, 1923, No. 332. 15, 75-101.

45. Corner, G. W. Oestrus, ovulation, and menstruation. Physiological Reviews, 1923. 3, 457-482.

46. Cruickshank, C., Hersey, F., & Lewis, C. Isocitric dehydrogenase activity of human epidermis. J. Invest. Derm., 1958. 30, 33-37.

47. Cruickshank, R. & Sharman, H. The biology of the vagina of the human subject. I. Glycogen in the vaginal epithelium and its relation to ovarian activity. J. Obstet. Gynecol. Brit. Empire, 1934. 41, 190-226.

48. Cruickshank, C. & Trotter, M. D. The oxygen uptake, glucose utilization and lactic acid production in guinea pig skin in relation to oxygen tension. Biochem. J., 1956. 62, 57.

49. Cruickshank, C. N. D., Trotter, M. D., & Cooper, J. R. Studies on the carbohydrate metabolism of skin. Biochem. J., 1957. 66, 285-289.

50. Davis, M. E. & Hartman, C. G. Changes in vaginal epithelium during pregnancy in relation to the vaginal cycle. J. A.M.A., 1935. 104, 279-285.

51. DeAllende, I. L. C., Shorr, E., & Hartman, C. G. A comparative study of the vaginal smear cycle of the rhesus monkey and the human. Carnegie Inst. Wash. Contrib. to Embryol., 1945, No. 557. 31, 1-26.

52. DelCastillo, E. & DiPaola, G. Cyclical vaginal response to the daily administration of estradiol to castrated rats. Endocrinology, 1942. 30, 48.

53. Dickinson, R. L. & Hartman, C. G. Similarity in cervix of rhesus monkey and woman. Am. J. Ob. Gyn., 1936. 32, 813-822.

54. Dierks, K. Der normale mensuelle Zyklus der menschlichen Vaginalschleimhaut. Arch. f. Gynäkol., 1927. 130, 46-69.

55. Dierks, K. Experimentelle Untersuchungen an menschlicher Vaginal Schleimhaut. Arch. f. Gynäk., 1929. 138, 111-130.

56. Eddy, E. M. & Walker, B. E. Cytoplasmic fine structure during hormonally controlled differentiation in vaginal epithelium. Anat. Rec., 1969. 164, 205-217.

57. Erickson, L. B. Sex skin turgescence, vaginal smear changes, and determination of the period of ovulation in the chimpanzee. Fertility & Sterility, 1963. 14, 273-283.

58. Fishman, W. H. Beta-glucuronidase. Adv. Enzymol., 1955. 16, 361.

59. Fishman, W., Kasdon, S., Bonner, C., Fishman, L., & Homburger, F. Beta-glucuronidase studies in women. V. The menstrual cycle: and serum beta-glucuronidase activity in estrogen treated postmenopausal subjects. J. Clin. Endocrinol., 1951. 11, 1425.

60. Fishman, W. & Mitchell, G. Studies on Vaginal Enzymology. Ann. N.Y. Acad. Sci., 1959. 83(2), 105-121.

61. Ford, D. H. A study of the changes of vaginal alkaline phosphatase activity during the estrous cycle in adult and in young "first estrus" rats. Anat. Rec., 1956. 125, 261.

62. Ford, D. M. & Perkins, E. M. The skin of the chimpanzee. In G. Bourne (Ed.) The chimpanzee, vol. 3. Basel: S. Karger, 1970. pp. 82-119.

63. Forsberg, J. G. The periodic-acid-schiff reaction in the vaginal epithelia of fetal, immature, and adult rats. J. Histochem. & Cytochem., 1962. 10, 29-35.

64. Freinkel, R. K. Metabolism of glucose-^{14}C by human skin in vitro. J. Invest. Derm., 1960. 34, 37-42.

65. Freinkel, R. K. Carbohydrate metabolism in the skin. In W. Montagna & W. Lobitz (Eds.) The epidermis. New York: Acad. Press, 1964. pp. 485-492.

66. Gillman, J. The cyclical changes in the external genital organs of the baboon (P. porcarius). Sci. Jour. S. Africa, 1935. 32, 342-355.

67. Gillman, J. The cyclical changes in the vaginal smear in the baboon and its relationship to the perineal swelling. S. Afr. J. Med. Sci., 1937. 2, 44-56.

68. Godlewski, H. G. & Skurzak, H. Phosphorylase and branching enzyme in the vagina, uterus and liver of castrated rats treated with estrogens. A histochemical approach. Folia Biol., 1961. 9, 101-110.

69. Gomori, G. Microscopic histochemistry. Chicago: Univ. Chicago Press, 1952. pp. 184 & 210-212.

70. Goss, C. M., ed. Gray's anatomy, 28th ed. Philadelphia: Lea & Febiger, 1966. Chapter 17.

71. Gregoire, A. & Parakkal, P. The glycogen content of the immature, castrate, normal and estrogen-treated rhesus monkey vaginal tissue. Submitted to Biol of Reproduction in 1971.

72. Griesemer, R. & Gould, E. A method for the study of the intermediary carbohydrate metabolism of epidermis. J. Invest. Derm., 1954. 22, 299-315.

73. Halprin, K. & Ohkawara, A. Glucose and glycogen metabolism in the human epidermis. J. Invest. Derm., 1966. 46, 43-50.

74. Ham, A. W. Histology. Philadelphia: J. Lippincott, 1965.

75. Hamilton, Clara Eddy. Observations on the cervical mucosa of the rhesus monkey. Carnegie Inst. Wash. Contrib. to Embryology, 1949, No. 217. 33, 83-101.

76. Hammond, J. & Marshall, FHA. Oestrous and pseudopregnancy in the ferret. Proc. Roy. Soc. London, Series B, 1930. 105, 607-629.

77. Hanschke, H. J. & Schulz, H. Elektronenmikroskopische Befunde an Zellen von Vaginal- und Portioabstrichen. Arch. Gynäk., 1960. 192, 393-411.

78. Harris, R. & Cohen, S. The influence of ovarian hormones on the enzymic activities of tissues. Endocrinology, 1951. 48, 264-272.

79. Hartman, C. Menstruation without ovulation in Macacus rhesus (Abstr.) Anat. Rec., 1927. 35, 13.

80. Hartman, C. G. Studies in the reproduction of the monkey Macacus rhesus with special reference to menstruation and pregnancy. Carnegie Inst. Wash. Contrib. to Embroyology, 1932, No. 134. 23, 1-161.

81. Hendrickx, Andrew. The menstrual cycle of the baboon as determined by the vaginal smear, vaginal biopsy, and perineal swelling. In H. Vagtborg (Ed.) The baboon in medical research II. Austin: U. Texas Press, 1967.

82. Hershey, F. B. Hormone and enzyme mechanism in sebaceous gland excretion. J. Invest. Derm., 1959. 32, 1.

83. Hershey, F. B. Quantitative histochemistry of skin. In W. Montagna & W. Lobitz (Eds.) The epidermis. New York: Acad. Press, 1964. pp. 145-160.

84. Hershey, F. B., Lewis, C. Murphy, J., & Schiff, T. Quantitative histochemistry of human skin. J. Histochem., 1960. 8, 41-49.

85. Hershey, F. & Mendle, B. Quantitative histochemistry of burned and normal skin. Surgical Forums, 1954. 5, 745-749.

86. Hess, R., Scarpelli, D., & Pearse, A. The cytochemical localization of oxidative enzymes. II. Pyridine nucleotide linked dehydrogenases. J. Biophy. Biochem. Cytol., 1958. 4, 753-760.

87. Hisaw, F. L. Effects of simultaneous oestrin-corporin treatment on the uterus, cervix, vagina and sex skin of castrated monkeys. Anat. Rec., 1935. 64, 54.

88. Hisaw, F. L. & Greep, R. O. Effects of synthetic progesterone on female genital tract of the monkey. Proc. Soc. Exp. Biol. Med., 1936. 35, 29-30.

89. Hisaw, F. L. & Greep, R. O. The inhibition of uterine bleeding with estradiol and progesterone and associated endometrial modifications. Endocrin., 1938. 23, 1-14.

90. Hisaw, F. L., Greep, R., & Fevold, H. The effects of oestrin-progestin combinations on the endometrium, vagina and sexual skin of monkeys. Am. J. Anat., 1937. 61, 483-503.

91. Hisaw, F. L., Greep, R. O., & Fevold, H. L. The effects of progesterone on the female genital tract after castration atrophy. Proc. Soc. Exp. Biol. & Med., 1937. 36, 940-842.

92. Hisaw, F. L. & Lindrun, F. C. Squamous metaplasia in the cervical glands of the monkey following oestrin administration. Endocrinology, 1936. 20, 228.

93. Hoerr, N. L. Cytological studies by Altmann-Gersh freeze-drying method; recent advances in technique. Anat. Rec., 1936. 65, 293-317.

94. Hopper, B. & Tullner, W. W. Urinary estrone and plasma progesterone levels during the menstrual cycle of the rhesus monkey. Endocrinology, 1970. 86, 1225-1230.

95. Huffman, J. The structure and bacteriology of the premenarchal vagina. Ann NY Acad. Sci., 1959. 83(2), 227-236.

96. Humason, G. L. Animal Tissue Techniques. San Francisco: W. H. Freeman, 1962.

97. Im, Michael Jae-Chul. Quantitative enzyme histochemistry on experimental injuries in the epidermis of the rhesus monkey Macaca mulatta. Unpublished doctoral dissertation, Univ. Oregon Med. Sch., 1967.

98. Im, M. J.-C. & Adachi, K. Quantitative histochemistry of primate skin.V. Glucose-6-phosphate dehydrogenase and 6-phosphogluconate dehydrogenase. J. Invest. Derm, 1966. 47, 121-124.

99. Im, M. J.-C. & Adachi, K. Quantitative histochemistry of the primate skin. VI Lactate dehydrogenase. J. Invest. Derm., 1966. 47, 286-288.

100. Im, M. J.-C., Yamasawa, S., & Adachi, K. Quantitative histochemistry of the primate skin. III. Glyceraldehyde-3-phosphate dehydrogenase. J. Invest. Derm., 1966. 47, 35-38.

101. Johansson, E. O. B., Neill, J. D., Knobil, E. Periovulatory progesterone concentration in the peripheral plasma of the rhesus monkey with a methodologic note on the detection of ovulation. Endocrinology, 1968. 82, 143-148.

102. Kahn, R. H. Effect of locally applied vitamin A and estrogen on the rat vagina. Am. J. Anat., 1954. 95, 309-335.

103. Kahn, R. H. Effect of œstrogen and of vitamin A on vaginal cornification in tissue culture. Nature, 1954. 174, 317.

104. Kahn, R. H. Vaginal keratinization in vitro. Ann. N.Y. Acad. Sci., 1959. 83(2), 347-355.

105. Kaplan, N. O., Colowick, S., & Barnes, C. Effect of alkali on DPN. J. Biol. Chem., 1951. 181, 461-472.

106. Katz, J. Landau, B., & Bartsch, G. The pentose cycle, triose phosphate isomerization, and lipogenesis in rat adipose tissue. J. Biol. Chem., 1966. 241, 727-740.

107. Kligman, A. M. The biology of the stratum corneum. In W. Montagna & W. Lobitz (Eds.) The epidermis. New York: Acad. Press, 1964. p. 397.

108. Koelle, G. B. & Friedenwald, J. S. A histochemical method for localizing cholinesterase activity. Proc. Soc. Exp. Biol. Med., 1949. 70, 617-622.

109. Krantz, K. Innervation of the human vulva and vagina; a microscopic study. Obstet. & Gyn., 1958. 12, 382-396.

110. Ladinsky, J. L. & Peckham, B. M. The kinetics of the generative compartment of the estrogen dependent vaginal epithelium. Exp. Cell Res., 1965. 40, 447-455.

111. Laidlaw, G. F. & Blackberg, S. N. Melanoma studies. II. Simple technique for the dopa reaction. Am. J. Path., 1932. 8, 491.

112. Lamar, J. K., Shettles, L., & Delfs, E. Cyclic penetrability of human cervical mucus to spermatozoa in vitro. Am. J. Physiology, 1940. 129, 234-241.

113. Langley, J. N. & Sherrington, C. S. On pilomotor nerves. J. Physiol., 1891. 12, 279.

114. Lawrence, D. J. & Bern, H. A. Mucous metaplasia and mucous gland formation in keratinized adult epithelium in situ treated with vitamin A. Exp. Cell Res., 1960. 21, 443-446.

115. Lillie, R. D. Histopathologic technic and practical histochemistry (3rd edition). New York: McGraw-Hill, 1965.

116. Linderstrøm-Lang, K., Holter, H., & Ohlsen, A. Studies on enzymatic histochemistry. XIII. The distribution of enzymes in the stomach of pigs. Compt.-rend., Lab. Carlsberg, Ser. Chim., 1935. 20, 66-125.

117. Linderstrøm-Lang, K. & Møgensen, K. Studies on enzymatic histochemistry. XXXI. Histological control of histochemical investigations. Comp.-rend. Lab. Carlsberg, Serie Chim., 1938. 23, 27-35.

118. Ling, K.-H., Marcus, F. & Lardy, H. Purification and some properties of rabbit skeletal muscle phosphofructokinase. J. Biol. Chem., 1965. 240, 1893-1899.

119. Long, J. A. & Evans, H. M. The oestrous cycle in the rat and its associated phenomena. Mem. Univ. Calif, 1922. 6, 1-148.

120. Lowry, O. H. A quartz fiber balance. J. Biol. Chem., 1941. 140, 183-189.

121. Lowry, O. H. A simple quartz torsion balance. J. Biol. Chem., 1944. 152, 293-294.

122. Lowry, O. H. The quantitative histochemistry of the brain: histological sampling. J. Histochem. Cytochem., 1953. 1, 420-428.

123. Lowry, O. H., Passonneau, J., Schulz, D., & Rock, M. The measurement of pyridine nucleotides by enzymatic cycling. J. Biol. Chem., 1961. 236, 2746-2755.

124. Lowry, O. H., Roberts, N. & Kappan, J. The fluorometric measurement of pyriding nucleotide. J. Biol. Chem., 1957. 224, 1047-1064.

125. Lowry, O. H., Roberts, N., Leiner, K., Wu, M., & Farr, A. L. The quantitative histochemistry of brain. I. Chemical methods. J. Biol. Chem., 1954. 207, 1-17.

126. Lowry, O. H., Roberts, N., Wu, M., Hixon, W., & Crawford, E. The quantitative histochemistry of brain. II. Enzyme measurements. J. Biol. Chem., 1954. 207, 19-37.

127. Mandt, C. Zur Anatomie der weiblichen Scheide. Z. rat. Med., 1849. 7, 1-13.

128. Markee, J. E. & Berg, B. Cyclic fluctuations in blood estrogen as a possible cause of menstruation. Stanford Med. Bull., 1944. 2, 55-60.

129. Matschinsky, F., Passonneau, J., & Lowry, O. Quantitative histochemical analysis of glycolytic intermediates and cofactors with an oil well technique. J. Histochem. and Cytochem., 1968. 16, 29-39.

130. Mauro, J., Serrone, D., Somsin, P., & Stein, A. Cyclic vaginal cytologic patterns in the Macaca mulatta. Acta Cytologica, 1970. 14, 348-352.

131. Meyer, J. & Medak, H. Keratinization of the oral mucosa. In E. Butcher & R. Sognnaes (Eds.) Fundamentals of keratinization. Washington, D.C.: AAAS, 1962.

132. Miura, H. Beiträge zum Studium der Vaginalsekrete. Kyoto-Idakaigaka Zasshi (Mitteil Med. Akad. Kioto), 1928. ii, Heft I., Abt. B. 2, 1-71.

133. Montagna, W. The structure and function of skin. New York: Acad. Press, 1962.

134. Montagna, W., Chase, H. B., & Melaragno, H. P. Histology and chtochemistry of human skin. I. Metachromasia in the mons pubis. J. Nat. Cancer Inst., 1951. 12, 591-597.

135. Montagna, W., Chase, H. B., & Lobitz, W. C. Histology and cytochemistry of human skin. IV. The eccrine sweat glands. J. Invest. Derm., 1953. 20, 415-423.

136. Montagna, W., & Ellis, R. A. Histology and cytochemistry of human skin. XII. Cholinesterases in the hair follicles of the scalp. J. Invest. Derm., 1957. 29, 151-157.

137. Montagna, W., Yun, J. S., & Machida, H. The skin of primates. XVIII. The skin of the rhesus monkey (Macaca mulatta). Am. J. Phys. Anthrop., 1964. 22, 307-320.

138. Nachlas, M., Crawford, D., & Seligman, A. The histochemical demonstration of leucine aminopeptidase. J. Histochem. Cytochem., 1957. 5, 264-278.

139. Parakkal, P. & Gregoire, A. Differentiation of the vaginal epithelium in the normal and hormone-treated rhesus monkey. Submitted to Biology of Reproduction, 1971.

140. Passman, J., Radin, N., & Cooper, J. Liquid scintillation technique for measuring carbon-14-dioxide activity. Anal. Chem., 1956. 28, 484-486.

141. Passonneau, J., Gatfield, P., Schulz, D., & Lowry, O. H. An enzymic method for measurement of glycogen. Analytical Biochemistry, 1967. 19, 315-326.

142. Peckham, B., Barash, H., Emlen, J., Kiekhofer, W., & Ladinsky, J. Changes in vaginal cellular activity elicited by varying doses of natural and synthetic estrogens. Exp. Cell. Res., 1963. 30, 339-343.

143. Peckham, B. & Kiekhofer, W. Cellular behavior in the vaginal epithelium of estrogen-treated rats. Am. J. Obstet. Gynecol., 1962. 83, 1021-1027.

144. Perrotta, C. A. Initiation of cell proliferation in the vaginal and uterine epithelia of the mouse. Am. J. Anat., 1962. 111, 195-204.

145. Petry, G., Overbeck, L., & Vogell, W. Untersuchungen über den funktionell bedingten Formwandel des Vaginalepithels. Verh. anat. Ges. (Jena), 1961. 57, 285-291.

146. Pocock, R. I. The external characteristics of the catarrhine monkeys and apes (Papio theropithecus). Proc. Zool. Soc. London, 1926. 2, 1479-1579.

147. Pollard, I., Martin, L., & Shorey, C. D. The effect of intravaginal oestradiol-3,17 β on the cell structure of the vaginal epithelium of the ovariectomized mouse. Steroids, 1966. 8, 805-823.

148. Rappaport, B. Z. A semiquantitative dopa reaction by use of frozen-dried skin. A.M.A. Arch. Path., 1955. 60, 444.

149. Reinhart, J. & Abul-Haj, S. An improved method for histologic demonstration of acid mucopolysaccharides in tissues. Arch. Pathol. (A.M.A.), 1951. 52, 189-194.

150. Rhodin, J. & Reith, E. Ultrastructure of keratin in oral mucosa, skin, esophagus, claw, and hair. In E. Butcher & R. Sognnaes (Eds.) Fundamentals of keratinization. Washington, D.C.: AAAS, 1962.

151. Rognstad, R. & Katz, J. The balance of pyridine nucleotides and ATP in adipose tissue. Proc. Nat. Acad. Sci., 1966. 55, 1148-1156.

152. Roman, N., Ford, D., & Montagna, W. The demonstration of cutaneous nerves. J. Invest. Derm., 1969. 53, 328-331.

153. Roman, N., Perkins, S., Perkins, E., & Dolnick, E. Orcein-hematoxylin in iodized ferric chloride as a stain for elastic fibers, with metanil yellow counterstaining. Stain Tech., 1967. 42, 199-202.

154. Rosa, C., & Velardo, J. Histochemical localization of vaginal oxidative enzymes and mucins in rats treated with estradiol and progesterone. Ann. N.Y. Acad. Sci., 1959. 83(2), 122-144.

155. Schultz, A. H. Studies on the growth of gorilla and of other higher primates with special reference to a fetus of gorilla, preserved in the Carnegie Museum. Mem. Carnegie Mus., 1927. 51, 1.

156. Seligman, A., Tsou, K., Rutenburg, S., & Cohen, R. Histochemical demonstration of β-D-glucuronidase with synthetic substrate. J. Histochem. Cytochem., 1954. 2, 209-229.

157. Smith, A., Perkins, E., & Machida, H. Durable mounts of the iodine stain for the phosphorylase reaction. Stain Technol., 1966. 41, 346-348.

158. Smith, B., & Brunner, E. The stature of the human vaginal mucosa in relation to menstrual cycle and to pregnancy. Am. J. Anat., 1934. 54, 27-85.

159. Steiner, D., Rauda, V., & Williams, R. Effects of insulin, glucagon, and glucocorticoids upon hepatic glycogen syntheses from uridine diphosphate glucose. J. Biol. Chem, 1961. 236, 299-304.

160. Stewart, T. D. The skin and its appendages. In C. Hartman & W. Straus (Eds.) Anatomy of the rhesus monkey. New York, N.Y.: Hafner, 1961.

161. Takeuchi, T. & Kuriaki, H. Histochemical detection of phosphorylase in animal tissues. J. Histochem. Cytochem., 1955. 3, 153-160.

162. Taschdjian, C. L., Reiss, F. R., & Kozinn, P. J. Experimental vaginal candidiasis in mice. J. Invest. Dermatol., 1960. 34, 89.

163. Teague, R. S. The conjugates of D-glucuronic acid of animal origin. Adv. Carbohydrate Chem., 1954. 9, 185.

164. Tinklepaugh, O. L., & VanCampenhout, E. The vaginal cell content of the mature and immature chimpanzee. Anat. Rec., 1931. 48, 309-322.

165. VanDyke, H., & Ch'en, G. Observations on the biochemistry of the genital tract of the female macaque particularly during the menstrual cycle. Am. J. Anat., 1936. 58, 473-499.

166. Vianney, M. J. Vaginal cytodiagnosis of the estrus cycle of the mouse with fluorescence microscopy. Fertil. Steril., 1965. 16, 401-414.

167. Wells, L. J. Embryology and anatomy of the vagina. Ann. N.Y. Acad. Sci., 1959. 83(2), 80-88.

168. Winkelmann, R. K. A silver impregnation method for peripheral nerve endings. J. Invest. Derm., 1955. 24, 57-64.

169. Winkelmann, R. & Schmidt, R. A simple silver method for nerve axoplasm. Staff Mtg. Mayo Clinic, 1957. 32, 217.

170. Wislocki, G. B. On the female reproductive tract of the gorilla, with a comparison of that of other primates. Carnegia Inst. Wash. Contributions to Embryol., 1932, No. 135. 23, 163-204 et seq.

171. Wislocki, G. B. The reproductive systems. In C. G. Hartman & W. L. Strauss (Eds.) The anatomy of the rhesus monkey Macaca mulatta, Ch. XI. New York: Hafner Publ. Co., 1961.

172. Wislocki, G. B., Fawcett, D. W., & Dempsey, E. Staining of stratified squamous epithelium of mucous membrane and skin of man and monkey by the PAS method. Anat. Rec., 1951. 110, 359.

173. Wohlgemuth, J & Ikebata, T. Die Fermente der Haut. Biochem. Zeitschr., 1927. 186, 43.

174. Wohlgemuth, J. & Klopstock, E. Die Fermente der Haut. V. Atmung und Glykolysis der Haut und ihre Beeinflussung durch Hormone. Biochem. Zeitschr., 1926. 175, 202-215.

175. Wood, H., Katz, J., & Landau, B. Estimation of pathways of carbohydrate metabolism. Biochemische Zeitschr., 1963. 338, 809-847.

176. Young, W. C. (Ed.) Sex and internal secretions. Vol. 1. Baltimore: Williams & Wilkins, 1961. 3rd edition.

177. Zuckerman, S., & Fulton, J. The menstrual cycle of the primates. VII. The sexual skin of the chimpanzee. J. Anat., 1934. 69, 38-46.

178. Zuckerman, S. The histogenesis of tissues sensitive to oestrogens. Biol. Rev., 1940. 15, 231-271.

179. Zuckerman, S. The histogenetic potency of the cloacal region. Arch. Anat. Microscop., 1950. 39, 608-617.

APPENDIX A

Menstrual Histories of Three Test Animals

MENSTRUAL HISTORIES OF THREE TEST ANIMALS

305 00664 F

	1 5 10 15 20 25 30
10-1969	M MM
11-1969	MMM
12-1969	MMM
01-1970	MMM
02-1970	MMM
03-1970	MMM
04-1970	MMM
05-1970	MMM
06-1970	MMM
	MMM

305 02074 F

	1 5 10 15 20 25 30
10-1969	M
11-1969	MMMM
12-1969	MMM
01-1970	MMM
02-1970	MMMMMMMM
03-1970	MM
04-1970	
05-1970	MMM
06-1970	MMM
07-1970	MMM
	MMM

305 02259 F

	1 5 10 15 20 25 30
10-1969	MMMM
11-1969	MMMM M
12-1969	MMMM MM
01-1970	MM MMMM
02-1970	MMMM
03-1970	MMM
04-1970	MMMMM
05-1970	MMMMM
06-1970	MMM

M = Menstruating

APPENDIX B

Fixatives and Solutions

HELLY'S FIXATIVE

100 ml stock solution:

(1) 5 gm. $HgCl_2$, 2.5 gm. KCr_2O_7, and 1 gm. $NaSO_4$ in 100 ml. distilled H_2O.

(2) Just before use, add 5 ml 37% formaldehyde to 95 ml stock solution.

FORMALIN, 10%

10 ml 37% formaldehyde into 90 ml distilled water

GLUTARALDEHYDE-CACODYLATE

4.6% glutaraldehyde in 0.1 M cacodylate buffer (pH 7.2)

(1) 18 ml glutaraldehyde + 82 ml buffer

(2) Add 9 gm. sucrose per 100 ml

cacodylate buffer

(1) 21.4 gm. sodium dimethyl arsenate in 500 ml distilled H_2O

(2) 42 ml 0.2 M HCl

(3) 458 ml distilled water

(4) Adjust pH to 7.2

PERMOUNT

60% xylene solution of the synthetic β-pinene from Fisher Scientific

HOLLANDE-BOUIN

picric acid.....4.0gm
cupric sulfate.....2.5gm
acetic acid.....1.5ml
formaldehyde (37%).....10.0ml
distilled water.....100.0ml

APPENDIX C

Histological Procedures

ACID MUCOPOLYSACCHARIDE TECHNIQUE

(Reinhart and Abul-Haj, 1951)

PROCEDURE

(1) Bring deparaffinized sections down to water and back up to 70% alcohol.

(2) Place in 3% glacial acetic acid . . . . . 5 min.

(3) Stain in acid-collodal complex iron solution . . . . . 10 min.

(4) Wash in distilled water until sections are colorless.

(5) Immerse in ferrocyanide-hydrochloric acid solution . 10 min.

(6) Rinse in two changes distilled water.

(7) Stain in aluminum ammonium sulfate - cochineal solution . . . . . 15 min.

(8) Wash in running tap water . . . . . 5 min.

(9) Rinse in distilled water . . . . . 2 min.

(10) Stain in picrofuchsin solution . . . . . 6 min.

(11) Without washing, pass quickly to 95% alcohol and dehydrate in absolute alcohol.

(12) Clear in xylene and mount in Permount.

REACTION

Nuclear chromatin . . . . . delicate brownish-gray

Collagen . . . . . red

Mucopolysaccharides . . . . . bright blue

Mucoproteins . . . . . buff - orange

Fibrin . . . . . buff - orange

Glycoproteins . . . . . buff - orange

Cell cytoplasm . . . . . greenish-yellow to orange

PREPARATION

(1) Colloidal iron -

To 333 ml. distilled water add 100 gm. ferric chloride and 133 ml. glycerin. Then add 33 ml. conc. ammonium hydroxide and mix until precipitate dissolves. Repeat addition of ammonium hydroxide using the following successive quantities: 16.6 ml., 10.0 ml., and 6.6 ml. The product of this reaction is a clear, deep red-brown colloidal solution of ammonium ferric glycerate.

This solution is then dialyzed as follows -

For 5 min. soak a sausage bag (18" x 1 7/8") in distilled water. Tie off one end and add 533 ml. of solution. Tie off other end at the 18" mark, place in large beaker of distilled water and use magnetic stirrer. This requires 8-10 changes over a 72 hour period. Solution will increase to approximately 1400 ml. and is quite stable.

(2) Acid-colloidal complex iron solution -

To 40 ml. colloidal iron solution add 10 ml. glacial acetic acid.

(3) Ferrocyanide-hydrochloric acid solution -

To 20 ml. 2% potassium ferrocyanide [$K_4Fe(CN)_6$] add 40 ml. 1% HCl.

(4) Aluminum ammonium sulfate - cochineal solution -

To 450 ml. distilled water add 26 gm. aluminum ammonium sulfate [$AlNH_4(SO_4)_2.12H_2O$]. Dissolve by heating to 85°C and add 30 gm. powdered cochineal. Stir thoroughly. At 85°C add 5 ml. conc. ammonium hydroxide SLOWLY and stir until precipitate dissolves. Now boil vigorously 35 minutes. Add 150 ml. distilled water, cool, filter, and add several phenol crystals.

(5) Picrofuchsin solution -

To 95 ml. sat. sq. picric acid add 6 ml. 1% acid fuchsin (Matheson).

HARRIS' HEMATOXYLIN AND EOSIN

(Lillie, 1965)

PROCEDURE

(1) Deparaffinize slides with two 5 minute changes of xylene

(2) Bring slides through alcohol series to water

If tissues were fixed with $HgCl_2$, the procedure must include a 5 minute rinse in 0.5% iodine in 80% alcohol and, after reaching water, a 5 minute rinse in 5% sodium thiosulfate.

(3) 5 minutes in running tap water

(4) 5 minutes in distilled water

(5) 7 minutes in hematoxylin staining solution

(6) 5 minutes in running tap water

(7) Fast dip in 30% alcohol acidified with 1 NHCl (1 ml/ 200 ml)

(8) 10-30 minutes in running tap water

(9) Dehydrate through 30, 50, 60, 70, and 80% alcohol

(10) Dip in 0.25% eosin G in 80% alcohol

(11) Rinse twice in 80% alcohol

(12) Complete dehydration through three 5 minute changes of 95% and 100% alcohol

(13) Clear in three 5 minute changes of xylene

(14) Mount in Permount

REACTION

Nuclei	blue
Cartilage	dark blue
Calcium deposits	dark blue
Cytoplasm	pink
Muscle	pink
Mucin	often light blue
Keratohyalin	often dark blue

PREPARATION. Harris' hematoxylin solution

(1) Dissolve 1 gm hematoxylin in 10 ml absolute alcohol

(2) Dissolve 20 gm potassium aluminum sulfate ($AlK(SO_4)_2 \cdot 12 H_2O$) in 20 ml distilled water. Heat may be required.

(3) Add hematoxylin solution and bring to rapid boil

(4) Turn off flame and carefully add 0.5 gm mercuric oxide

(5) Cool the solution quickly

(6) Filter into stock bottle

ORCEIN-HEMATOXYLIN IN IODIZED FERRIC CHLORIDE (AOV)

(Roman, Perkins, Perkins and Dolnick, 1967)

PROCEDURE

(1) Bring deparafffinized sections down to water and back up to 70% alcohol.

(2) Stain in orcein-hematoxylin solution . . . . . 2 hrs.

(3) Rinse in distilled water until excess stain is removed.

(4) Differentiate in 1.2% ferric chloride (observe every 5 sec.).

(5) Wash in running tap water . . . . . 5 min.

(6) Agitate in 0.01% HCl in 70% alcohol . . . . . 1 min.

(7) Rinse briefly in 70% alcohol and place in distilled water . . . . . 2 min.

(8) Counterstain in 0.25% aq. metanil yellow . . . . . 10 sec.

(9) Dehydrate in absolute alcohol, clear in xylene, and mount in Permount.

REACTION

Coarse and fine elastic fibers . . . . intense purple

Nuclei . . . . . violet

Other tissue elements . . . . . yellow

PREPARATION

(1) Acid orcein -

Dissolve 0.25 gm. orcein (Roboz) in 125 ml. 70% alcohol.

Add 1 ml. conc. HCL and filter.

(2) Hematoxylin -

Dissolve 2 gm. hematoxylin (Roboz) in 40 ml. absolute alcohol and filter.

(3) Orcein-hematoxylin staining solution -

Add ingredients in order listed: orcein, 0.2% in 70% alcohol (125 ml.); hematoxylin, 5% in absolute alcohol (40 ml.); ferric chloride, 6% aq. (25 ml.); and iodine, 1% in 2% aq. potassium iodide (25 ml.). Prepare fresh each time and filter before use.

(4) 0.25% Metanil yellow -

To 200 ml. distilled water add 0.5 gm. metanil yellow and 1 ml. 1% acetic acid.

PERIODIC ACID-SCHIFF

(Montagna, Chase and Lobitz, 1953)

PROCEDURE

(1) Deparaffinize control slides and bring down to distilled water.

(2) Incubate control slides in diastase solution at 37°C . . . 15 min.

(3) Wash control slides in running tap water . . . . . 30 min.

(4) At this time deparaffinize all PAS slides, hydrating to distilled water.

(5) Combine ALL slides in freshly prepared 0.5% periodic acid at 37°C . . . . . 15 min.

(6) Place in two changes distilled water . . . . . 3 min. each

(7) Place in dilute Schiff reagent . . . . . 30 min.

(8) Place in 10% potassium metabisulfite . . . . . 4 min.

(9) Repeat . . . . . 4 min.

(10) Wash in running tap water . . . . . 5 min.

(11) Place in distilled water . . . . . 3 min.

(12) Stain in Harris' hematoxylin (filter before use) . . . 1/2 min.

(13) Rinse in acid water (5 ml. 1N HCl in 100 ml. distilled water).

(14) Dip in lithium carbonate until blue.

(15) Wash in running tap water . . . . . 5 min.

(16) Place in distilled water, dehydrate through alcohols, and clear in xylene.

(17) Mount in Permount.

REACTION

Polysaccharides (glycogen, starch, cellulose);
Muco- and glycoproteins (reticulin, collagen);
Unsaturated lipids and phospholipids;
Glycolipids; and neutral
Mucopolysaccharides . . . . . rose to red-violet
Nuclei . . . . . blue

PREPARATION

(1) Diastase solution -

To 1 gm. sodium chloride, 0.163 gm. dibasic sodium phosphate (Na_2HPO_4 anhyd.), and 0.1 gm. monobasic sodium phosphate ($NaH_2PO_4 . H_2O$) add 125 ml. distilled water. Pour off 25 ml. and to remaining 100 ml. add 1 gm. malt diastase.

(2) Schiff reagent -

To 100 ml. bioling distilled water add 1 gm. basic fuchsin and stir. Cool to 50°C and filter. Add 20 ml. 1N HCl and cool to 25° C. Add 1 gm. potassium metabisulfite ($K_2S_2O_5$ anhyd.) and keep in dark several days. After sulfurous acid has decolorized as much of fuchsin as it will, add one spatula decolorizing carbon,

mix, and filter. Store in dark bottle in refrigerator, protected by layer of xylene.

(3) Dilute Schiff reagent -

To 60 ml. conc. Schiff reagent add 240 ml. 10% potassium metabisulfite.

TOLUIDINE BLUE

(Montagna, Chase and Melaragno, 1951)

PROCEDURE

(1) Bring deparaffinized sections down to distilled water.

(2) Place in toluidine blue solution (pH 4.5) . . . . . 15 min.

(3) Rinse in distilled water.

(4) Place tissue sections in tert-butyl alcohol . . . . . 5 min.

(5) Repeat with fresh tert-butyl alcohol . . . . . 5 min.

(6) Cover sections with absolute alcohol . . . . . 5 min.

(7) Cover sections with toluene . . . . . 5 min.

(8) Cover with fresh toluene . . . . . 5 min.

(9) Repeat . . . . . 5 min.

(10) Mount in Permount.

REACTION

Acid Mucopolysaccharides . . . . metachromatic

Other tissue elements . . . . . light blue

PREPARATION

(1) McIlvaine buffer -

0.1 M Citric acid (to 25 ml. 25% methanol add 1.1 gm. citric acid)

0.2 M Sodium phosphate (to 0.71 gm. dibasic sodium phosphate -Na_2HPO_4 anhydrous--add 25 ml.

25% methanol)

(2) Toluidine blue solution -

To 23 ml. 0.1 M citric acid and 17 ml. 0.2 M sodium phosphate add 1000 ml. distilled water. Mix and pour off 40 ml. To remaining 1000 ml. add 500 mg. o-toluidine blue (Roboz). Mix and store in refrigerator. Check pH before use.

APPENDIX D

Histochemical Procedures

ACID PHOSPHATASE

(Barka and Anderson, 1963)

PROCEDURE

(1) Fixation: four possible treatments, sections from 40 to 80 microns.

(a) Fix the entire tissue in glutaraldehyde fixative for 2 hours, then cut frozen cryostat sections. Place free floating sections directly into 0.1 M cacodylate buffer pH 7.2 and 8% sucrose overnight in refrigerator; OR adhere sections to slides, air dry, and wash in the cacodylate buffer sucrose solution overnight in refrigerator.

(b) If the entire block of tissue cannot be fixed, cut fresh frozen sections and adhere them to the slide, air dry at room temperature, fix in glutaraldehyde fixative for two hours, and wash overnight in the cacodylate buffer sucrose solution refrigerated; cut fresh frozen sections directly into fixative and proceed as for the slides.

(2) Place slides in the incubating substrate for 30 minutes at room temperature.

(3) Wash in several changes of distilled water.

(4) Place into ammonium sulfide solution (0.5 to 1.0%) for 30 seconds.

(5) Wash in distilled water 3 to 4 times.

(6) Mount in glycerol gelatin, or place in cold 10% formalin overnight; next day wash in distilled water and mount in glycerol jelly or dehydrate and mount in Permount.

Reaction: sites of enzyme activity . . . . . brown to black

FIXATIVE:

(1) Prepare 0.1 M cacodylate buffer pH 7.2

(a) Sodium cacodylate, $3H_2O$ (sodium dimethyl arsenate) . . . 21.4 gm.

(b) Distilled water . . . . . 500.0 ml.

(c) Add 0.2 M hydrochloric acid . . . 42.0 ml.

(d) Distilled water . . . . . 458.0 ml.

(e) Adjust pH to 7.2

(2) Prepare 4.6% glutaraldehyde in 0.1 M cacodylate buffer pH 7.2 and add 8.0 gm. of sucrose.

STOCK SOLUTIONS

Tris-maleate solution 0.2 M

(a) Tris (hydroxymethyl) aminomethane . . . . . 12.1 gm.

(b) Maleic acid . . . 11.6 gm "or" maleic anhydride . . . 9.8 gm.

(c) Distilled water . . . . . 500.0 ml.

Sodium hydroxide 0.2 M

(a) 1 N sodium hydroxide . . . . . 20.0 ml.

(b) Distilled water . . . . . 80.0 ml.

1.25% Sodium glycerophosphate pH 5.0

(a) Sodium glycerophosphate . . . . . 1.25 gm.

(b) Distilled water . . . . . 100.0 ml.

(c) Adjust to pH 5.0 using 1N HCl

0.1 M Tris-maleate buffer pH 5.0

Prepare fresh and use the same day.

(a) Tris- maleate stock solution 0.2 M . . . . . 50.0 ml.

(b) Sodium hydroxide stock solution 0.2 M . . . . . 7.0 ml.

(c) Add distilled water to 100.0 ml. and pH to 5.0

INCUBATING SUBSTRATE

(1) 0.1 M Tris-maleate buffer pH 5.0 . . . . . 10.0 ml.

(2) Distilled water . . . . . 10.0 ml.

(3) 1.25% sodium glycerophosphate pH 5.0 . . . . . 10.0 ml.

(4) Mix thoroughly

(5) 0.2% lead nitrate . . . . . 20.0 ml. "Constantly stirring."

(6) Check the pH of the incubating substrate and adjust to 5.0 if necessary using normal HCl.

(7) Incubating substrate should be clear; if it appears cloudy or turbid, discard it.

(8) Incubating substrate should be prepared fresh each time.

ALKALINE PHOSPHATASE

(Gomori, 1952)

(1) Cut frozen tissue at 80 & 100 microns and affix sections to slides precoated with Tissue-Tac.

(2) Remove from cryostat and bring to room temperature for 15 minutes. Spray very slightly with distilled water and allow to air dry 2 hours.

(3) Fix tissue in cold 10% formalin in the refrigerator for 2 hours.

(4) Wash slides in cold distilled water 2 or 3 times for 15 to 30 minutes.

(5) Place slides in preheated substrate in the 37° C oven for 2-1/2 hours.

(6) Place slides directly from substrate into 2% calcium chloride for . . . 3 min.

(7) Rinse slides 4 to 6 times in distilled water.

(8) Place slides in freshly prepared 2% cobalt chloride for . . . . . 5 min.

(9) Rinse slides 6 to 8 times in distilled water.

(10) Place slides in ammonium sulfide solution from 15 to 30 seconds

. . . . . ammonium sulfide . . . 1.0 ml.

dist. water . . . . . 74.0 ml.

(11) Rinse slides immediately 4 to 6 times in distilled water.

(12) Place slides in 10% formalin in refrigerator overnight.

(13) Rinse slides in two or three changes of distilled water, then dehydrate through grades of alcohol and xylene and mount in Permount.

Reaction: sites of enzyme activity brown to black.

BUFFERED SUBSTRATE FOR ALKALINE PHOSPHATASE:

(1) 2% calcium chloride	10.0 ml.
(2) 2% sodium glycerophosphate	10.0 ml.
(3) 2% sodium barbitol	5.0 ml.
(4) Distilled water	25.0 ml.
(5) 10% magnesium sulfate	.5 ml.
	50.5 ml.

BETA - D - GLUCURONIDASE

(Seligman et al., 1954)

PROCEDURE

(1) Cut frozen sections in the cryostat, adhere sections to UNCOATED (NOT TISSUE TAC) slides, cut at 20 & 40 microns.

(2) Remove from the cryostat and air dry slides at room temperature for about 15 minutes.

(3) Fix slides in "Cold" 10% neutral formalin (neutralized with disodium phosphate) for 10 to 30 minutes.

(4) Wash in "cold" distilled water for 3 changes, each change 5 minutes.

(5) *Incubate slides in incubating substrate mixture in 37°C oven for 4 to 6 hours.

(6) Remove slides from incubator and wash in running tap water for less than 1 minute.

(7) Place slides in Diazo Blue B (tetrazotized diorthoanisidine), prepared immediately before use for 2 minutes. Prepared by using 1.0 mg. in 1.0 ml. of cold phosphate buffer (0.02 M, pH = 7.5).

(8) Rinse slides in two changes of cold distilled water.

(9) Rinse slides in 0.1% acetic acid solution.

(10) Mount slides in glycerol - gelatin.

Reaction: sites of enzyme activity . . . . . purple to blue

SOLUTIONS:

*Incubating Substrate Mixture

(1) Dissolve 6-bromo, 2 naphthyl, β-D-glucopyranose . . . . 30.0 mg.

Into absolute methanol . . . . . 5.0 ml.

(2) Add phospho-citrate buffer pH 4.95 . . . . . 20.0 ml.

(3) Add distilled water . . . . . 75.0 ml.

Phospho-citrate buffer pH = 4.95

0.1 M Citric acid ($C_6H_8O_7 \cdot H_2O$) . . . M.W. = 210.146

2.1 gm. of citric acid, and dilute with distilled water to 100.0 ml.

0.2 M Sodium phosphate dibasic, anhydrous (Na_2HPO_4); MW = 141.96

2.84 gm. of disodium phosphate in 100 ml. distilled water.

Mix equal volumes of citric acid and disodium phosphate and pH to exactly 4.95.

Phosphate Buffer (0.02 M) pH = 7.5 (Buffer used in step #7)

0.02 M Sodium phosphate, dibasic, anhydrous (Na_2HPO_4) . . .

M.W. = 141.96

2.84 gm. of disodium phosphate in 100 ml. distilled water.

0.02 M Sodium phosphate, monobasic ($NaH_2PO_4 \cdot H_2O$); MW = 138.01

.276 g. sodium phosphate in 100 ml. distilled water.

Mix 3 parts Na_2HPO_4 to 1 part NaH_2PO_4; pH to 7.5 while mixing.

Neutral buffered formaldehyde solution (pH = 7.0) . . . Step #3

37-40% (concentrated) formaldehyde	100.0 ml.
Distilled water	900.0 ml.
Acid sodium phosphate - monohydrate	4.0 gm.
Anhydrous disodium phosphate	6.5 gm.

DOPA OXIDASE

(Laidlaw & Blackberg, 1932; and Rappaport, 1955)

(1) Unfixed frozen sections, 20, 40, 80 μ, placed in small jar within cryostat.

(2) Add cold 10% formalin, buffered to pH 7.0.

Fix for two hours.

(3) Wash with distilled water.

(4) Add substrate solution and incubate at 37° C until reaction can be seen in tissue under microscope.

To avoid contamination resulting from autoxidation, the substrate solution is changed as soon as it begins to darken. Two or three changes may be necessary.

(5) Rinse in distilled water.

(6) Counterstain as desired.

(7) Dehydrate and mount.

Reaction: sites of enzyme activity . . . . brown to black granules of melanin.

SUBSTRATE SOLUTION:

0.1% DOPA (dihydroxyphenylalanine) buffered to pH 7.3-7.5 with 0.1 M phosphate buffer, pH 7.4.

PHOSPHATE BUFFER:

Mix a. and b. below:

a. 0.1 M sodium phosphate dibasic (Na_2HPO_4) MW = 141.96

Na_2HPO_4 . . . . . 7.1 gm.

Distilled H_2O . . . . . 500.0 ml.

b. 0.1 M sodium phosphate monobasic (NaH_2PO_4) MW = 138.01

NaH_2PO_4 . . . . . 1.38 gm.

Distilled H_2O . . . . . 100.0 ml.

GLUCOSE 6-PHOSPHATE DEHYDROGENASE (G-6-PDH)

(Hess, Scarpelli, & Pearse, 1958)

PROCEDURE

(1) Cut frozen sections in the cryostat and adhere sections to tissue-tac slides; sections are cut at 40 microns.

(2) Remove from cryostat, bring to room temperature, spray slides slightly with distilled water, air dry.

(3) Add a few drops of incubating substrate to each section in 37° C oven for 45 minutes.

(4) Rinse slides in distilled water.

(5) Postfix slides in "Cold" 10% formalin for a period of 10 minutes to overnight at 4°C.

(6) Wash slides 2-3 times in "Cold" distilled water, allow slides to remain in cold distilled water until they reach room temperature before coverslipping. This will prevent many bubbles.

(7) Mount slides in glycerol-gelatin (Sigma Stock No. GG-1).

Reaction: sites of enzyme activity . . . . red to violet

INCUBATING SUBSTRATE MIXTURE

(1) Glucopyranose-6-phosphate disodium salt

M.W. = approx. 284.00, require 0.5 M solution. (Use 140.0 mg. / 1.0 ml.) . . . . . 1.0 ml.

(2) Triphosphopyridine nucleotide (TPN)

M. W. = 800. (Use 12.0 mg./3.0 ml. or 8.0 mg./2.0 ml.: final concentration 1.0 mM.) . . . . . 2.0 ml.

(3) Sodium azide (NaN_3)

M. W. = 65.02, require 0.1 M. (Use 650.0 mg./100.0 ml.) . . . . . 1.0 ml.

(4) Manganese chloride ($MnCl_2.4H_2O$)

M. W. = 197.91, require 0.05 M. (Use 1.0 gm./100.0 ml.) . . . . . 1.0 ml.

(5) Veronal buffer (0.05 M . . . pH = 7.6) . . . . . 2.5 ml.

To prepare veronal buffer (0.05 M, pH = 7.6)

(a) Barbital sodium (sodium veronal) $C_8H_{11}N_2O_3Na$

M. W. = 206.18 . . . . . 456.0 mg.

Add distilled water . . . 49.2 ml., and thoroughly dissolve.

(b) Use a weak solution of hydrochloric acid (0.1 N), very slowly and carefully one drop at a time to the above solution (a) until you reach pH 7.6.

(c) Make the final dilution up to 80.0 ml.

(6) Nitro blue tetrazolium chloride (NBT) . . . 1.0 mg./1.0 ml. . . 2.5 ml.

LEUCINE - AMINOPEPTIDASE (LAP)

(Nachlas, Crawford, Seligman, 1957)

PROCEDURE FOR STAINING

(1) Cut tissue in the cryostat and adhere sections to PLAIN (no affixative) slide; sections cut at 20 and 60 microns.

(2) Remove slides from cryostat to room temperature for 5 to 15 minutes, spray slightly with distilled water. Allow to air dry.

(3) Place unfixed slides directly into preheated incubating substrate mixture at 37°C oven for 20 minutes.

(4) Rinse in normal saline for 2 minutes.

(5) Transfer to 0.1 M cupric sulfate solution for 2 minutes.

(6) Fix in 10% formalin for 3 minutes.

(7) Wash in distilled water, dehydrate through grades of alcohol, clear in xylene, and mount in Permount.

Reaction: sites of enzyme activity . . . . . pink to purple

INCUBATING SUBSTRATE

(1) L-leucyl-B naphthylamide hydrochloride (8 mg. dissolved in 1 ml. dist. water) . . . 1.0 ml.

(2) Acetate buffer (0.1 M) pH 5.7 to 5.9 . . . . . 10.0 ml.

(3) Sodium chloride (0.85%) . . . . . 8.0 ml.

(4) Potassium cyanide (.002 M) . . . . . 1.0 ml.

(5) Naphthanil Diazo Blue B . . . . . 10.0 mg.

REAGENTS

(1) Acetate buffer (0.1 M) pH = 5.7 to 5.9

To 100 ml. of 0.1 M acetic acid add 0.1 M sodium acetate until pH 5.8 is reached.

0.1 M Sodium acetate ($NaC_2H_3O_2 . 3H_2O$) M.W. = 136.08

1.36 gm. of sodium acetate in 100.0 ml. with distilled water.

0.1 M Acetic acid (CH_3COOH) m.W. = 60.05

6.0 ml. of glacial acetic acid diluted to 1000.0 ml. with distilled water.

(2) .002 M Potassium cyanide (KCN) M.W. = 65.12

13.0 mg. of potassium cyanide in 100.0 ml. distilled water.

(3) 0.1 M Cupric sulfate ($CuSO_4 . 5H_2O$) M.W. = 249.68

25.0 gm. of cupric sulfate ($CuSO_4 . 5H_2O$) in 1000.0 ml. distilled water.

(3a) 0.1 M Cupric sulfate ($CuSO_4$ anhydrous) M.W. = 159.61

16.0 gms. of cupric sulfate anhydrous in 100.0 ml. dist. water.

Note: Use either (3) or (3a), but be sure to consider molecular water in molarity calculation.

PHOSPHORYLASE

(Takeuchi and Kuriaki, 1955; Smith, Perkins and Machida, 1966)

PROCEDURE

(1) Incubate fresh frozen, 40 micron tissue sections in substrate at 37°C . . . . . 20 min.

(2) Continue to incubate in substrate at room temperature . . . . . 15 min.

(3) Agitate in 10% aq. Lugol's iodine solution until color develops.

(4) Dehydrate in two changes absolute alcohol (to which 1 mg./ml. iodine is added) . . . . . 5 min. each

(5) Clear in two changes xylene (to which 1 mg./ml. iodine is added) . . . . . 5 min. each

(6) Mount in Histoclad (to which 1 mg./ml. iodine is added).

REACTION

Glycogen . . . . . henna

Amylose . . . . . gray-violet

PREPARATION

(1) 0.1 M Acetate buffer (pH to 5.8) -

0.1 M Acetic acid (to 497 ml. distilled water add 3 ml. glacial acetic acid)

0.1 M Sodium acetate (to 6.8 gm. sodium acetate add 500 ml. distilled water)

Buffer (to 25 ml. 0.1 M acetic acid add 475 ml. 0.1 M sodium acetate). Adjust pH.

(2) Substrate -

To 100 mg. glucose-1-phosphate, 20 mg. adenosine-5-phosphoric acid, and 10 mg. glycogen (Nutribio) add 30 ml. distilled water, 20 ml. 0.1 M acetate buffer, 1 ml. insulin (1 ml. = 40 units), and 10 ml. absolute alcohol.

(3) Lugol's iodine solution -

To 2 gm. potassium iodide and 1 gm. iodine crystals add 1000 ml. distilled water.

ELASTIC FIBER STAIN IN FRESH FROZEN SECTIONS

(modified from N. Roman, et al., 1967)

PROCEDURE

(1) Fresh frozen sections are cut in the cryostat at desirable thickness. In our laboratory sections are varied from 10 to 30 microns in thickness. Affix sections to slides precoated with Tissue-Tac.

(2) Allow slides to air dry at room temperature for not less than two (2) hours and preferably overnight; longer periods for air drying are not harmful to the demonstration of elastic fibers.

(3) Immerse the slides in 70% alcohol for not less than one (1) hr.

(4) Remove the slides from 70% alcohol and place in the A. O. V. stain for 2 hours.

(5) Wash slides in 4 to 6 changes of distilled water to remove the excess stain. While the slides are in distilled water, check the slides microscopically for the black elastic fibers. Slides may be returned to the stain for additional time if fibers appear brown or purple in color; it is important to check the stain here before the next step.

(6) Differentiate slides one at a time in 1. 2% ferric chloride

($FeCl_3.6H_2O$). Differentiation time varies with region and thickness of the tissue. Check the slide under the microscope for proper contrast after short periods of 5 to 10 seconds differentiation. Look for dark fibers (thick & fine structures) and a lightened background (as compared with undifferentiated slides). The slide must be rinsed in distilled water before checking it microscopically.

(7) Rinse in 3 changes of distilled water: The slide may be left in running tap water while others are differentiated.

(8) Counterstain with 0.25% aqueous solution of metanil yellow: The length of time for counterstaining again depends on both the region and thickness of tissue. After one to two dips, the slides are rinsed in distilled water and checked microscopically for the effect of color and detail that is desired. From distilled water they may be returned to metanil yellow for further staining.

(9) Rinse in 95% alcohol, dehydrate, clear and mount coverslips using Permount (a Fischer modified beta-pinene dissolved in toluene).

Reaction: elastic fibers . . . . blue to black

STAIN

Note: Prepare solutions fresh each time and mix them together in the order that they are listed.

(a) Acid orcein: Dissolve orcein pur (Chroma-Gesellschaft

product) 0.25 gm. in 125.0 ml. of 70% alcohol and add 1.0 ml. of concentrated hydrochloric acid; mix well and filter.

(b) Hematoxylin: Dissolve hematoxylin (Hematoxylin puriss., Chroma-Gesellschaft product) 2.0 gm. in 40.0 ml. of absolute alcohol. Mix well and filter.

(c) 6% Ferric chloride ($FeCl_3.6H_2O$): Dissolve 2.4 gms. of ferric chloride in 25.0 ml. dist. water.

(d) Lugol's solution: 1% crystalline iodine in 2% KI; make 25.0 mls.

(3) Add together a, b, c, d, in this given order. Though the amount of staining solution may be increased or decreased, the proportions must be maintained exactly.

DIFFERENTIATOR (1.2% Ferric chloride)

Dissolve 1.7 gm. of ferric chloride ($FeCl_3.6H_2O$) in 100.0 ml. of distilled water.

COUNTERSTAIN (0.25% metanil yellow)

Dissolve 0.25 gm. of metanil yellow in 100.0 ml. of distilled water, acidified with 3 to 4 drops of 10% acetic acid per 100 ml. of solution. The color becomes rather orange; should it become purple, the solution is too acid.

WINKELMANN'S TECHNIQUE FOR PERIPHERAL NERVE ENDINGS

PROCEDURE

(1) Fix tissue in Winkelmann's fixative for not less than one day. Longer fixation is desirable.

(2) Dehydrate tissue by placing into three changes of ascending ethanols for one hour each change (70%, 95%, 100%).

(3) Clear in xylene for 1/2 to 1 hour.

(4) Rehydrate tissue by placing into three changes of descending ethanols for one hour each change (100%, 95%, 70%).

(5) Store in 10% formalin until needed.

(6) Cut tissue at 50 microns in the cryostat into jars equilibrated to -20°C.

(7) Remove jars from cryostat and pour cold 10% formalin over the sections in the jars. Sections may be stored in cold 10% formalin until needed. (Very important . . . The tissue must remain in the 10% formalin for at least 10 minutes. A longer period (up to many days) may be used if convenient).

(8) Remove sections from 10% formalin and rinse in two changes of distilled water; allow sections to remain for 30 minutes in a third change of distilled water. (Excess formalin is associated with extensive background staining.)

(9) Immerse sections in 20% silver nitrate solution for 20 minutes.

(10) Immerse sections ONE AT A TIME in three changes of distilled water for approximately THREE SECONDS EACH CHANGE.

(11) Place tissue sections flat on the bottom of a dish containing 0.2% hydroquinone in 1% sodium sulfite for 10 minutes.

(12) Wash in two changes distilled water.

(13) Place sections into 0.2% gold chloride for 2 minutes.

(14) Rinse in one change of distilled water.

(15) Place sections in 5% sodium thiosulfate for 5 minutes.

(16) Wash in distilled water.

(17) Dehydrate through grades of alcohol, clear in xylene and mount with Permount.

Reaction: nerves (even finest) . . . . . black

REAGENTS

(1) Fixative: 1% ammonium hydroxide and 15% sucrose in 10% formalin.

(2) 20% silver nitrate.

(3) 0.2% hydroquinone in 1% sodium sulfite. Use within 8 hrs. after preparation.

(4) 0.2% gold chloride (15 grains = 1.0 gm.). Use the entire vial diluted to 500.0 ml. with distilled water.

(5) 5% sodium thiosulfate.

SILVERED CHOLINESTERASE

(Roman, Ford, Montagna, 1969)

***NOTE: At all times handle sections very carefully and allow to lie flat at bottom of all reagents.

PROCEDURE

(1) Tissue sections are cut in the cryostat at 60, 70, 80, 100 μ, and placed into screw cap jars.

(2) Remove the jars from the cryostat and fix in cold 10% formalin for 1 to 2 hours in the refrigerator.

(3) Wash 4 to 6 times in distilled water.

(4) Transfer sections to the "cholinesterase incubating substrate" and place in 37° C oven for 4 to 5 hours.

(5) Wash the sections through 8 changes of saturated sodium sulfate.

(6) Transfer into ammonium sulfide for 3 minutes.

(7) Wash in 6 changes of distilled water. Store the tissue overnight in 10% formalin in the refrigerator.

(8) De-fat the tissue the next day in this manner: Wash the tissue two to three times in distilled water; dehydrate, starting with 30% alcohol up to 100% alcohol (allow plenty of time in xylene to clear the tissue); hydrate the tissue back to distilled water and into 10% formalin overnight at 4° C.

***NOTE: After de-fatting allow tissue to remain for at least two or three days in 10% formalin at 4°C.

(9) Wash the tissue 4 to 6 times in distilled water before going to the next step. Allow at least one hour total for washing.

(10) Immerse sections in 20% silver nitrate for . . . 20 minutes.

(11) Wash sections in three changes of distilled water; allow a total of 10 seconds for all three changes.

(12) Place sections in the hydroquinone-sulfate solution for 10 minutes or for gross observation of color developing.

(13) Wash in four different changes of distilled water.

(14) Place sections in 0.2% solution of gold chloride for 3 minutes.

(15) Wash in four different changes of distilled water.

(16) Place sections in 5% sodium thiosulfate for 5 minutes.

(17) Wash in four changes of distilled water, then dehydrate starting with 30% alcohol, clear in xylene and mount; in the dehydration you may counterstain with paracarmine if so desired.

Reaction: nerves . . . . . dark brown to black

melanocytes . . black

INCUBATING SUBSTRATE FOR CHOLINESTERASE ACTIVITY

ACETYLTHIOCHOLINESTERASE (ACHE)

Acetyl thiocholine iodide . . . . . 20.0 mg.

Stock solution . . . . . 10.0 ml.

BUTYRYLTHIOCHOLINESTERASE (BCHE)

Butyryl thiocholine iodide . . . . . 25.0 mg.

Stock solution . . . . . 10.0 ml.

CHOLINESTERASE STOCK SOLUTION: (This must be prepared fresh each time and used the same day.)

First prepare . . . sodium sulfate anhydrous (Na_2SO_4) . . 50.0 gm. dissolved into 170.0 ml. dist. water (apply heat if necessary).

Second prepare . . maleic anhydride ($C_4H_2O_3$) . . . 1.75 gm. dissolved in 30.0 ml. of 1N (4%) sodium hydroxide (NaOH). ***Note: This reagent is used to "pH" the stock solution.

Add the remaining reagents to the sodium sulfate EXACTLY in the order given.

(a) Cupric sulfate ($CuSO_4 . 5H_2O$) . . . . . 0.3 gm.

(b) Glycine (Aminoacetic acid; anhydrous) . . . . . 0.375 gm.

(c) Magnesium chloride ($MgCl_2 . 6H_2O$) . . . . . 1.0 gm.

Using the second reagent prepared, pH this solution to 5.2; store in 37°C oven until ready for use the same day.

REAGENTS FOR WINKELMANN'S TECHNIQUE

FIXATIVE . . . 1% ammonium hydroxide and 15% sucrose in 10% formalin.

Reagents . . . . (a) 20% silver nitrate

(b) hydroquinone . . . . 0.2 gm.
sodium sulfite . . . 1.0 gm.
} Dissolved in 100.0 ml. dist. H_2O

(c) 0.2% gold chloride (15 grains = 1.0 gm.) entire vial diluted in 500.0 ml. distilled water = 0.2%

(d) 5% sodium thiosulfate

APPENDIX E

Glucose Metabolism Procedures

GLUCOSE METABOLISM PROCEDURES

REAGENT PREPARATION

(1) Krebs-Ringer bicarbonate buffer, made to 100 mg% glucose. Make enough for 100λ for each sample tube and blank tube, a small amount for tissue holding solution, and 20 ml for dilutions of standard. Mix salt solutions separately and combine immediately before use. Bubble oxygen-CO_2 into the bicarbonate solution for 15 minutes before use.

Salt Solutions	Proportions
.154 M NaCl	100
.154 M KCl	4
.11 M $CaCl_2$	1
.154 M KH_2PO_4	1
.154 M $NaHCO_3$	21

(2) Incubation mixture

Into 2 ml test tube place Krebs-Ringer bicarbonate buffer to provide 100λ for each sample and blank tube. Add radioactive glucose to give activity of 0.25 μc/100 λ reagent mixture. (If the specific activity of the ^{14}C is high enough, the amount of hot glucose can be disregarded in the consideration of a 100 mg% glucose solution. The Krebs-Ringer buffer made to 100 mg% glucose may be used.

(3) Apparatus for incubation and CO_2 collection

Items

10 x 75 mm disposable flintglass test tubes

1/2 inch amber latex tubing

medium weight filter paper cut in strips about 2 x 12 cm

Assembly

Cut the test tubes in half (3.5-4 cm). Save the bottom half of each tube. Two half-tubes are necessary for each sample and blank. Cut the latex tubing into 2-2.5 cm lengths. Insert the paper strips into half of the cut tubes. Shortly before use, the tubes and tubing will be connected to appear as depicted in the following illustration.

(4) Reagents for assays

20% Cupric Sulphate ($CuSO_4$)
Calcium hydroxide powder ($Ca(OH)_2$)
Double distilled water
2N Sodium Chloride (NaCl)
10% glycogen (aqueous solution)
1% glucose (aqueous solution)
95% ethanol
chloroform
methanol
heptane

BIOPSY PROCEDURE

(1) Rongeur biopsy with sterile rongeur forceps
Place the biopsy specimen on watch glass on ice; add small amount of buffered 100 mg% glucose.

(2) In weighing toom, dissect pieces of epithelium as free as possible from underlying connective tissue. The pieces are to weigh about 5 mg after two quick blottings with tissue paper. Weigh specimens on small, 20-40 mg squares of aluminum foil in balance. Place weighed samples with foil on cold glass (on ice); cover samples with a drop or two of buffered 100 mg% glucose.

INCUBATION AND CO_2 ASSAY

(1) Add 300 λ of hyamine hydroxide (or similar solubilizer) to the filter papers in half of the cut tubes. Connect the rubber tubing to those tubes. Add 100λ of the incubation mixture to each of the empty cut tubes, including those to be used as blanks. Blot the sample tissues with filter or tissue paper and place each tissue in its tube. Hold the blank tissues in 100 mg% glucose on ice. Connect the rubber rubing and CO_2 collector to the incubation tube, taking care not to splash the radioactive mixture.

(2) Incubate at 37°C for one hour in a shaking water bath. Stop the reaction by immersing the apparati in ice water slush. Add 100 λ 10% Trichloracetic acid to the incubation mixture by a syringe via the rubber tubing. Slide the tubing down the incubation tube until the injection hole has been blocked. Continue incubation at 37°C for 45 minutes.

(3) Cut the tubing from the CO_2 collection tube and remove the filter paper to a scintillation counting vial with 20 ml of .5% PPO-.03% POPOP scintillation fluid (toluene).

HOMOGENIZATION

Add blank tissues to blank tubes. Remove tissues and incubation mixtures one by one to tissue grinders in ice. Beware of cross contamination. After removing a tissue and its reagents, wash the incubation tube twice with 500 λ 3% TCA. Add the washings to the tissue. Homogenize the tissue samples and blanks thoroughly; maintain at 4°C.

LACTATE ASSAY

A 100 λ aliquot of the homogenate will suffice for the lactate assay. To the homogenate add 100 λ 20% $CuSO_4$, 800 λ double distilled water, and 100 mg

$Ca(OH)_2$. Mix vigorously. Allow to stand 15 minutes. Mix again. Centrifuge 5-10 minutes at 9000 RPM. Apply 100 λ of the supernatant to filterpaper, allow to dry, and place in counting vial with 20 ml scintillation fluid.

GLYCOGEN ASSAY

(1) Centrifuge the 1000 λ of homogenate remaining after the lactate assay for 10 minutes at 9000 RPM. The glycogen assay will be carried out on the supernatant, which is to be removed from the sediment without the buffy nuclear layer, an easily disturbed interface zone.

(2) To the relatively clear supernatant add 100 λ 10% glycogen and two drops of 2N NaCl. Mix well. Add 1.5 ml 95% EtOH, mix well, and scratch the inside walls of the tube with glass until a flocculent precipitate appears. Chill the tubes at -18°C for 15 minutes. Centrifuge 5-10 minutes at 9000 RPM. Decant and discard supernatant.

(3) Repeat the following washing operation three times: dissolve the sedimented glycogen in 300 λ 1% glucose; add 2 drops 2N NaCl; mix well; add 1.3 ml 95% EtOH; mix and scratch tube walls until ppt. forms; chill at -18°C 15 min.; centrifuge and

decant supernatant. Dissolve the sediment from the third wash in 250 λ double distilled water. Apply a 200 λ aliquot to filter paper, allow to dry, and place in a counting vial with 20 ml scintillation fluid.

LIPID ASSAY

Wash the residue remaining from step 1 of the glycogen assay three times with 500 λ of a 2:1 chloroform-methanol mixture. Combine the three washes of each sample and blank. Evaporate these extractions to near dryness (not dry) under a nitrogen atmosphere. Add 300 λ of heptane to the lipid extract and mix. Repeat the following washing procedure three times: add 200 λ of double distilled water; mix well; discard the aqueous phase. After the third washing, apply the organic phase to filter paper, allow to dry, and place in a counting vial with 20 ml scintillation fluid. Alternatively the heptane may be added directly to the counting vial.

PROTEIN-DNA ASSAY

Suspend the residue remaining from the chloroform extractions in 250 λ double distilled water. Apply

a 200 λ aliquot of the suspension to filter paper, allow to dry, and place in a counting vial with 20 ml scintillation fluid.

166 Glucose Metabolism data collected from Pages 79–100a

Recounting

(formly labeled) Glucose Cycle – d1-5		1x		100x	÷.8	Glycogen		if NG, don't use ^{14}C-U-G	CO_2
	^{13}C	μmole/Kg/hr.	Lactate	μmole/Kg/hr.	PI	% incorporation	% CO_2	% dpm	
V15 d3	15.5	$\times 10^4$	19.27	$\times 10^{35}$		.26 .33	9.95	26.6	
V25 d3	15.0		14.4			.11 .14	4.55	15.7	
V20 d.	19.3		17.96			.12 .15	3.62	13	
V34 d5	17.4		11.7			.21 .26	7.1	35.2	
V30 d5	21.4		14.0			.2 .25	5.6	28.4	
d7-15									
V16 d7	12.1		9.89			.12 .15	6.5	25	
V28 d11	21.6		12.2			.1 .13	2.88	17.2	
V37 d11	10.42		5.94			.13 .16	7.59	44.4	V37 NG .684?
V41 d13	10.95		6.32			.05 .06	2.87	16.59	V41 8.28
V38 d11	7.35		7.9			.04 .05	3.5	11.0	V38 NG 1.15
V42 d10	15.2		10.53			.03 .04	1.01	4.84	V42 NG 3.29?
V19 d11	17.9		16.01			.26 .33	8.9	33.2	
V36 d15	16.62		9.34			.21 .26	7.51	44.56	
V40 d11	8.38		8.35			.21 .26	14.98	50.27	V40 5.65
V43 d7	12.7		16.5			.18 .23	8.4	21.59	V43 15.4
d17-25									
V33 d23	21.7		12.8			.11 .14	3.08	17.4	
V24 d23	17.56		24.94			.12 .15	4.2	9.89	
V31 d23	16.2		16.3			.18 .23	6.75	22.3	
V14 d17	10.6		15.49			.41 .51	23	52.5	
V21 d23	NOT AVAILABLE		5.85			.23 .29	—	79.7	
V29 d25	25.0		16.5			.26 .33	6.23	31.3	
	^{14}C-1-Glucose								^{14}C-1-Glucose
V41 d13	12.78	Ratio c1/c6 10.2 → 10.9	2.42			.03 .04	1.3	22.93	V41 9.05
V42 d10	34.5	24.1 25.9	9.6			.04 .05	7.59	9.09	V42 16.6
V43 d7	15.7	11.4 10.7	26.4			.08 .1	3.13	6.18	V43 19.1
	^{14}C-6-Glucose								
V41 d13	1.258		3.2			.03 .04	13.72	17.96	V41 .989
V42 d10	1.43		6.37			.08 .1	34.52	25.78	V42 NG .483
V43 d7	1.38		12.2			.13 .16	55	20.63	V43 1.62

APPENDIX F

Glucose Metabolism Data and Sample Calculations

SAMPLE GLUCOSE METABOLISM CALCULATIONS

	U		1		6	
	cpm	%	cpm	%	cpm	%
CO_2	717	4.4	2309	10.6	63.33	1.8
Lactate	154 = 15400	94.9	193 = 19300	88.99	34 = 3404	96.5
Glycogen	19.67 = 24.58	.15	23 = 28.75	.13	19.33 = 24.17	.7
Lipid	26	.16	23	.1	9.33	.3
Protein	44 = 55	.33	20.67 = 25.84	.1	21.33 = 26.67	.7
Total cpm	16222.58		21686.59		3527.5	

Pentose Cycle

100 mole glucose yields 600 moles carbon x 4.4% = 26.4

CO_2 Method:

$$\frac{S}{3-2S} \times 100 = \% \text{ glucose utilization}$$

$$\frac{.0888}{3-.1776} = \frac{.0888}{2.8224} = .03145 \times 100 = 3.145\%$$

$$S = \text{specific yields } \frac{G_1CO_2 - G_6CO_2}{1-G_6CO_2}$$

$$S = \frac{0.106 - .018}{1 - .018}$$

$$S = \frac{.088}{.992} = .0888$$

Lactate Method:

$$\frac{1-\gamma}{1+2\gamma} = \%\ \text{gluc. util.} \qquad \gamma = \frac{G_1\ \text{Lact}}{G_6\ \text{Lact}}$$

$$\frac{1-.922}{1+1.844} = \frac{.078}{2,844} = .0274 \times 100 = 2.74\% \qquad \gamma = \frac{.8899}{.965}$$

$$\gamma = .922$$

Products (^{14}C-U)

CO_2 -- Total 600 molecules carbon x 4.4% = 26.4

CO_2 (Pentose) -- 500 x .5 x .03 = 9

CO_2 (Pyruvate decarboxylase) -- pyruvate kinase - Lactate = 591 - 570 = 21 (1/3 as CO_2 = 7)

CO_2 from TCH cycle = Total CO_2 - Σ(Pentose and Pyr. decarboxyl.) = 26.4 - 16 = 10.4

Lactate = 94.9% of 600 = 570

Lipids = 600 x .0016 = .96 = <1

Glycogen = 600 x .0015 = .9 = ≤1

Protein/DNA = 600 x .0033 = 1.98 = ~2

Intermediate Steps

Hexokinase -- 600 carbons

PFK -- 600 - 18 = 582

G3PDH and PK -- PFK + 9 = 582 + 9 = 591

Pyridine Nucleotide Balance (100 moles glucose)

Formation:

Cytoplasmic:

Pentose cycle (TPNH) -- ($3CO_2$ x 2 TPNH) x PC% = TPNH

100moles x $3CO_2$ x 2TPNH x 3%=18 mole

G-3PDH (DPNH)--

591 carbons÷ 3 carbons of G3P= 197 mole

Σ (DPNH+TPNH) = total reduced pyridine nucleotide

= 215 mole

Mitochondrial:

Pyruvate DH (DPNH)= $\frac{\text{PK-Lact.}}{3} = \frac{591-570}{3} = 7$

Utilization:

Fatty Acid-- negligible

Glycerol (from G3P)-- negligible

Lactate formation-- 570÷3 carbon of lactate= 190mole

Net reduced energy formation= ΣDPNH,TPNH - Lactate

= 215-190

= 25

ATP Balance(metabolism of 100 moles glucose)

Utilization:

Hexokinase-- 100

PFK-- 582÷6 = 97

Acetyl CoA,etc.-- negligible

Net utilization = 197

Formation: (at G-3-PDH)

G3PDH-- 197

PK-- 197

PyruvateDH-- $\frac{\text{PK-Lactate}}{3}$ = 7x3 = 21

Krebs cycle-- Acetyl CoA= 10.4÷2= 5.2

ATP= (AcCoA)x 12 = 62.4

Net ATP formation = Σ G3P,PK, PDH,ATP(TCA)=477.4

Energy gainedfrom 100 moles glucose= 477.4-197

=280 moles

APPENDIX G

Classification of Enzymes

CLASSIFICATION OF ENZYMES

Name in Thesis	IUB	Systematic Name	Reaction
Lactic dehydrogenase	1.1.1.27	L-Lactate:NAD oxidoreductase	L-Lactate + NAD^+ → pyruvate + NADH
Malate dehydrogenase	1.1.1.37	L-Malate:NAD oxidoreductase	L-Malate + NAD^+ → NADH
Isocitrate dehydrogenase	1.1.1.42	L-Isocitrate:NADP oxidoreductase	L-Isocitrate + $NADP^+$ → 2 oxoglutarate + CO_2 + NADPH
Glucose-6-phosphate dehydrogenase	1.1.1.49	D-Glucose-6-phosphate:NADP oxidoreductase	D-Glucose-6-phosphate + $NADP^+$ → D-glucono-δ-lactone-6-phosphate + NADPH
Glyceraldehyde-3-phosphate dehydrogenase	1.2.1.12	D-Glyceraldehyde-3-phosphate: NAd oxidoreductase	D-Glyceraldehyde-3-phosphate + orthophosphate + NAD^+ → 1,3-diphospho-D-glyceric acid + NADH
Phosphorylase	2.4.1.1	α-1,4-glucan:orthophosphate glucosyl transferase	Glycogen + inorganic phosphate → glucose-1-phosphate
Phosphofructokinase	2.7.1.11	ATP:D-Fructose-6-phosphate-1-phosphotransferase	Fructose-6-phosphate + ATP → Fructose-1,6-phosphate + ADP
Pyruvate kinase	2.7.1.40	ATP:pyruvate phosphotransferase	Pyruvate + ATP → phosphoenol pyruvate + ADP
Acetylcholinesterase	3.1.1.7	Acetylcholine acetyl hydrolase	Acetylcholine + H_2O → choline + acetic acid
Butyrylcholinesterase	3.1.1.8	Butyrylcholine butyryl hydrolase	Butyrylcholine + H_2O → choline + butyric acid
Alkaline phosphatase	3.1.3.1	Orthophosphoric monoester phosphohydrolase	Orthophosphoric monoester + H_2O → alcohol + H_3PO_4
Acid phosphatase	3.1.3.2	Orthophosphoric monoester phosphohydrolase	Orthophosphoric monoester + H_2O → alcohol + H_3PO_4
Leucine aminopeptidase	3.4.1.1	α-Aminopeptide (Leucine) aminoacid hydrolase	hydrolyses L-peptides, splitting off leucine, an N-terminal residue with a free α-amino group

APPENDIX H

Quantitative Enzyme Assay Procedures

QUANTITATIVE ENZYME ASSAY PROCEDURES

A. Standardization of NAD^+ and $NADP^+$

NAD^+:

10 ml	0.1 M Tris buffer, pH 8.5-9.0
5	100 mM NAD^+ stock solution
400	98% EtOH
10	Alcohol dehydrogenase (5-6 mg/300 H_2O)

$NADP^+$:

1 ml	0.1 M Tris buffer, pH 8.5-9.0
5	10 mM $NADP^+$ stock solution
10	100 mM Glucose-6-phosphate
10	100 mM $MgCl_2$
1	Glucose-6-phosphate dehydrogenase

Take 1 ml. of the standardization mixture to spectrophotometric cuvette.

Read at 340 m every 10 minutes for 20 minutes. Make sure OD will not change; read long enough to assure reaction completion.

Add 50 6N HCl to cuvette. Read at 340 m for blank value.

NAD^+ calculation: $X = \dfrac{OD \times \frac{10415}{5}}{6275} = OD \times 0.332$

$NADP^+$ calculation: $X = \dfrac{OD \times \frac{1027}{5}}{6275} = OD \times 0.0326$

Molar Extinction Coefficient = $E_{340} = 6270$

B. NADH Standardization

Add 5 of freshly prepared 50 mM NADH to 5 ml. 0.1 M Tris buffer, pH 8.5-9.0.

Take a 1 ml. aliquot to spectrophotometric cuvette.

Read at 340 m .

Add 50 λ 6N HCl; read at 340 mμ for blank values.

C. Glucose-6-Phosphate Dehydrogenase (G-6-PDH)

1. Reaction mixture:

Final Concentration	Reagent	Aliquot
2.0 mM	G-6-P, 100 mM	20 λ
0.3 mM	NADP, 10 mM	30 λ
2.5 mM	$MgCl_2$, 100 mM	25 λ
0.5 mM	EDTA, 100 mM	5 λ
0.05%	BPA, 5%	10 λ
0.1 M	Tris buffer, 0.5 M pH 8.2-8.8	200 λ
	H_2O to make 1000 λ	710 λ

2. Procedure

0.5-2 μg samples + 10-15 λ reaction mix.
Incubate 60 minutes at 37°C.
10 λ aliquot + 1 ml carbonate buffer.
Read NADPH in fluorometer.

3. Blank and standard

To be run pari passu with samples

Blank tubes contain an aliquot of reagent mixture the same size as used with samples.

Standard tubes contain aliquots of diluted NADH equal to the aliquots of samples. The dilution is as follows: 5 λ of 50 mM NADH (freshly prepared) is diluted with 500 λ double distilled water. Three 10 λ aliquots are then diluted with 100 λ of reaction mix, 50 λ of reaction mix, and 25 λ of reaction mix, respectively. Aliquots of the same magnitude as those for samples are then removed to the standard incubation tubes.

Make a 1000-fold dilution of NADH with Tris buffer, pH 8.2-8.8. Determine the absolute value for the NADH with a spectrophotometer (340 mμ).

D. Phosphofructokinase (PFK)

1. Reaction mixture

Final Concentration	Reagent	Aliquot
0.1 M	Tris buffer, 0.5 M, pH 7.9	200 λ
7.5 mM	F-6-P, 50 mM	150 λ
2.5 mM	ATP, 100 mM	25 λ
2.5 mM	$MgCl_2$, 1.0 M	2.5 λ
1.0 mM	NADH, 50 mM	20 λ
0.5%	BPA, 5%	10 λ
	Aldolase, 10 mg/ml	0.5 λ
	Triose isomerase + α glycerophosphate DH	0.5 λ
	H_2O to make 1000 λ	591.5 λ

2. Procedure

0.5-1 µg + 10 reaction mix.
Incubate 30 minutes at 37°C.
Add 5 λ 1N HCl.
Mix.
Remove a 10 λ aliquot to 100 λ 6.6M NaOH.
Incubate 30 minutes at 37°C (or 15 min. at 60°C).
Add 1.0 ml H_2O.
Read NAD^+ in fluorometer.

3. Blank and standard

To be run pari passu with samples

Blank tubes contain 10 λ reaction mix.

Standard tubes:

I. 3 λ of 100 mM NAD^+ + 400 H_2O
II. 3 λ of 100 mM NAD^+ + 200 H_2O

6-8 λ aliquots of I and II + 50 λ reaction mixture
10 λ of above to incubation tubes
Then treat as sample tubes.

NB: Calculations carry 0.5 factor resulting from production of 2 moles of NAD^+ from 1 mole of substrate.

E. Glyceraldehyde-3-Phosphate dehydrogenase (G-3-PDH)

1. Reaction mixture

Final Concentration	Reagent	Aliquot
5 mM	Fructose-1,6-diphosphate, 50 mM	100 λ
30 mM	Arsenate, 0.4 mM	75 λ
3 mM	NAD^+, 100 mM	30 λ
5 mM	Mercaptoethanol, 1M	5 λ
1 mM	EDTA, 100 mM	10 λ
0.1 mM	BPA 5%	20 λ
	Aldolase, 10 mg/ml suspension	1.25λ
0.1 mM	AMP_2 buffer, 0.5 M, pH 8.6-8.8	200 λ
	triose isomerase 10 mg/ml	1 λ
	H_2O to make 1000 λ	567.5

2. Procedure

1 µg or less samples
+ 17 λ reaction mixture
Incubate 1 hr. at 37°C.
12 λ aliquot to 1 ml carbonate buffer
Read NADH in fluorometer.

3. Blank and standard

To be run pari passu with samples.

Blank tubes contain 17 λ of reaction mixture.

Standard tubes contain 17 λ of the following dilution: 2.5 λ 50 mM freshly prepared NADH diluted with 200 λ H_2O; a 10 λ aliquot added to 50 λ reaction mixture provides the standard for incubation.

NB: Aldolase facilitates the splitting of FDP to DHAP (dehydroxyacetone phosphate) and G-3-P (glyceraldehyde-3-phosphate). Accordingly, a compensation in the calculations must be made.

F. Pyruvate Kinase (PK)

1. Reaction Mixture

Final Concentration	Reagent	Aliquot
0.1 M	Imidazole, 0.2 M, pH 7.0	500 λ
4 mM	PEP, 100 mM	40 λ
2 mM	ADP, 50 mM in 0.1 M Tris, pH 7.6	40 λ
5 mM	$MgSO_4$, 1M	5 λ
50 mM	KCl, 1M	50 λ
0.25 mM	NADH, 50 mM	5 λ
5 mg/ml rgt.	LDH, 10 mg/ml	0.5λ
0.05 %	BPA 5%	10 λ
	H_2O to make 1000 λ	350 λ

2. Procedure

1 µg sample
+ 18 λ reaction mixture
Incubate 30 minutes at 37°C.
+ 3 λ 2N HCl
12 λ aliquot to 100 λ 6.6N NaOH
Incubate 30 min. at 37°C.
+ 1 ml H_2O
Read DPN^+ correlate with fluorometer.

3. Blank and standard

To be run pari passu with samples

Blank tubes contain 18 λ of the reaction mixture.

Standard tubes contain 18 λ aliquots of the following dilution: 2.9 λ 100 mM NAD^+ diluted with 155 λ H_2O. 5 λ aliquot of above removed to 40 λ reaction mixture from which incubation aliquot is taken.

G. Lactic Dehydrogenase (LDH)

1. Reaction mixture

Final Concentration	Reagent	Aliquot
0.1 M	Tris buffer, 0.5 M, pH 7.5	200 λ
1 mM	Pyruvate, 100 mM	10 λ
2 mM	NADH, 50 mM	40 λ
0.05%	BPA 5%	10 λ
	H_2O to make 1000 λ	740 λ

2. Procedure

0.5-5 µg samples
+ 18 λ reaction mixture
Incubate 30 minutes at 37°C.
+ 5 λ 1N HCl
15 λ aliquot of above to 100 λ 6.6N NaOH
Incubate 30 minutes at 37°C.
+ 1 ml H_2O
Read NAD^+ correlate on fluorometer.

3. Blank and standard

To be run pari passu with samples

Blank tubes contain 18 λ of reaction mixture.

Standard tubes contain 18 λ of each of the following dilutions:

I. 5 λ of 100 mM NAD^+ diluted with 100λ H_2O
II. 5 λ of 100 mM NAD^+ diluted with 50 λ H_2O

10 aliquots of I and II diluted with 50 λ reaction mixture provide the incubation standard.

H. Malate Dehydrogenase (MDH)

1. Reaction mixture

Final Concentration	Reagent	Aliquot
0.1 M	Tris buffer, 0.5 M, pH 8	200 λ
1 mM	Oxaloacetic acid, 100 mM, pH 2.3-2.4 Made fresh with Tris, pH 8.6	10 λ
2 mM	NADH, 50 mM	40 λ
0.05%	BPA, 5%	10 λ
	H_2O to make 1000 λ	740 λ

2. Procedure

1.5-1 µg samples
+ 15 λ reaction mixture
Incubate 30 minutes at 37°C.
+ 5 λ 1N HCl
Mix.
Remove 10 λ aliquot to 100 λ 6.6 N NaOh
Read NAD^+ correlate with fluorometer.

3. Blank and standard

To be run pari passu with samples

Blank tubes contain 15 λ reaction mixture

Standard tubes contain 15 λ of the following dilution: 5 λ to 100 mM NAD^+ diluted with 100 λ H_2O. 10 λ aliquot of above diluted with 50 λ reaction mixture.

I. Isocitrate Dehydrogenase (ICDH)

1. Reaction mixture

Final Concentration	Reagent	Aliquot
0.1 M	Tris buffer, 0.5 M, pH 7.8-8.0	200 λ
5 mM	Isocitrate, 33 mM	150 λ
0.25 mM	$MnCl_2$ 50 mM	5 λ
1 mM	NADP, 10 mM	100 λ
0.05%	BPA, 5%	10 λ
	H_2O to make 1000 λ	535 λ

2. Procedure

0.5-1 µg samples
+ 10-15 λ reaction mixture
Incubate 30-60 minutes at 37°C.
+ 1 ml carbonate buffer
Read NADPH from fluorometer.

3. Blank and standard

To be run pari passu with samples

Blank tubes contain "sample size" aliquot of reaction mixture.

Standard tubes contain "sample size" aliquots of the following dilutions:

I. 5 λ of 50 mM NADH diluted with 500 λ H_2O

II. 5 λ of 50 mM NADH diluted with 250 λ H_2O

10 aliquots of I and II added to 50 λ reaction mixture provide the incubation standards.

APPENDIX I

Enzyme Activity in Course of Cycle for Three Test Animals

ENZYME ACTIVITY IN COURSE OF CYCLE FOR THREE TEST ANIMALS

(mean values of 5-15 determinations in moles/kg/hr)

Day	3	5	7	11	15	17	23	25
G6PDH								
664	7.97*		2.89	3.82*			2.04	
2074		5.99		1.998			5.65*	
2259			1.07		1.25	1.19	5.94	8.93
PFK								
664	.107**		.159	.045				
2074		.01		.07			.065	
2259			.06	.02	.076	.074	.063	.01
LDH								
664	4.72**		5.6	4.21*			2.17	
2074		4.67		1.43			5.43*	
2259			2.86	1.43	4.55	5.14	6.85	7.34
P Kinase								
664	2.4**		2.21	1.714*			1.104	
2074		1.138		.9548			3.05*	
2259			.536	.441	.8308	2.24	2.98	2.03
G3PDH								
664	.538**		.25	.256*			.103	
2074		.112		.173			.338*	
2259			.439	.047	.104	.906	.237	.142
ICDH								
664	.246**		.076	.118*			.072	
2074		.059		.024			.128*	
2259			.044		.033	.034	.138	.194
MDH								
664	4.46**		4.8	4.69*			3.34	
2074		3.71		4.16			7.05	
2259			3.16		4.52	7.39	5.63	4.33

* n = 10

** n = 15

APPENDIX J

Equipment and Suppliers

EQUIPMENT AND SUPPLIERS

paraplast -- cat. no. 48667, Van Waters and Rogers, Inc., Los Angeles, Calif.

57° paraffin oven -- model no. B-1-P, Electrical Heat Control Apparatus Co., Newark, N.J.

microtome blade -- Jung 5 inch and 9 inch steel blades

Spencer microtome -- model no. 820, American Optical Co., Buffalo, N.Y.

microscope slides -- cat. no. 2951, Erie Scientific, Buffalo, N.Y.

electric tissue float -- model no. 375, Lipshaw Mfg. Co., Detroit, Mich.

Tissue-Tac -- cat. no. M-7645, Dade Reagent, Inc., Miami, Florida.

Surital -- sodium thiemylal, Parke-Davis & Co., Detroit, Mich. 25 mg/cc injected I.V. to effect. Dose 6-15 mg/kg.

Neo-Predef -- Neomycin sulfate, 9-Fluoroprednisolone acetat tetracaine hydrochloride, and myristyl-gamma-picolinium chloride in powder base. The Upjohn Company, Kalamazoo, Mich.

45° slide warmer -- cat. no. 26000, Chicago Surgical & Electrical Co., Div. Lab-Line Instruments, Inc., Chicago, Ill.

slide boxes -- cat. no. M-6285, Scientific Products, Div. American Hospital Supply Corp., Evanston, Illinois.

cryostat -- model CTI, International Equipment Co., Needham Heights, Mass.

small slide boxes -- cat. no. A-1604 B, Clay-Adams, Inc., New York, N.Y.

mounting medium -- Permount, a 60% solution of synthetic resin (β-pinene). Cat. no. 12-568, Fisher Scientific Co., FairLawn, N.J.

large glass slides -- 3" x 2" cat. no. 66518 Scientific Products, Div. Am. Hosp. Supply Corp., Evanston, Ill.

Microscope -- Carl Zeiss GFL standard microscope with 1, 2.5, 10, 40, and 100x objectives, Kpl 8x eye pieces, and a 50-60 Hertz 39-25-24 type transformer

photomicroscope -- Ultraphot II Carl Zeiss from Brinkmann Instruments, Great Neck, N.Y.

film -- 4 x 5 inch Panatomic-X, Eastman Kodak Co., Rochester, N.Y.

rectal biopsy rongeur forceps -- Lawton Inst., New York.